Elastomer Friction –Fundamental and Footwear Research

Jakobsen, Lasse

Publication date:
2023

Document Version
Publisher's PDF, also known as Version of record

DTU Construct
Department of Civil and Mechanical Engineering

Elastomer Friction – Fundamental and Footwear Research

Lasse Jakobsen

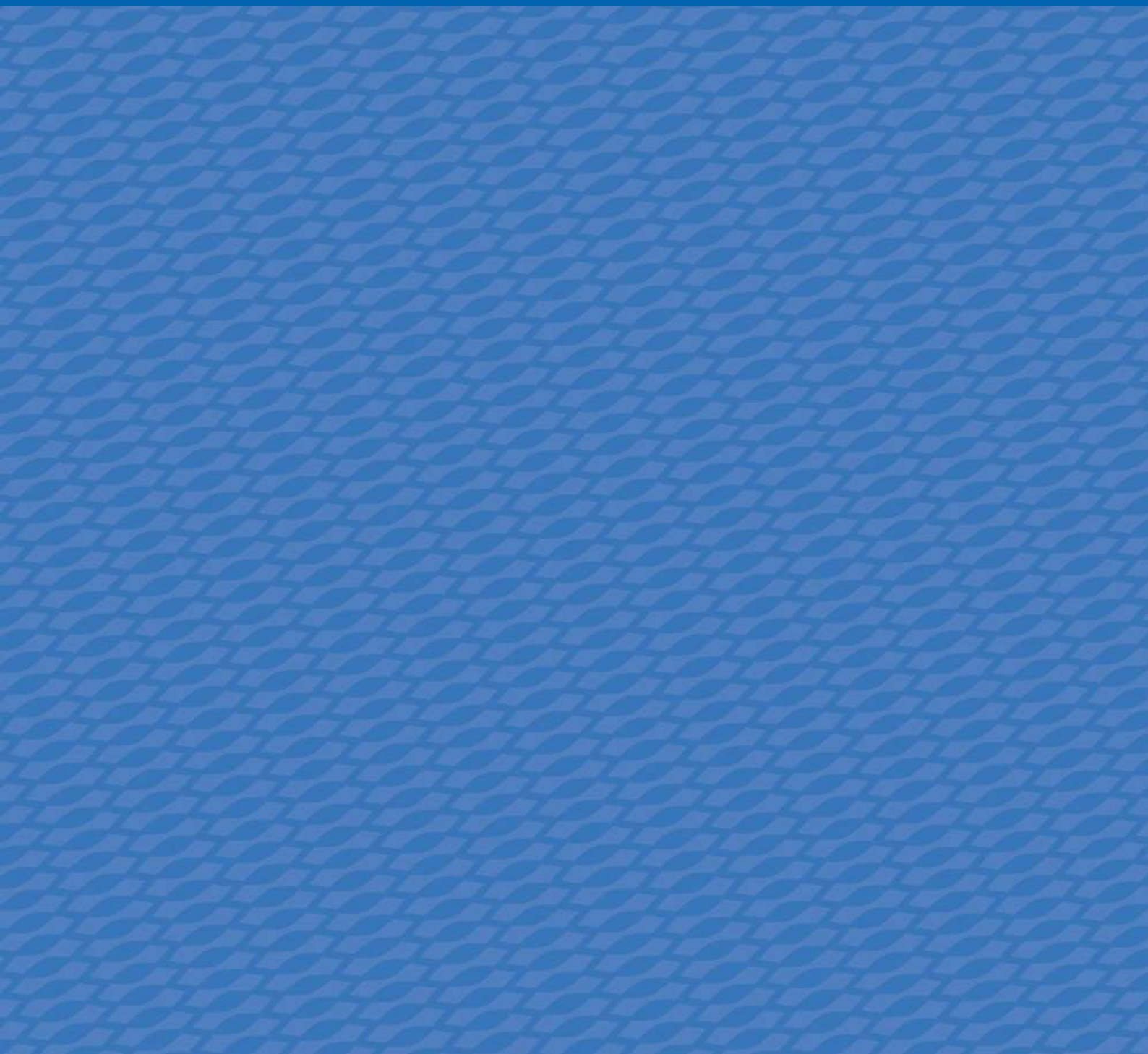

PREFACE

This PhD thesis is centered around slip resistance of footwear. The thesis is based on five separate studies, with different methodology and ranges from friction research of elastomer block specimens to application-oriented research in relation to slipping accidents and the role of footwear. The studies methodologies and results are presented numerically and tight together in the discussion. The materials and methods chapter briefly summarize the different studies methodologies to give the reader an understanding of how the results are obtained. Therefore, detailed methodology descriptions are left out and the reader is referred to the appended articles for methodology elaborations. In addition, if the reader is new to/unfamiliar with the severity of slipping accidents, biomechanics of slipping and elastomer friction, the reader is urged to peruse the introduction, which provides a short, however necessary theoretical background.

Kongens Lyngby, 28th February 2023

Lasse Jakobsen

Elastomer Friction –Fundamental and Footwear Research

March 2023

ISBN: 978-87-7475-707-8

Author:

Lasse Jakobsen

Technical University of Denmark

Main supervisor:

Associate Professor Ion Marius Sivebæk

Technical University of Denmark

Co-Supervisor:

Professor Jesper Henri Hattel

Technical University of Denmark

DTU Construct

Section of Manufacturing Engineering

Technical University of Denmark

Produktionstorvet, Bld. 425

DK-2800 Kgs. Lyngby

Denmark

Tlf.: +45 4525 4763

www.construct.dtu.dk

CONTENTS

LIST OF PUBLICATIONS

This dissertation consists of a summary of five studies in total:

Study I: **L. Jakobsen**, F.G. Lysdal, T. Bagehorn, U.G. Kersting, I.M. Sivebaek, (2022). Evaluation of an actuated force plate-based robotic test setup to assess the slip resistance of footwear. International Journal of Industrial Ergonomics, https://doi.org/10.1016/j.ergon.2021.103253. (ACCPETED MANUSCRIPT IS ATTACHED).

Study II: **L. Jakobsen**, F.G. Lysdal, T. Bagehorn, U.G. Kersting, I.M. Sivebaek, (2022). The Effect of Footwear Outsole Material on Slip Resistance on Dry and Contaminated Surfaces with Geometrically Controlled Outsoles. Ergonomics, https://doi.org/10.1080/00140139.2022.2081364. (ACCPETED MANUSCRIPT IS ATTACHED).

Study III: **L. Jakobsen**, S.B. Auganæs, A. F. Buene, I.M. Sivebaek, A. KleinPaste, (2022). Dynamic and Static Friction Measurements of Elastomer Footwear Blocks on Ice Surface. Tribology International, https://doi.org/10.1016/j.triboint.2022.108064. (ACCPETED MANUSCRIPT IS ATTACHED).

Study IV: **L. Jakobsen**, T. Bagehorn, I.M. Sivebaek, F.G. Lysdal, (2022). Evaluation of Footwear Slip Resistance Certifications and Measurements Conducted on a Force Actuated Robotic Test Setup. International Journal of Industrial Ergonomics, (SUBMITTED. MANUSCRIPT UNDER REVIEW IS ATTACHED).

Study V: **L. Jakobsen**, A. Tiwari, I.M. Sivebaek, and B.N.J. Persson. Footwear Outsole Friction on Steel and Tile Surfaces: Experiments and Modelling. (IN PREPARATION. PRELIMINARY MANUSCRIPT IS ATTACTED).

ABBREVIATIONS

COF	Coefficient of Friction
RCOF	Required Coefficient of Friction
ACOF	Available Coefficient of Friction
DCOF	Dynamic Coefficient of Friction
SCOF	Static Coefficient of Friction
DMA	Dynamic Mechanical Analysis
PU	Polyurethane
TPU	Thermoplastic Polyurethane
RU	Vulcanized Rubber
SLS	Sodium Lauryl Sulfate
ISO 13287	ISO 13287:2019 - Personal protective equipment – Footwear – Test method for slip resistance
Biofidelic	Testing parameters optimized to simulate realistic slipping events
Tile surface	Eurotile 2
Steel surface	Steel number 1.4301

ENGLISH SUMMARY

Slipping, tripping and falling is with 18.9% in Denmark the second most frequent cause of serious occupational accidents. In fact, general fall accidents in 2016 were estimated to result in annual additional costs of 3.9 billion DKK due to lost production and further 4.8 billion DKK for treatment and care.

The cause of fall/slip accidents is complex and multi-factorial, but is most often a result of insufficient friction between footwear and surface. However, varying work environments where different surfaces and contaminants (oil, dirt and food residues) are present, makes it difficult to maintain sufficient friction. Friction occurs as a result of contact between shoe sole and surface, but is difficult to determine realistically, as the friction between footwear and surface is strongly influenced by the test methodology. It is therefore necessary to replicate realistic slipping accidents, to gain the best possible insight into the slipping mechanisms.

Shoe soles are often made from elastomers, which are viscoelastic materials in nature. This means that elastomers have both viscous (behaves like liquids) and elastic (behaves like solids) characteristics and the friction properties are therefore extremely complicated. This is due to a complex combination of material properties such as low modulus of elasticity, adhesive and hysteresis components, real contact area, as well as dependence on sliding velocity, temperature normal load and frequency of normal load.

The purpose of this PhD thesis is to investigate the shoe/surface slipping phenomena from a basic research perspective, using elastomer blocks and from an application-oriented perspective, using actual footwear. The thesis is thus divided into research that deals with elastomer friction of block specimens and research that is applied to a system, which, in this case, is shoe slip resistance.

Study I has dealt with the application-oriented research and presented and evaluated a test system to quantify the slip resistance of footwear. The system can operate in accordance with "ISO 13287 Personal protective equipment – Footwear – Test method for slip resistance" and at the same time can be adjusted to accommodate testing parameters replicating realistic slip accidents. Studies II and IV have used this test system to determine the slip resistance properties of footwear models using an application-oriented research approach. In study II, three shoes constructed from the same model, but with different outsole materials, have been studied. The three materials are referred to as PU, TPU and RU. In study IV, five commercially available footwear models have been studied, all of which are certified as slip resistant according to ISO 13287.

Studies III and V have been characterized as more fundamental research of elastomer friction, since they use elastomer blocks and do not include whole shoes. The complexity of the tribosystem is thereby reduced and the results are to a certain extent more generic and can therefore be used in other applications.

In Summary, the studies (Studies II, III and V) have showed that material selection have a large impact on the friction properties and is context dependent. The RU material has exhibited the highest dynamic friction on a cold (-10 °C) ice surface, whereas the PU has exhibited the highest dynamic and static friction on a warm (0 °C) ice surface. PU has also demonstrated the highest dynamic friction on tile and steel surfaces contaminated with glycerin and canola oil. TPU has exhibited the highest dynamic friction on dry steel surface at high sliding velocity (up to 2.4 m/s). Thereby, all three materials have showed the highest friction under different conditions. This concludes that material performance/friction properties are highly dependent on testing conditions and environmental circumstances. Furthermore, study IV has showed that the test conditions and footwear design have influenced slip resistance considerably. Future research should therefore focus on optimizing slip resistant footwear to meet area- and industry-specific environments, where different surfaces and contaminants are present. At the same time, the focus should be on reducing the gap that exists between the academic research in slip resistance

and the industrial stakeholders in the footwear industry, who produce slip resistant footwear and surfaces, as well as the industrial buyers/users of non-slip footwear.

DANSK RESUME

Glid, fald og snublen er i Danmark den næst hyppigste årsag til anmeldte alvorlige arbejdsulykker og svarer til 18,9% af alle alvorlige arbejdsulykker. Faktisk er generelle faldulykker i 2016 beregnet til at resultere i årlige ekstra omkostninger på 3,9 mia. kr. i forbindelse med tabt produktion og yderligere 4,8 mia. kr. til behandling og pleje.

Årsagen til fald- og glideulykker er dog kompleks og multifaktoriel, men er oftest et resultat af utilstrækkelig friktion mellem fodtøj og underlag. Varierende arbejdsmiljøer, hvor forskellige overflader og forureninger (olie, snavs og madrester) er til stede, gør det vanskeligt at bevare tilstrækkelig friktion. Friktion opstår som et resultat af kontakt mellem skosål og underlag, men er dog vanskelig at fastlægge realistisk, da friktionen mellem fodtøj og underlag er stærkt influeret af testmetodikken. Det er derfor nødvendigt at replikere virkelighedstro glideulykker i forskningsøjemed for at få bedst mulig indsigt i de mekanismer, der forårsager glideulykker.

Skosåler fremstilles ofte af elastomerer, som er viskoelastiske materialer af natur. Det betyder, at elastomerer både har viskose (opfører sig som væsker) og elastiske (opfører sig som faststoffer) egenskaber, og friktionsegenskaberne er derigennem særdeles komplicerede. Dette skyldes bl.a. en kompleks kombination af materialeegenskaber som lavt elasticitetsmodul, adhæsiv- og hysterese-komponenter, reelt kontaktareal samt afhængighed af glidehastighed, temperatur, normal last og frekvens af normal last.

Formålet med denne ph.d.-afhandling er at belyse elastomerers friktion fra et grundforskningsperspektiv og fra et applikationsnært perspektiv. Afhandlingen er således inddelt i forskning, der beskæftiger sig med friktion af elastomerblokke og forskning, der er anvendt i et system, som i dette tilfælde er skoskridsikkerhed.

Studie I beskæftiger sig med den applikationsnære forskning og præsenterer samt evaluerer et testsystem til at kvantificere skridsikkerheden af fodtøj. Systemet kan operere i overensstemmelse med "ISO 13287 Personlige værnemidler – Fodtøj – Metode til prøvning af skridsikkerhed" og kan samtidig justeres, så testparametre replikerer virkelighedstro glideulykker. Studie II og IV anvender dette testsystem til at bestemme skridsikkerhedsegenskaberne for fodtøjsmodeller, og disse studier er derfor også en del af den applikationsnære forskning. I studie II er der konstrueret tre sko af samme model, men med forskellige ydersålsmaterialer. De tre materialer benævnes som RU, PU og TPU. I Studie IV studeres fem kommercielt tilgængelige fodtøjsmodeller, som alle er certificeret som skridsikre i henhold til ISO 13287.

Studie III og V drejer sig om forskning af friktion af elastomerblokke, da der i disse ikke anvendes hele sko, men i stedet for kvadratiske elastomerelementer. Kompleksiteten af tribosystemet er herved reduceret, og resultaterne er i et vist omfang mere generisk og kan derfor også anvendes i andre applikationer. De samme tre materialer, som blev studeret i studie II (RU, PU og TPU), anvendes her som kvadratiske elastomerblokke.

Kort fortalt viser studierne (II, III og V), at materialevalg har stor indvirkning på friktionsegenskaberne og er kontekstafhængig. RU materialet udviser højest dynamisk friktion på kold (-10 °C) isoverflade, hvorimod PU udviser højest dynamisk og statisk friktion på varm (0 °C) isoverflade. PU demonstrerer også højest dynamisk friktion på flise- og ståloverflade forurenet med glycerin og rapsolie. TPU udviser højest dynamisk friktion på tør ståloverflade ved høje glidehastighed (op til 2.4 m/s). Derved udviser alle tre materialer højest friktion under forskellige betingelser. Konklusionen er derfor, at materialet, der resulterer i højest friktion, er bestemt af konteksten og afhænger derfor af miljøet (overflader, forureninger og temperaturer) og kontaktbetingelsen (last og glidehastighed). Ydermere viser studie IV, at testbetingelserne og ydersålsgeometrier influerer skridsikkerheden betragteligt. Fremtidig forskning bør derfor fokusere på at optimere skridsikkerhedsfodtøj til at imødekomme område- og branchespecifikke miljøer, hvor forskellige overflader og forureninger er til stede. Samtidig bør der

fokuseres på at reducere det gab, der eksisterer imellem den akademiske forskning inden for skridsikkerhed og de industrielle interessenter i fodtøjsbranchen, der producerer skridsikkert fodtøj og overflader samt de industrielle aftagere/brugere af skridsikkert fodtøj.

ACKNOWLEDGEMENTS

This PhD projected is funded by the Danish Working Environment Research Fund (Arbejdsmiljøforskningsfonden - grant number: 20195100816). In that regard, I wish to express my gratitude to the fund, for believing and investing in this project.

Data collection in studies I, II and IV was conducted at Aalborg University, Department of Health Science and Technology. Data collection in Study III was conducted at Norwegian University of Science and Technology (NTNU), Department of Civil and Environmental Engineering. Lastly, data collection of study V was conducted at Forschungszentrum Jülich GmbH, Institute for Advanced Simulation and at Technical University of Denmark, Department of Civil and Mechanical Engineering.

In addition, I wish to thank a number of people, whose assistance was essential to the completion of this project.

First, I wish to express my appreciation to my main supervisor Associate Professor Ion Marius Sivebæk (DTU), who introduced me to the complex "world of tribology" and provided professional guidance throughout the project. Especially, I enjoy your professional approach combined with a great sense of humour.

Secondly, I wish to thank Professor Jesper Henri Hattel (DTU), for welcoming me to the department, taking me under your wings and providing priceless guidance with various research applications.

In prolongation, I wish to recognize the extensive assistance of all my co-authors. Dr. Filip Gertz, Lysdal (St Mary's University) for being an invaluable close research partner and quality controller. Timo Bagehorn (Aalborg University) for especially software development and highly specialised knowledge from the footwear industry. Prof. Uwe G. Kersting (Aalborg University) for contributing with valuable discussions. My Norwegian colleagues. Dr. Audun Formo Buene (NTNU), Sondre Bergtun Auganæs (NTNU) and Prof. Alex Klein-Paste (NTNU) for inviting me for a lovely (and cold) stay in the winter lab. Dr. Bo Persson and Dr. Avinash Tiwari for inviting me to Forschungszentrum Juelich and introducing me to rheology and rubber friction.

To my partners in the footwear industry, I want to thank Kasper Vejergang Jepsen Lundh and Jane Bjerregaard Nielsen from SIKA Footwear for providing footwear samples. Not to mention Sophia Sachse from ECCO A/S for her extensive help and very fast execution with material and prototype delivery. Lastly, I appreciate Jesper Bøgelund, Senior R&D Engineer at DDS (device delivery & solutions) at Novo Nordisk for providing the DMA measurements in study III.

Finally, I wish to acknowledge the great love and support of my family and friends. I wish to thank my parents and Nathalie for listening to my frustrations and always being supportive. I wish to thank Kim Birch Olsen for putting a roof over my head and for numerous lovely coffee breaks during the Corona pandemic lock down.

INTRODUCTION

1.1. SEVERITY AND SCOPING

Slips, Trips and Falls (STF) have increased in the period 2016-2021 (Figure 1) [1] and are the second most frequent cause of work related injuries in Denmark and accounts for 18.9 % of serious reported accidents [2]. In Denmark, general fall accidents have annual expenses of DKK 3.9 billion (€524.405.700) as consequence of lost production and absence from work, and additional expenses of DKK 4.8 billion (€645.422.400) due to hospitalization and health care [3].

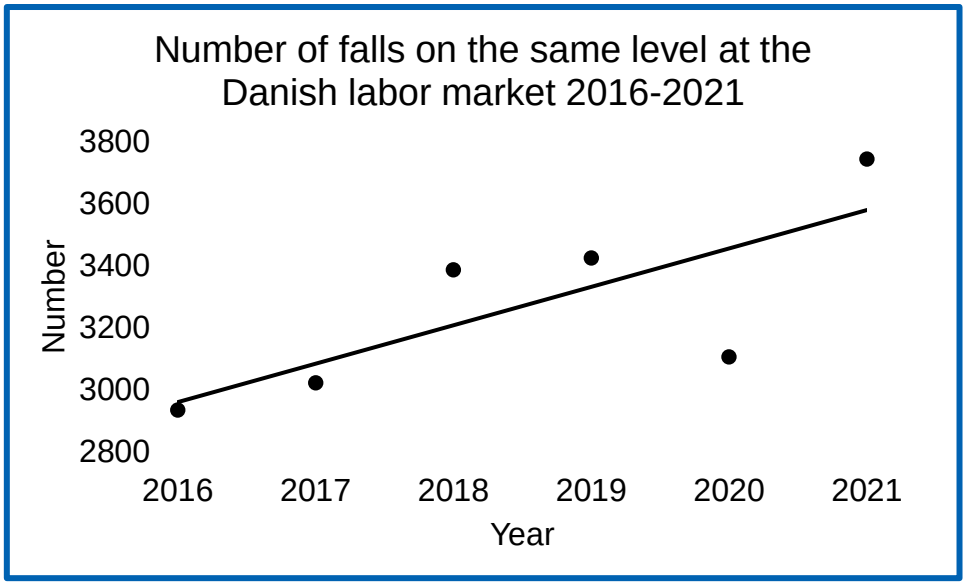

Figure 1 Number of falls on the same level at the Danish labor market 2016-2021. Numbers from the Danish Working Environment Authority [1].

Similar statistics are present in other western countries such as Finland, Norway, USA and Canada [4]–[7], which makes STF a global health problem.

Slipping is caused by insufficient friction between footwear and surface, whereas trips are caused when the foot is interrupted by an object or edge. Thus, falls can be caused by either slipping or tripping (see Figure 2).

Figure 2 Slips, Trips and Falls.

Slipping is commonly acknowledged as the major contributor to falls [8], why slipping is also the focus of this PhD thesis.

The friction properties between footwear and surface are crucial to avoid slipping and have long been recognised as direct risk factors for slip accidents [9]. The importance of these friction properties is also highlighted by recent enhanced friction requirements for certified slip resistant footwear by ASTM international [10].

The friction properties between footwear and surface are a multi-factorial challenge and are influenced by factors related to the footwear, surface, contaminants and human factors (Figure 3) and interact in a complex manner [11]. Hence, to study the factors presented in Figure 3, should all ideally be isolated, controlled and accommodated.

Figure 3 Factors affecting slip resistance.

Contaminants and, to some extent, surfaces are determined by the environment and can be difficult to manipulate. Contaminants are given by a specific industry, such as e.g. food industries, off shore industries, medical industries or outdoor pavements. Hence, contaminants such as rain water/sea water, soap, food scraps, frying oil, snow/ice etc. may be present and are determined by the industry/operating environment. Nonetheless, surfaces can be altered to accommodate slip resistance with various contaminants being present. E.g. by changing the surface topography [12]. However, some branches require high levels of hygiene standards, which limit the ability to alter surface topography [13]. Hence, the footwear counterpart should ideally be altered to accommodate slip resistance, with specific surfaces and contaminants present. Therefore, the focus of this research is limited to footwear parameters. Hence, industry standard surfaces and contaminants will be applied.

In relation to human factors (Figure 3), recommendations suggest that footwear slip resistance testing devices should replicate biomechanically relevant loading conditions and thus obtain more realistic slip resistance measurements [14]. These loading conditions are, for mechanical testing devices, referred to as biofidelic [15]. The reason why these loading conditions should be met can be attributed to the

complex friction properties of footwear outsoles. Footwear outsoles are often constructed of viscoelastic elastomer materials, which friction properties are dependent on, e.g. temperature, contact time, normal load and sliding velocity [16]. Thus, testing devices should ideally be simulating real slipping events in realistic environments under biofidelic loading conditions [14].

It is imperative to study the individual footwear parameters separately [17] [18]. This is, however, rarely seen in published scientific literature due to researchers' inability to manufacture a whole piece of footwear where only one parameter is changed at a time. Hence, individual parameters are often studied in more fundamental elastomer friction [19]–[21]. These kinds of studies provide an important and general understanding of the frictional behaviour of elastomers. Studies with whole footwear samples for commercial use [18] and prototypes [22] have also been performed. However, footwear used in scientific investigations are often prototypes and are expected to undergo substantial alterations in the ramp up process before serial production. Therefore, isolating individual parameters for production ready footwear is challenging. Hence, application-oriented studies of footwear slip resistance rely on contribution from footwear manufactures to construct actual footwear and controlling for individual factors. This project aims at contributing to both friction research of elastomer blocks and applied research within footwear slip resistance.

The following goals for this PhD thesis in relation to friction research of elastomer blocks and footwear slip resistance research were:

1. Develop test methodologies to qualify and quantify friction properties between footwear and surfaces under realistic biomechanical conditions.
2. Investigate the friction properties of elastomer block materials based on material characterization.
3. Investigate footwear slip resistance in relation to material and design properties.

The research questions were answered via five separate studies, which formed the PhD thesis as illustrated in Figure 4. The studies assessed contribution to either friction research of elastomer blocks or footwear application-oriented slipping research are illustrated in Figure 5.

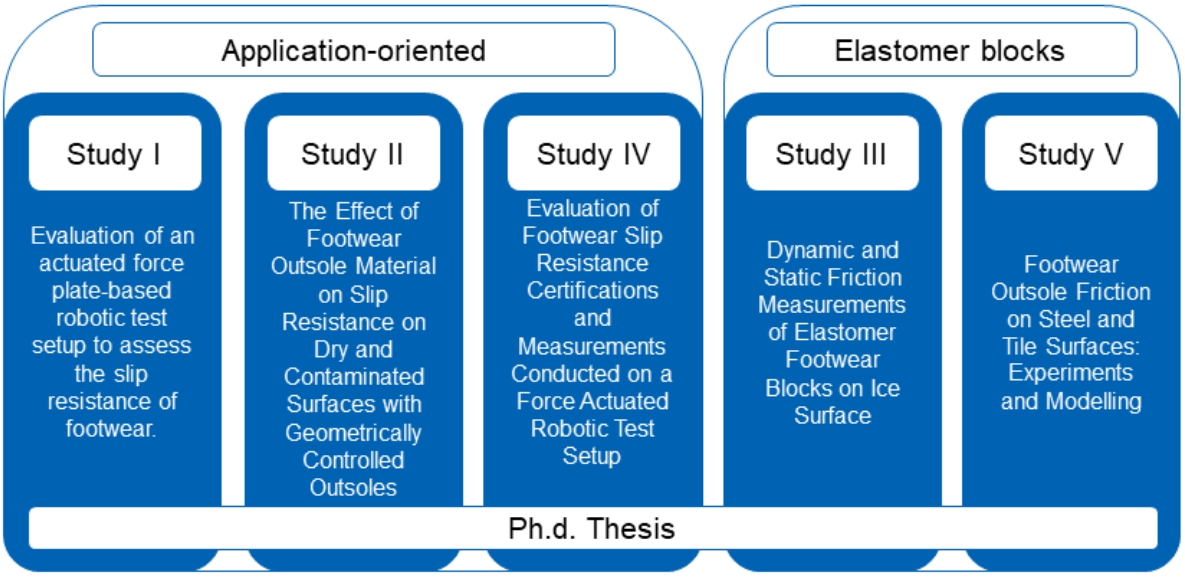

Figure 4 PhD thesis consolidating the studies (I – V).

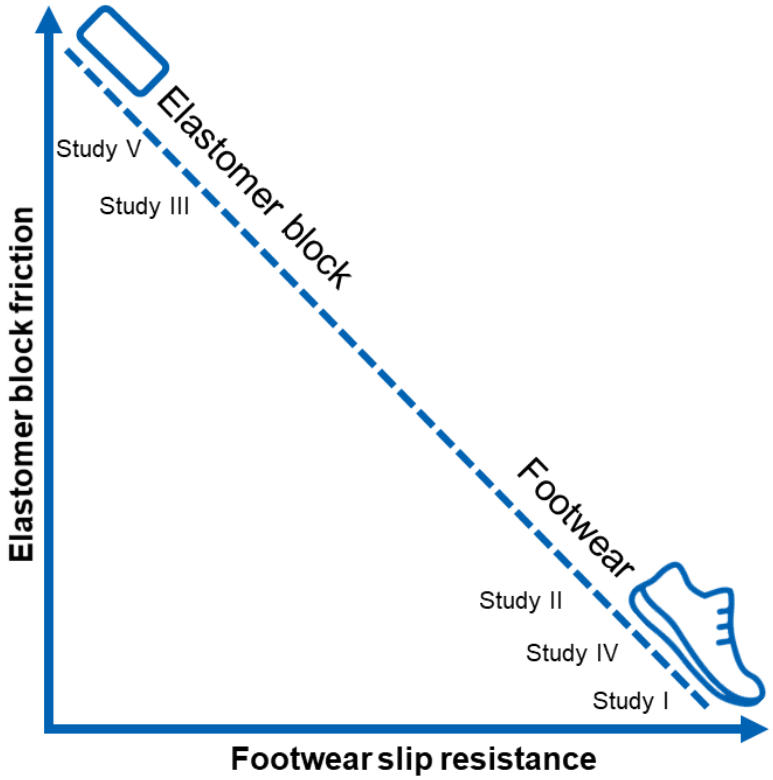

Figure 5 Relationship between elastomer block friction research and applied research of footwear slip resistance for the five individual studies.

Study I was related to the first research question and presented a device for conducting footwear slip resistance measurements and reported on the usability of the device. Study II was related to the third research question and focused on the impact of outsole materials on slip resistance, when controlling for outsole geometry. Study III dealt with the second research question, where the effect of material choice on ice surface was studied and related to material properties. Study IV was focused on research question three and evaluated the slip resistance of commercial available footwear models and related the outsoles design and material properties to the slip resistance performance. Study V was also centered on research question two and used an experimental and theoretical approach to evaluate the friction properties of outsole materials.

The five studies were to some extent conducted chronologically for practical reasons. Study I was necessary to proceed with Studies II and IV, since the device developed in Study I was used in Study II and IV. Studies III and V were independent of the three other studies and were conducted in parallel. For eased readability, the method, result and discussion sections are divided into research of elastomer block friction and application-oriented research. Hence, elastomer block friction research refers to square outsole elastomer elements, whereas application-oriented research refers to slip resistance research of footwear.

1.2. HUMAN FACTORS/ERGONOMICS

To accommodate the first goal of this PhD thesis in relation to developing test methodologies to quantify the friction properties between footwear and surfaces, it is crucial to understand the human factors related to slipping. Grönqvist and colleagues described safe walking as a dynamic interplay between the human sensory systems and the footwear/surface friction mechanism during walking [23]. The latter is the focus in this thesis and thus the biomechanical loading conditions between footwear and surface were taken into account, during the development of a footwear slip resistance test setup. Hence, the biomechanics of slipping and measurement of slipping will be briefly explained in the following.

A human gait cycle consists of various phases [24]. Nonetheless, in relation to slipping, an important phase of a normal gait cycle is the heel-strike and toe off [25]. The heel strike (illustrated in Figure 6) is the initial contact with the ground, where the foot is normally placed in front of the body, which results in an angled ground reaction force (GRF). The toe off phase is the end of a step, with the foot placed behind the body, which also results in an angled GRF, however in the opposite direction. Ultimately, this angled GRF causes a shear/friction force between footwear and surface. Hence, longer steps usually cause greater friction force between footwear and surface, compared to shorter steps [26]. In addition, when walking subjects anticipate slippery surfaces, the step length shortens [27], and therefore they unconsciously reduce the friction force between footwear and surface.

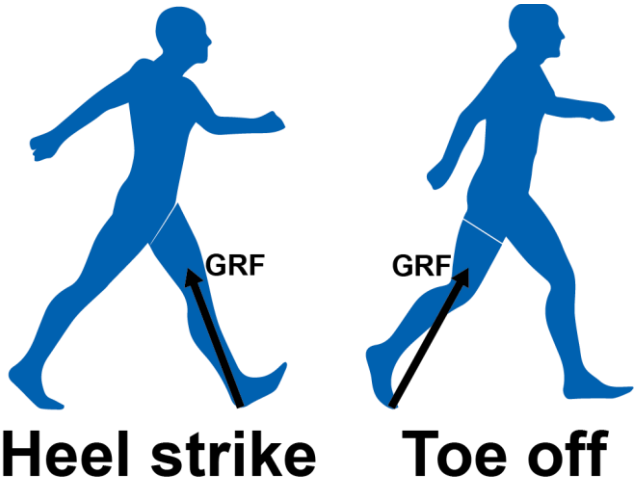

Figure 6 Heel strike and toe off with ground reaction forces (GFR) from a human gait cycle.

The required coefficient of friction (RCOF) for safe walking is a complex matter and is affected by human factors, thus disagreement between friction measurements with walking subjects and devices for determining the available coefficient of friction (ACOF) exists [28]. Due to this, it is important to replicate realistic conditions from real slipping events when designing/using ACOF devices to determine footwear slip resistance. These conditions are e.g. sliding velocity, normal load, static contact time, footwear/surface contact angle, surfaces and contaminants. To accommodate realistic measurements, the "ISO 13287:2019 - Personal protective equipment – Footwear – Test method for slip resistance" was established [29] (the specifications for ISO 13287 are elaborated in 2.2.1). In addition, commercially available test devices, such as the STM 603 (Satra Technology, Kettering, Great Britain) and the DW9530 (Fanyuan Instrument, Hefei, China) can operate in accordance with the ISO 13287. However, whether the testing parameters used in the ISO 13287 are replicating slipping events are debated [30], [31]. In academic context, various ACOF testing devices have been developed and are either portable or laboratory based [14], [32]–[35].

These devices determine either the dynamic coefficient of friction (DCOF) or the static coefficient of friction (SCOF) and are used as measures for the friction properties between footwear and surface. The SCOF is the coefficient of friction (COF) right at the time when the shoe starts moving relative to the surface. The DCOF is the relationship between the acting forces when the footwear moves relative to the surface and is calculated as an average over a time period. The COF is calculated by dividing the horizontal reaction forces (friction forces (F_x & F_y)) with the vertical reaction force (normal force (F_z)) as in equation 1.

$$\mathrm{COF} = \sqrt{\frac{F_x^2 + F_y^2}{F_z^2}} \qquad 1$$

Whether the SCOF or DCOF is the most important frictional measure for preventing slipping is controversial [9], [36]. It is argued that a high SCOF can prevent a slip initiation when a surface is

known/expected to be slippery, since walking subjects tend to reduce their heel velocity when anticipating slippery floors [27]. However, the magnitude of the DCOF is previously found related to the probability of slipping [15], [28], [37]. In relation to this thesis, the DCOF is quantified in all the studies, whereas the SCOF is also quantified in Study III.

1.3. FOOTWEAR FRICTION

1.3.1. FOOTWEAR PROPERTIES AFFECTING SLIP RESISTANCE

As mentioned previously, this PhD thesis was limited to footwear parameters affecting the slip resistance. More specific the outsole materials and the material characterization. Numerous of other footwear parameters also affect the slip resistance, such as e.g. thread patterns [22], [38]–[41], wear state [42]–[44], foam thickness [21] and heel shape [45]. In relation to outsole materials, previous research has revealed that microcellular polyurethane is a slip resistant outsole material on wet and oily surfaces [46]–[48]. In addition, outsole hardness also affects the slip resistance, with softer outsoles being more slip resistant [18], [49], [50]. Nonetheless, outsoles are often constructed of viscoelastic elastomers with complex material properties, and the static hardness measurement does not provide a comprehensive characterization.

1.3.2. ELASTOMER FRICTION

Strandberg pointed out that the friction mechanism between footwear and surface under wet conditions is similar to the friction mechanism between a rolling pneumatic tyre on a wet roadway [51]. He used the squeeze-film contact theory developed by Moore [52] and asserted that the foot rotates around the heel during heel strike (see Figure 6) in the stance phase of walking. This concept was also discussed by Grönqvist [50] and illustrated the theory by Moore. Figure 7 illustrates the squeeze-film concept adapted to a footwear/surface contact mechanism.

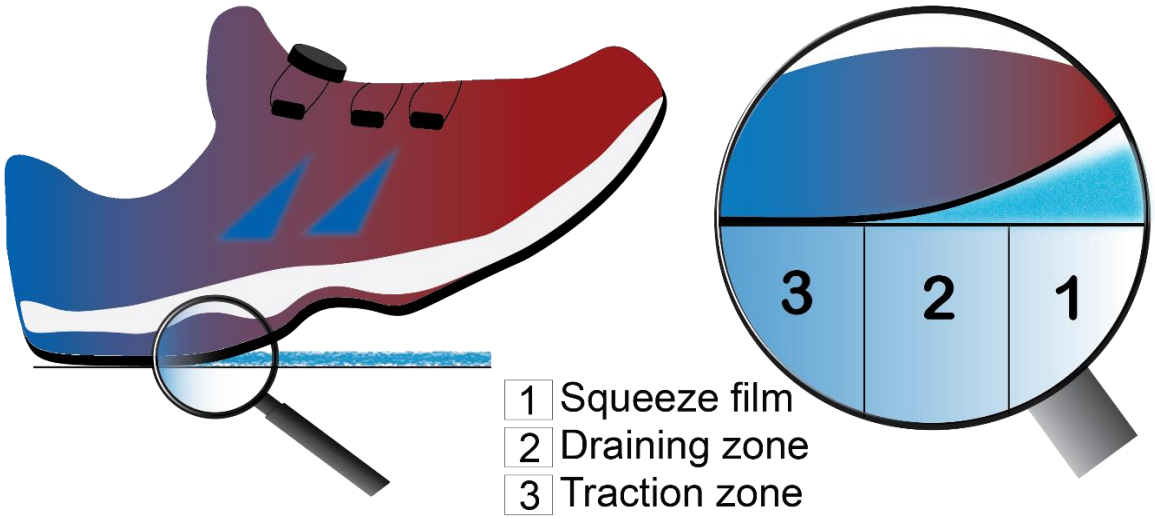

Figure 7 Squeeze-film theory adapted from [50], [52].

In addition to the squeeze-film process, Strandberg [51] mentioned the importance of the viscoelastic/hysteresis component and the adhesive component of footwear friction. The adhesive component is defined as the shearing of real contact area [53], whereas the viscoelastic component is the internal friction of the elastomer when sliding over surface asperities [16]. Under contaminated conditions and when sliding on rough surfaces, the viscoelastic component is found to be the most important component [48]. However, the viscoelastic properties of elastomers are complex and are dependent on load, load frequency, sliding velocity and temperature [16].

The viscoelastic properties of elastomers can be quantified with an apparatus named dynamic mechanical analysis (DMA) (also referred to as dynamic mechanical termal analysis (DMTA)). A typical DMA test setup is illustrated in Figure 8). Here an elastomer specimen is subjected to either tensile or shear deformation over a few decades of frequencies at various temperatures.

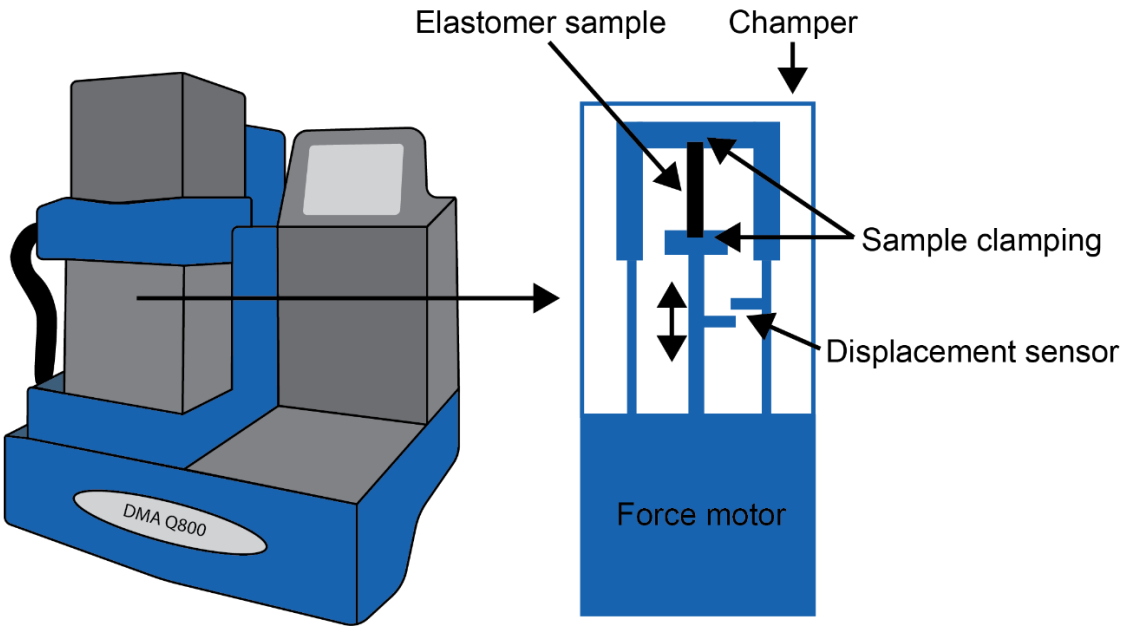

Figure 8 Left: Simplified illustration of a DMA test setup. Illustrations adapted from [54].

Elastomers are in general soft at high temperatures and under low load frequencies. In contrast, under low temperatures and high load frequencies they become hard [55]. The elastic modulus (E'/G') is a measure of the energy stored inside the material and the material elasticity. The loss modulus (E''/G'') represents the materials ability to damp and lose energy. The relation between the loss modulus and the storage modulus is called the loss factor (tan(δ)), hence tan(δ) = loss modulus/storage modulus. A high hysteresis friction component is expected at the peak, where the loss factor is at its maximum [56]. A plot of the DMA derivatives (storage modulus and loss factor) is found in Figure 9.

The DMA analysis tool has found its way into developing/optimizing skid resistance for rubber compounds for pneumatic tires [53], [57], [58]. However, it is sparsely seen in relation to optimizing slip resistance of footwear outsoles [19], [41], [59] and is therefore considered as novel in relation to footwear slip resistance. This method is used to characterize elastomers and discussed in relation to elastomer friction in Study III and V. The specific method for obtaining the DMA measurements are described in the method section 2.1. Throughout this thesis, three outsole materials namely; polyurethane (PU), thermoplastic polyurethane (TPU) and vulcanized rubber (RU) are studied and characterized.

MATERIALS AND METHODS

This chapter summarises and combines the essence of the method chapters from Studies I to V. Hence, a brief explanation of the different methods and approaches are described to provide the reader with a general understanding, necessary to proceed with the following result and discussion chapters.

2.1. METHODS – ELASTOMER BLOCK FRICTION RESEARCH

The friction properties of the three outsole elastomer materials (RU, PU and TPU), constructed as blocks were studied in Study III & Study V. Friction experiments were conducted with established tribometers presented in previous studies [60], [61]. Figure 10 illustrates the three materials as square elastomer blocks. Friction experiments were conducted on ice surface in Study III and on a steel and tile surface in Study V (the same steel and tile surfaces as in Study I, II and IV). Furthermore, the materials were characterized with hardness measurements, DMA and surface energy measurements.

The three materials represent a different and specific outsole manufacturing process, namely: low pressure injection of polyurethane (PU), injection moulding of a thermoplastic polyurethane (TPU) and vulcanized rubber (RU). The PU material has a porous core structure with air pockets, whereas the TPU and RU have a more dense core. The RU material is crosslinked by strong adhesive bonds, which means that RU decomposes by pyrolysis at high temperatures. PU and TPU melt.

The materials had a short term (< 10 s) shore A hardness of; PU = 56, TPU = 80 and RU = 68. Dynamic material properties were characterized with DMA using the time-temperature superposition (TTS) principle [54]. 8 mm samples of the three materials were cooled to -130 °C and a thermogram was measured from -130 °C to ~ 300 °C at 1 Hz and 2 °C/min. Frequency sweeps from 10 to 0,1 Hz were done at selected temperatures. TTS master curves were constructed with 23 °C as the reference temperature and are illustrated in Figure 9. The DMA measurements where used in both Study III and V and discussed in relation to friction properties.

Material surface roughness and topography were measured with a non-destructive elastomeric 3D imaging system and is presented in Figure 10. The hydrophobicity/wettability of the three materials were identified via surface energy measurements and performed with a Krüss Mobile Surface Analyser (Flexible Liquid) with distilled water (MilliPore) and diiodomethane (Merck). Due to the high density of diiodomethane (3.32 g/cm3) drops of 1 µL were deposited while for water, 1.5 µL drops were analysed. Five measurements were collected per sample and liquid. The surface free energy (SFE) of the elastomers was calculated with the Owens-Wendt-Rabel-Kaelble model by the Krüss ADVANCE software, yielding the total surface free energy (SFE^{tot}) as well as the dispersive and polar contributions. The surface energy properties are presented in

Table 1 [62].

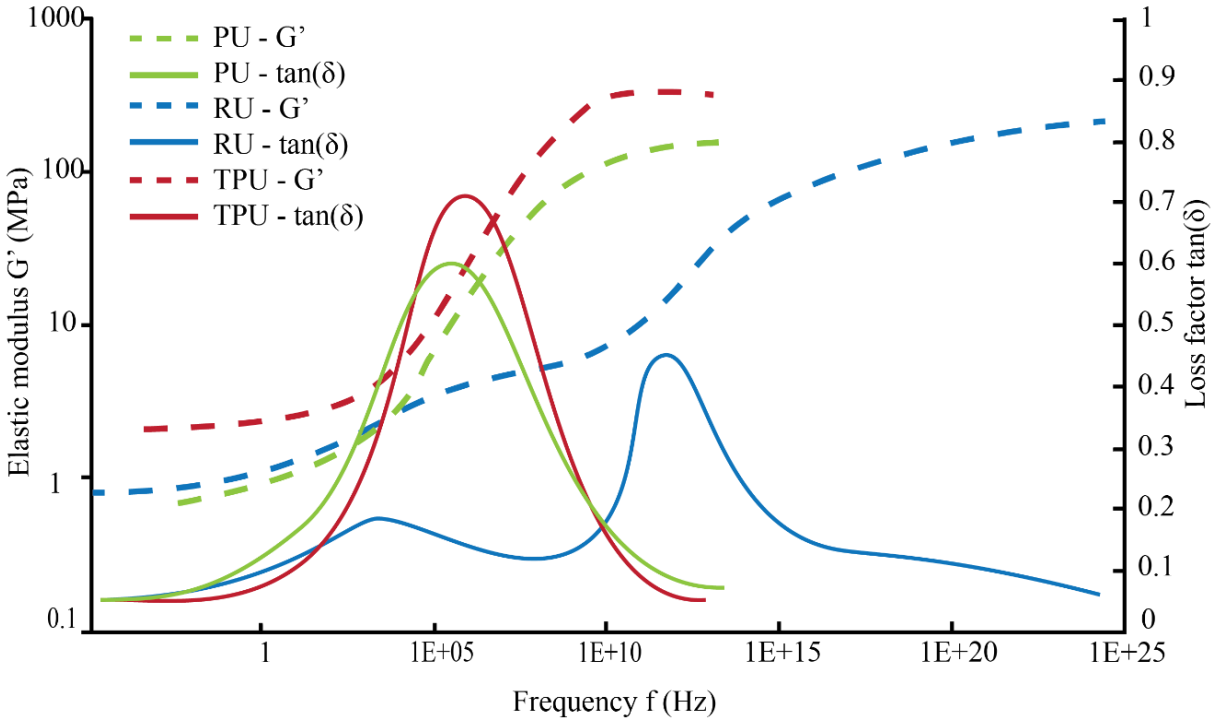

Figure 9 Master curves for the three materials obtained with Dynamic Mechanical Analysis (T 23 °C). Reused with permission from Study III [62].

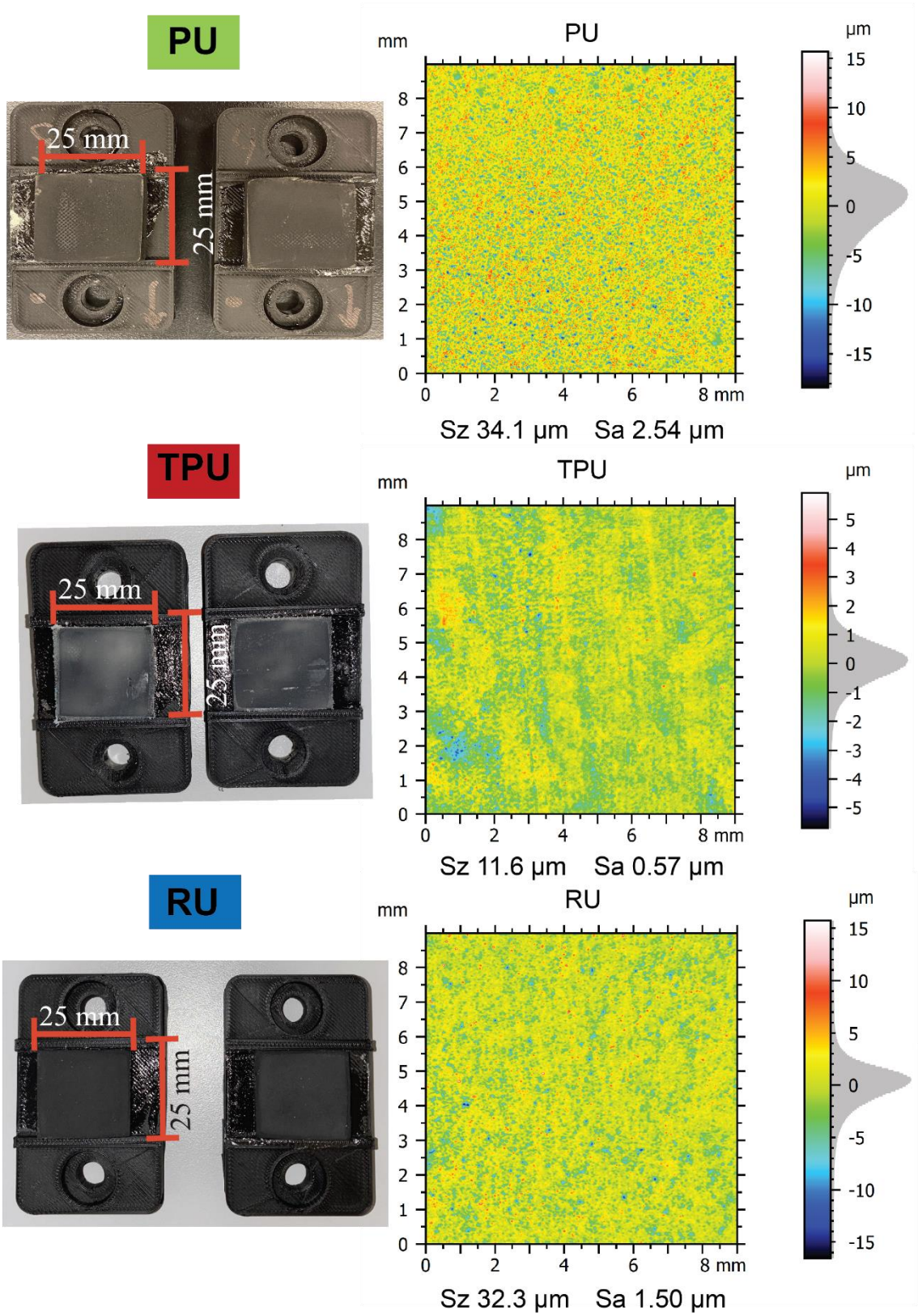

Figure 10 Visual appearance of the three elastomer material blocks. Reused with permission from Study III [62].

Table 1 Surface energy measurements. CA(H_2O) = contact angle with distilled water; CA(CH_2Cl_2) = contact angle with diiodomethane; SFE_{tot} = total surface free energy; P/D ratio = polar/dispersive ratio. Reused with permission from Study III [62].

Sample	CA(H_2O) [°]	CA(CH_2Cl_2) [°]	SFE^{tot} [mN/m]	P/D ratio
PU	97.39 ± 0.67	91.96 ± 2.05	16.65 ± 1.33	0.41
TPU	94.99 ± 0.07	54.46 ± 1.05	32.70 ± 0.67	0.03
RU	109.19 ± 0.18	91.24 ± 0.56	13.46 ± 0.31	0.11

2.1.1. SURFACES CHARACTERIZATION

Two surfaces were used throughout all friction experiments in Study I, II, IV and V: A ceramic tile (Eurotile 2 specified in ISO 13287:2019 Footwear – test method for slip resistance) with a roughness of 20.00 µm (Cut-off length of 2.5 mm) and a steel plate (number 1.4301) with a roughness of 1.65 µm (Cut-off length of 0.25 mm). From the roughness measurements the surface power spectra (Figure 11) was calculated as described elsewhere [55], [63]. The power spectra is useful to chareterize self-similar fractal surfaces, which have the same topography despite the magnification. All the information about the surface is contained in the power spectrum and is used as an input parameter for roughness in the rubber friction theory [16] used for calculating the viscoelastic contribution to friction. Basically, the surface profile is decomposed to its base frequency contents, using a Fast Fourier transform (FFT) algorithm. Hence, the power spectra data was used in Study V as input data for calculating the viscoelastic contribution to the friction.

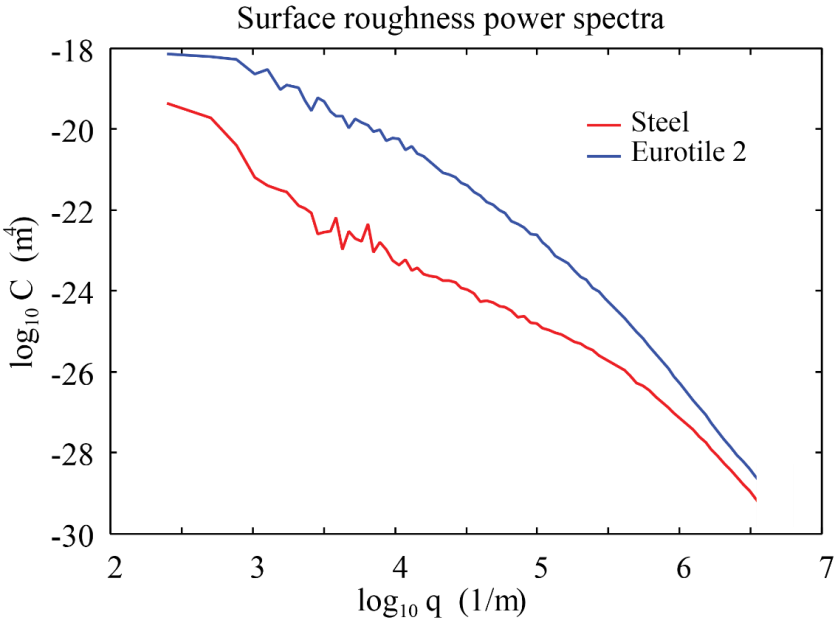

Figure 11 The surface roughness power spectra of the steel surface and the tile surface as a function of the wavenumber (log-log scale).

In study III friction measurements were conducted on ice surface, and the surface topography is plotted as a heat map in Figure 12, illustrating the ice surface roughness profile for one sliding track at 0 °C and -10 °C before and after friction measurements [62]. The surface roughness measurements were conducted with the same non-destructive elastomeric 3D as described in section 2.1. The effect of surface roughness at different ice temperatures was used to explain/discuss the friction measurements in Study III.

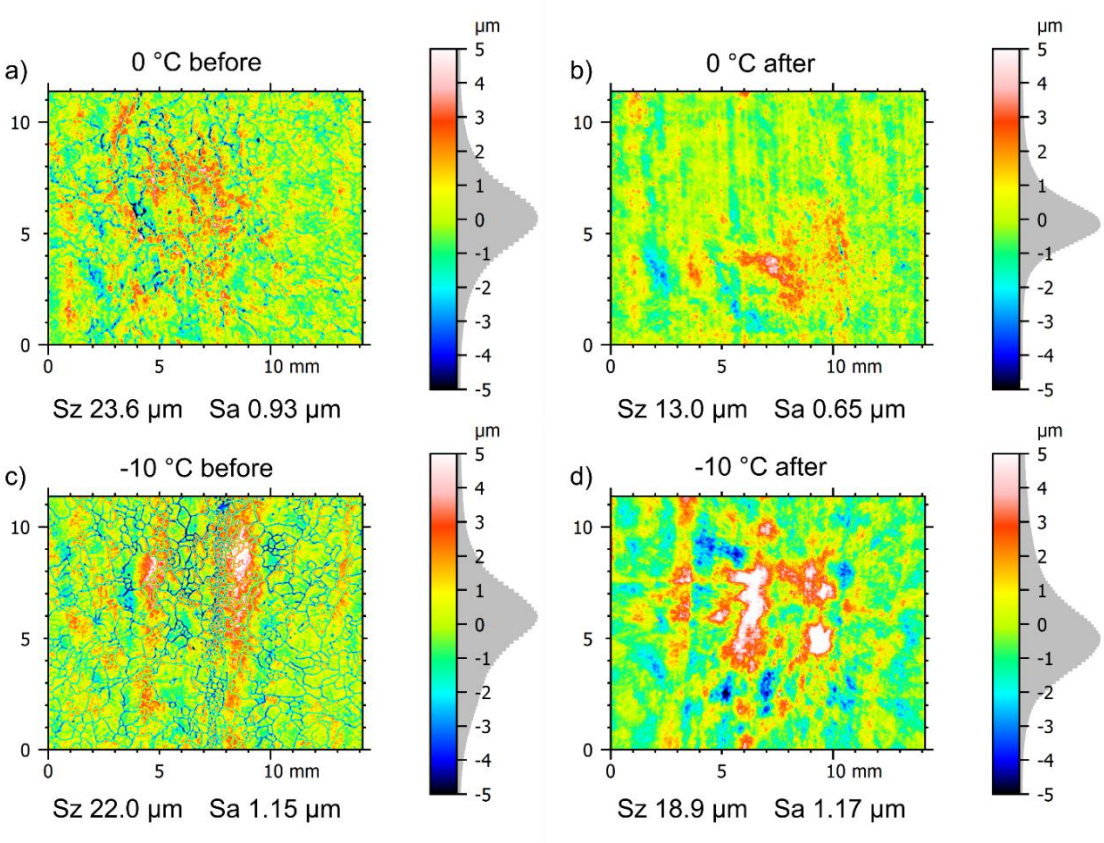

Figure 12 Topography GelSight images at the same approximate location of one ice track (TPU) surface at 0 °C and -10 °C before and after friction measurements (n = 40). The image size is 14 * 12 mm, where the forward sliding direction in the images is vertically upwards. Reused with permission from Study III [62].

2.1.2. ELASTOMER FRICTION ON ICE

In Study III friction experiments of the three elastomer blocks were conducted on an ice surface under four different ambient temperatures (-10, -5, -2 and 0 °C). A linear tribometer [60] with a custom-made trajectory program (see Figure 13 top) was used to quantify the SCOF and DCOF. 500 N normal force was applied in the middle of the material blocks, giving a contact pressure of 0.8 MPa. Friction measurements were performed with six different sliding velocities (0.3, 1, 2, 3, 4, 5 m/s) in a randomized order, for each temperature.

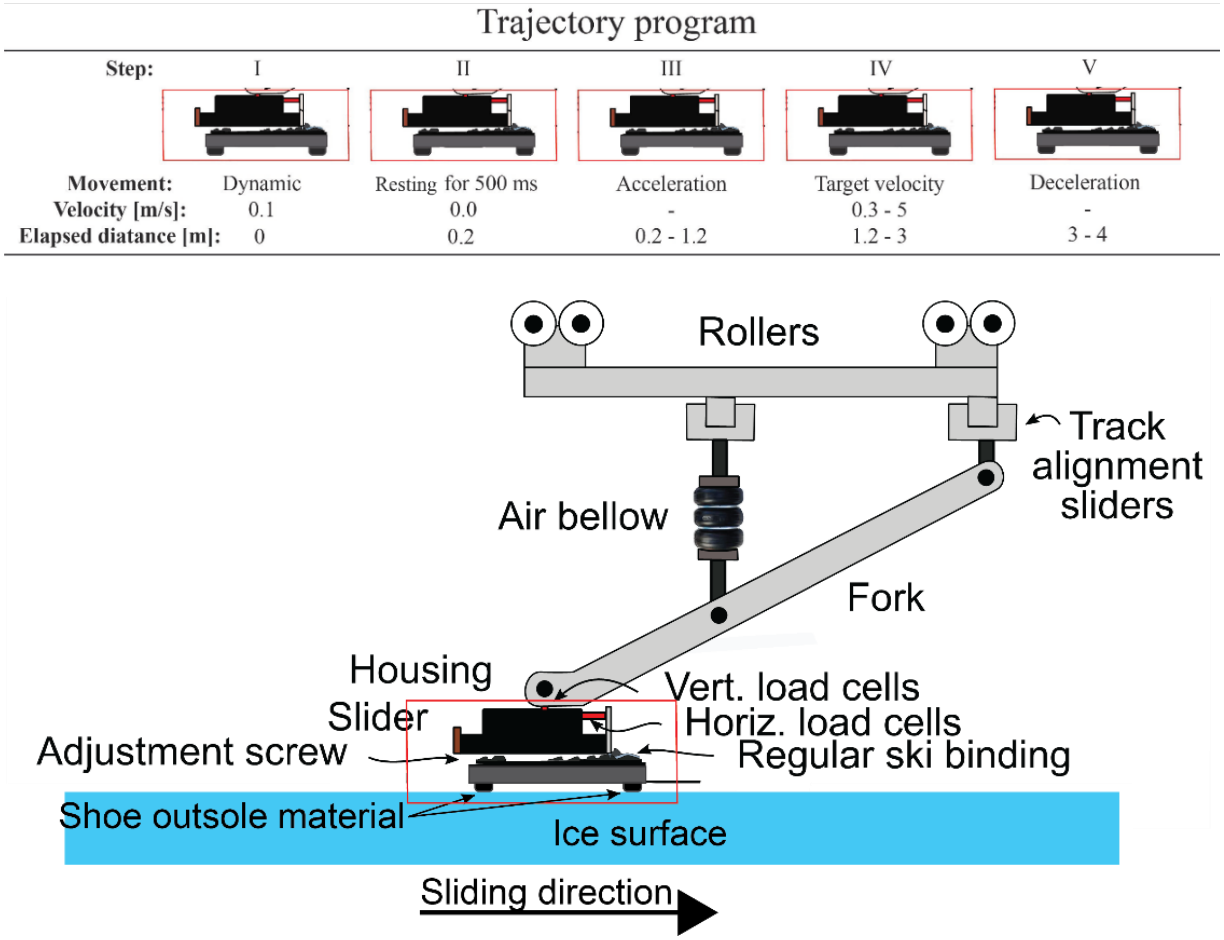

Figure 13 Top: Trajectory program for the tribometer. I. Slow dynamic sliding (0.1 m/s for 20 cm), II. Resting (500 ms), III. Acceleration, IV. Target-sliding velocity (alteration of the six different sliding velocities), V. Deceleration. Bottom: Illustration of the linear tribometer with shoe outsole material specimen sliding on ice surface. Reused with permission from Study III [62].

2.1.3. ELASTOMER FRICTION ON DRY SURFACES

In Study V friction experiments of the three elastomer blocks were conducted on the tile and steel surfaces in a dry state, with a tribometer [64] (Figure 14 A) with reciprocal sliding velocities ranging from 1 µm/s to 10 mm/s. Additional friction experiments were conducted with a pin-on-disk tribometer [65] (Figure 14 B) with the steel surface, during constant sliding velocities of 30 cm/s, 100 cm/s and 240 cm/s for approx. 1 s. For both tribometer setups, a normal pressure of 0.5 MPa was used.

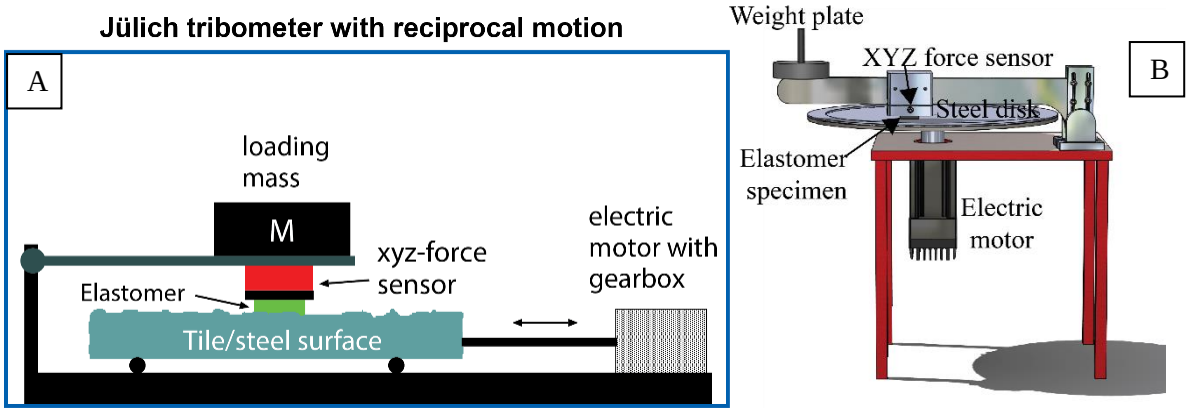

Figure 14 (A): Schematic illustration of the tribometer from Jülich with reciprocal motion [64]. (B): Illustration of the large-scale pin-on-disk tribosystem for elstomer ACOF measurements [65].

The viscoelastic contribution to friction was calculated (estimated), using the rubber friction theory developed and described elsewhere [16]. The rubber friction theory uses the power spectra (Figure 11) and the elastic modulus, obtaind with the DMA (Figure 9) to calculate the viscoelastic friction contribution for three outsole materials. In this thesis, the rubber friction theory was used as a part of Study V, as an externally provided tool for calculating the aforementioned viscoelastic friction contribution. The rubber friction theory is not the focus of this thesis and will not be described further. The reader is refered to [16] for exaborated explanation.

2.2. METHODS - APPLICATION-ORIENTED RESEARCH OF FOOTWEAR SLIP RESISTANCE

2.2.1. DEVELOPMENT OF A FOOTWEAR SLIP RESISTANCE TEST SETUP.

A test setup with a large degree of flexibility, able to accommodate various testing conditions and parameters was desired. Specifically, it should accommodate the device requirements presented by Chang and colleagues[14], based on biomechanics of slipping [66]. They proposed a list of requirements for mechanical slip resistance devices, which should be considered for most valid ACOF measurements [14]. These are as follows:

1. *Normal force build-up rate should be at least 10 kN s^{-1} for whole-shoe devices.*
2. *Normal contact pressure should be between 200 and 1000 kPa.*
3. *Sliding velocity at the interface should be between zero and 1.0 m s^{-1}. (Static tests would tend to have velocities near zero, while dynamic tests would tend to have velocities closer to the upper bound.)*
4. *Maximum time of contact prior to and during the COF computation should be 600 ms.*

In addition, the system should accommodate the European standard for measuring slip resistance (ISO 13287: 2019 Personal protective equipment — Footwear — Test method for slip resistance) [29], which is widely accepted in the footwear industry. The ISO 13287 has the following requirements for mechanical slip resistance devices:

1. *Normal force 400–500 ±25 N*
2. *Accuracy of device for friction measurement of 2% or better*
3. *Sliding velocity of 0.30 ±0.03 m/s*
4. *Static contact time between initial contact and start of movement of ≤1.0 s.*
5. *Measurement period shall start within 0.3 s of achieving the full normal force and end 0.6 s after start of movement*
6. *Shoe contact angle at 0 and 7.0 ± 0.5*
7. *Measurement period shall start within 0.3 s of achieving the full normal force*
8. *Able to include wet contaminants*
9. *Able to apply tile (Eurotile 2) and steel surface (Rz between 1.6 μm and 2.5 μm)*

To meet these requirements, a force plate was instrumented atop of a robotic hydraulic platform (Aalborg University, Aalborg, Denmark) as illustrated in Figure 15-Top. The test setup is a steel frame fixed with a shoe and last above a force plate. The last was fixed directly under linear bearings, with a vertical lead. This enabled movement in the vertical direction. Normal load is simply applied to the vertical lead with standard weight plates.

The platform movement trajectory is illustrated in Figure 15-Bottom. At event 1. no external force acts on the force plate. At event 2., the platform moves upwards in the vertical direction and initial contact between shoe and surface is reached. At event 3., the shoe is resting statically on the surface (i.e., full normal load reached). At event 4., the platform starts moving in the horizontal direction (from forefoot to heel) with a constant velocity. The DCOF measurement period starts at event 5. and ends at event 6. and is calculated based on equation 1. The horizontal movement ends at event 7. and is static in event 8. In event 9., the robotic platform moves horizontally (heel to forefoot) to prevent overshooting of the hydraulic rams and moves back towards the starting point. All events can be altered. Hence, it is possible to adjust sliding velocity, static contact time and sliding distance. The robotic test setup was evaluated in relation to ISO 13287, and an extended description and complete evaluation of the test setup is presented in Study I [67].

Three types of contaminants were used: A glycerine solution (85% glycerol and 15% water by volume solution with a viscosity of 110cP at 20 °C) in Study I, II and IV, canola oil (65cP at 20 °C) in Study I

and II and a detergent solution containing a mass fraction of 0.5% sodium lauryl sulfate (SLS) in demineralized water in Study IV.

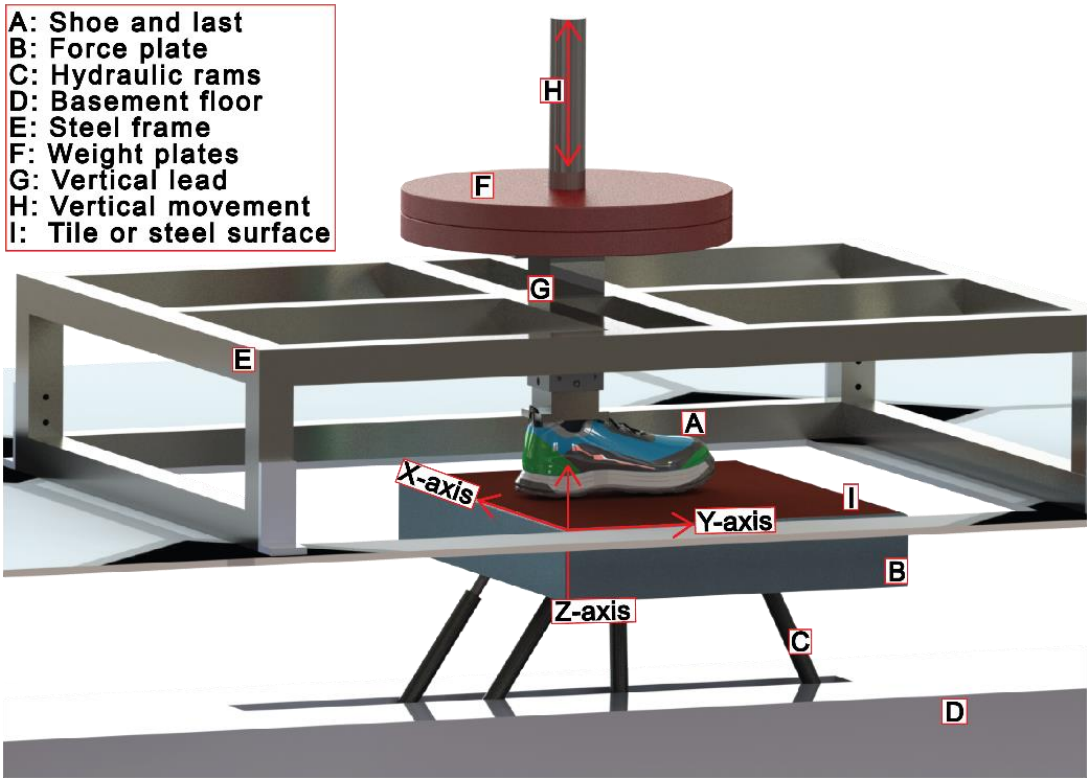

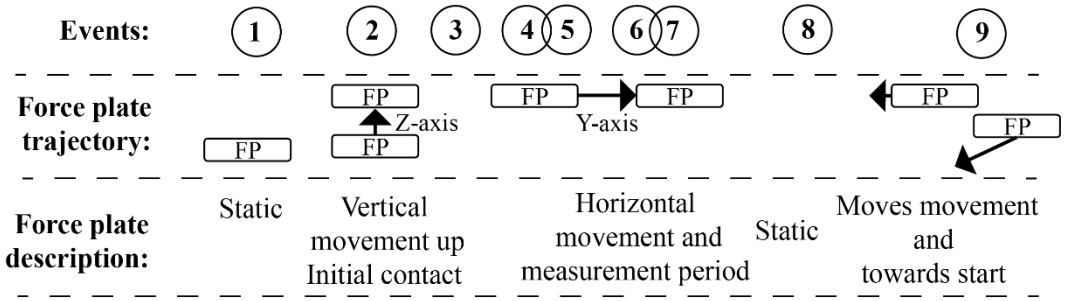

1 Force plate is static
2 Force plate moves up / initial contact
3 Full normal load is reached
4 Force plate horizontal movement starts
5 Friction measurement period starts
6 Friction measurement period ends
7 Force plate horizontal movement ends
8 Force plate is static
9 Force plate moves down and contact ceases

Figure 15 Top: Illustration of the force actuated robotic test setup. Bottom: Description of platform movement cycle. Reused with permission from Study I [67].

2.2.2. STUDIYNG FOOTWEAR SLIP RESISTANCE

The force actuated robotic test setup, from Study I [67], was used to study the friction properties of whole footwear samples in relation to test specifications in accordance with the ISO 13287 in Studies II and IV and with biofidelic optimized parameters in Study IV.

The effect of footwear outsole materials on slip resistance on dry and contaminated surfaces with geometrically controlled outsoles was under the scope in Study II. Here the aim was to compare slip resistance of geometrically identical shoes with varying outsole materials. Three Ecco Xpedition III (Ecco shoes A/S, Bredebro, Denmark) shoes were constructed of PU, TPU and RU. The shoes were tested for DCOF. Testing parameters and surface properties corresponded to the specifications of the ISO 13287 [29]. The testing mode and the footwear samples are illustrated in Figure 16. Ecco had no role in the data analysis and discussion.

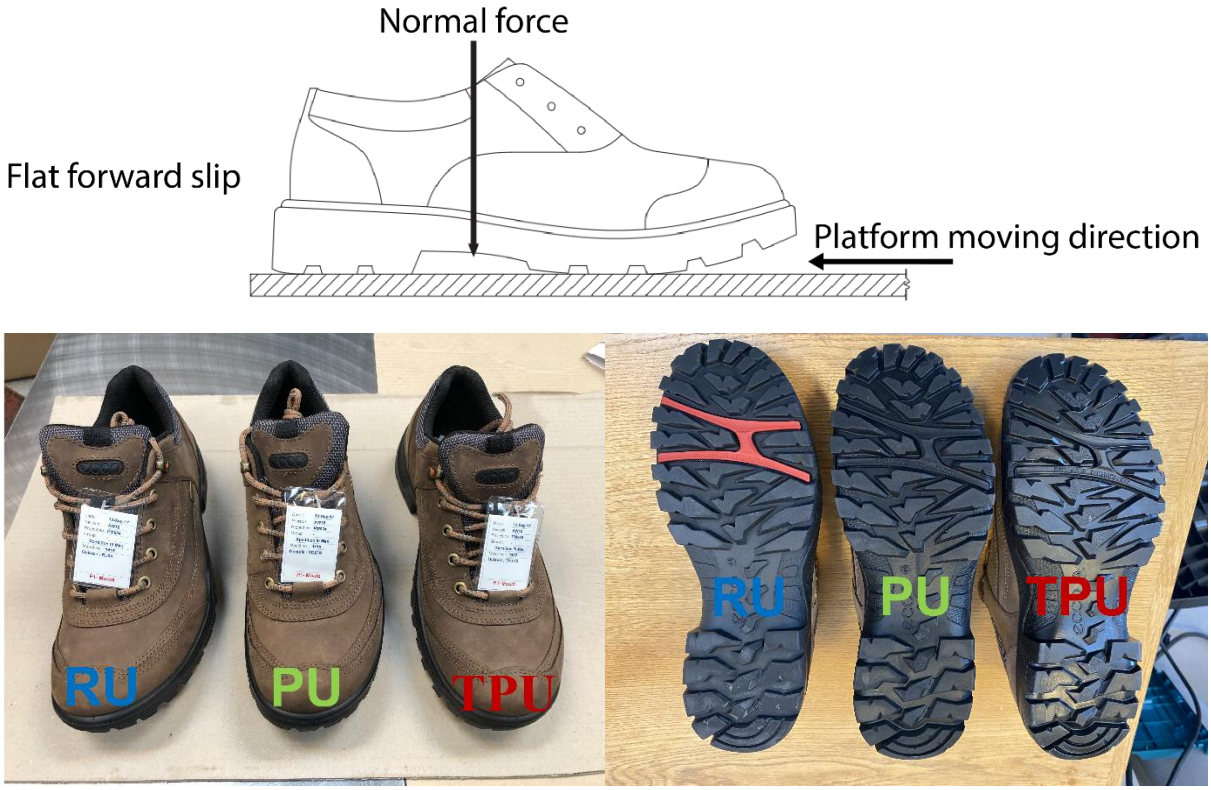

Figure 16 Top: Testing mode: flat forward. Adapted from ISO 13287 with permission from Danish Standards (ISO 13287, 2019). Bottom: Footwear constructed of RU (left – note the red part in the forefoot is also RU), PU (middle) and TPU (right). Reused with permission from Study II [68].

In addition, the force actuated robotic test setup [67] was used for comparison of mechanical friction evaluations from occupational footwear certified as slip resistant in Study IV. The aim was to compare slip resistance certification data from five slip resistance certified shoes (see Figure 17 bottom), with measurements performed on the force actuated robotic test setup [67] in accordance with the ISO 13287 standard [29]. A secondary goal was to determine their performance in a biofidelic setup (see Figure 17 top), which argubly resembles the biomechanics of slipping better. SIKA (SIKA Footwear A/S, Ikast, Denmark) provided the five shoes certified as slip resistant in accordance with the ISO 13287 standard and external certification data. SIKA had no role in the data analysis and discussion.

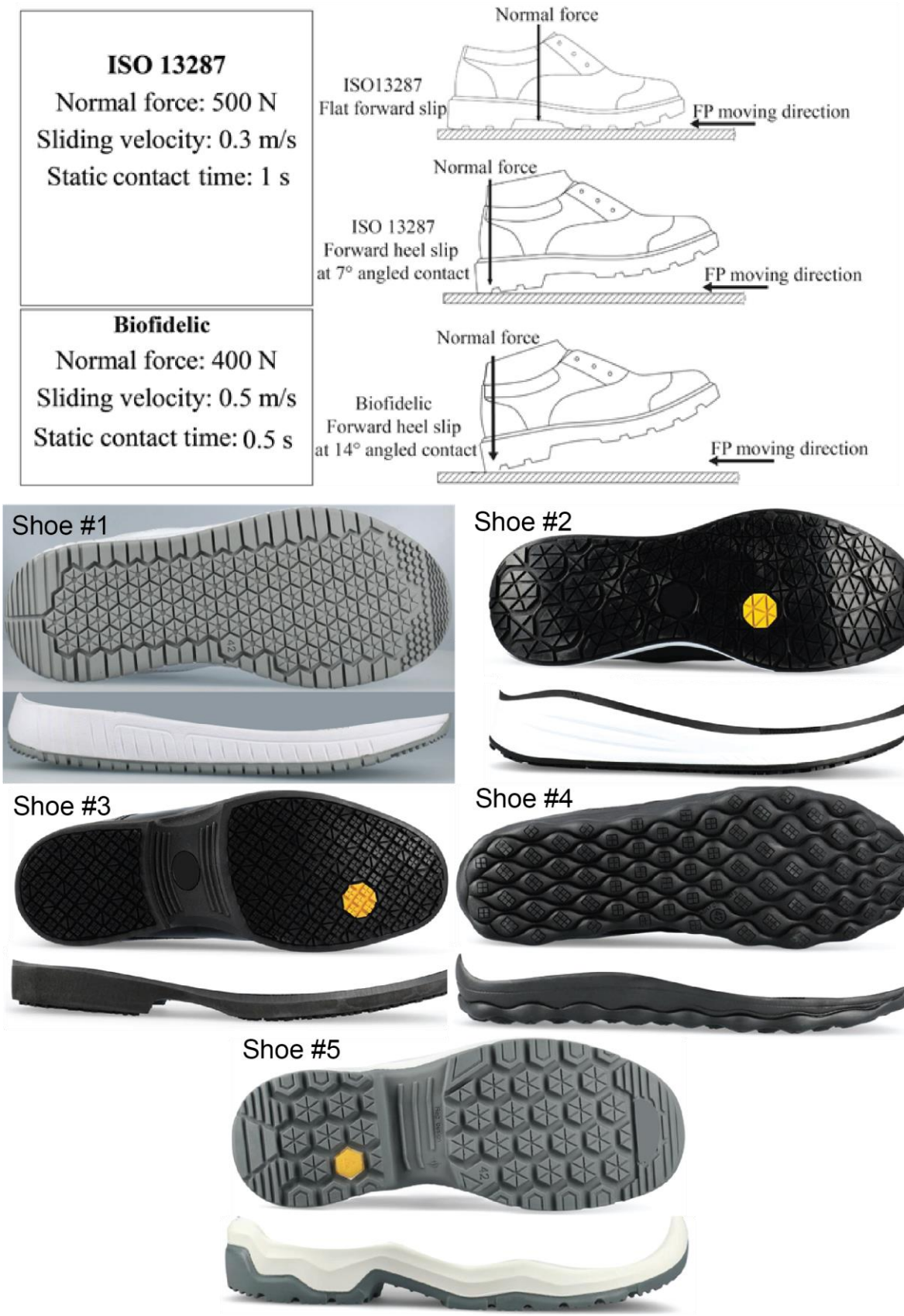

Figure 17 Top: Testing modes in accordance the ISO 13287 test standard and testing mode optimized for biofidelic parameters. Adapted from [69] with permission from Danish Standards (ISO 13287:2019). Buttom: Shoes outsole and profile view of the five occupational footwear certified as slip resistant. From Study IV.

RESULTS

3.1. RESULTS – ELASTOMER BLOCK FRICTION RESEARCH

The friction measurements with the three elastomer blocks (Figure 10) conducted on ice are presented in Figure 18. The RU showed the highest DCOF at low temperatures (-5 °C and -10 °C). However, at -5 °C and at sliding velocities above 2 m/s, the PU revealed highest DCOF at low temperatures. The PU showed the highest DCOF at high temperatures (-2 °C and 0 °C). However, the PU revealed much higher SCOF compared to the TPU and RU materials at 0 °C.

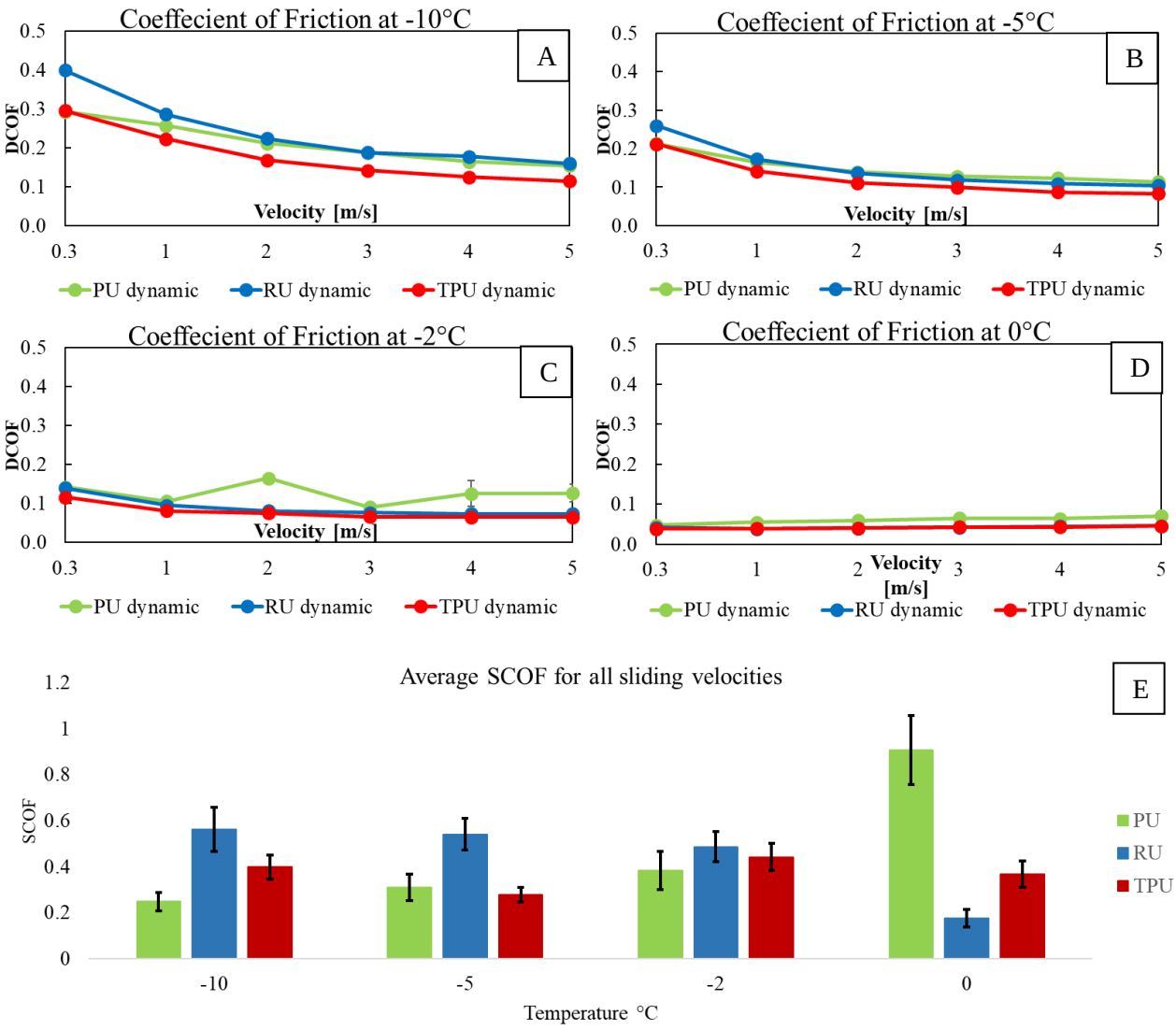

Figure 18 (A-D) Average dynamic coefficient of friction (DCOF) at – 10, -5, -2 and 0 °C as function of sliding velocity. Error bars with ± standard deviations < 0.02 are not visual and left out. (E) Average static coefficient of friction (SCOF) for all temperatures (0 °C to -10 °C). Average is taken for all 30 measurements conducted for each temperature. Adapted from Study III [62].

The friction measurements and calculated viscoelastic friction contribution as function of sliding velocity for the three elastomer blocks (Figure 10) conducted on dry Eurotile and steel are presented in Figure 19 A,B,C,D. The TPU material showed the highest DCOF for all sliding velocities on both the Eurotile and steel surface. The RU material showed the highest viscoelastic contribution to friction on

the Eurotile at slow sliding velocities. However the RU was overtaken by the PU material with increased sliding velocity. When sliding on the steel surface, the TPU had the highest viscoelastic friction contribution for all sliding velocities, which became even more pronounced with increased sliding velocities.

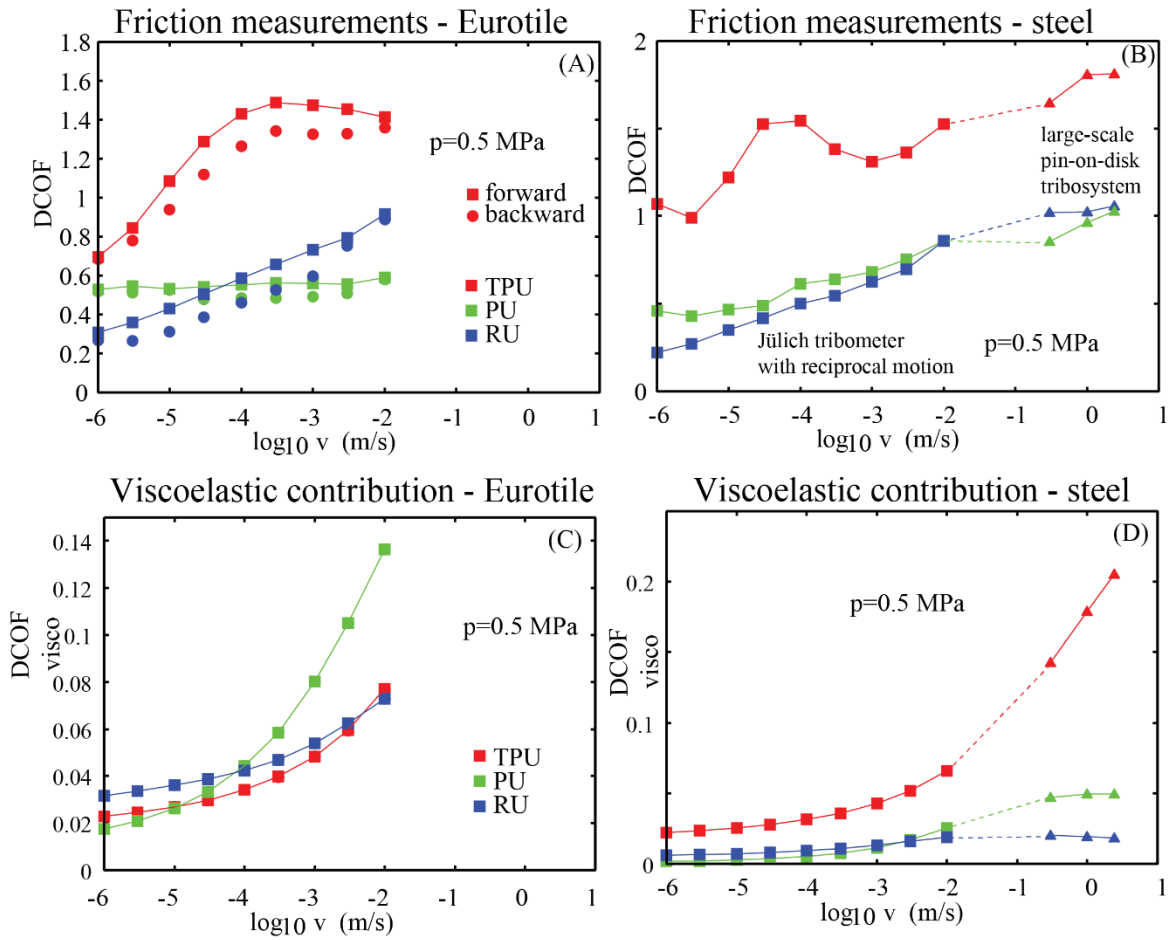

Figure 19 (A-B): Dynamic coefficient of friction (DCOF) on dry Eurotile (A) and steel (B) at 20°C as function of sliding velocity. (C-D): Viscoelastic friction contribution on Eurotile (C) and steel (D) as a function of the sliding velocity. Adapted from Study V.

3.1. RESULTS - APPLICATION-ORIENTED RESEARCH OF FOOTWEAR SLIP RESISTANCE

A typical movement cycle of the robotic platform developed in Study I [67], generated three force components and is displayed in Figure 20. Here it is visually evident that no forces acted on the system between 0.0 s and 0.5 s. After 0.6 s a peak in the Z-axis (vertical force) appeared and was caused by the initial contact between shoe and surface/platform. The horizontal movement started after 1.0 s and resulted in a friction force which was especially pronounced in the Y-axis (horizontal force). The DCOF was calculated from 1.1 s to 1.3 s and represents event 5-6. A plot of a typical DCOF measurement is presented in Figure 21. It appears that the DCOF fluctuates slightly. The average friction values presented in the following results (Figure 22 to Figure 27) are averaged in the time periode from events 5-6 in Figure 21.

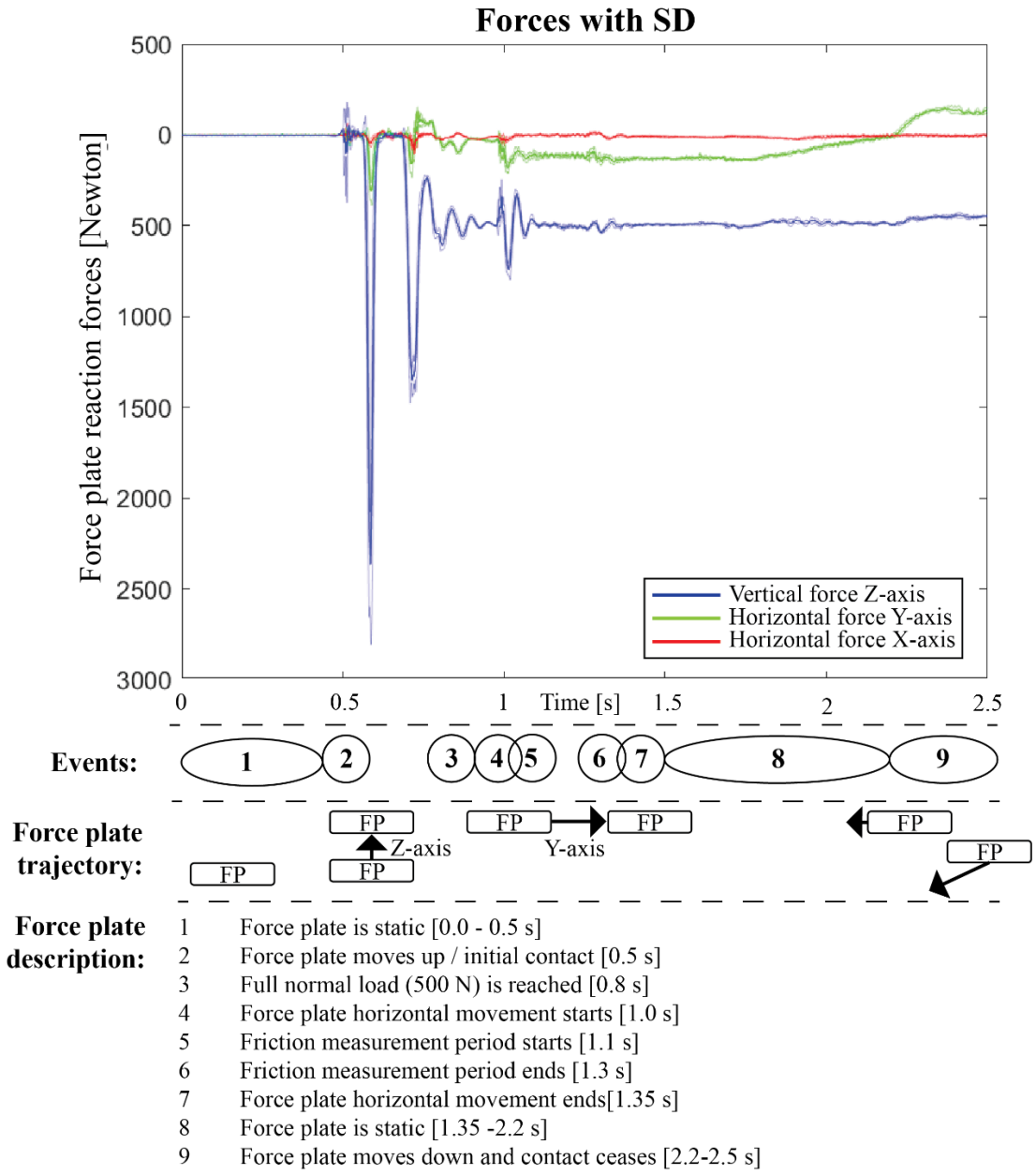

Figure 20 Vertical and Horizontal force components for an entire robotic platform movement cycle. Bold solid lines are the mean reaction forces (blue = vertical force Z-axis; green = horizontal force Y-axis; red = horizontal force X-axis). The thinner solid lines represent the corresponding standard deviation. Reused with permission from Study I [67].

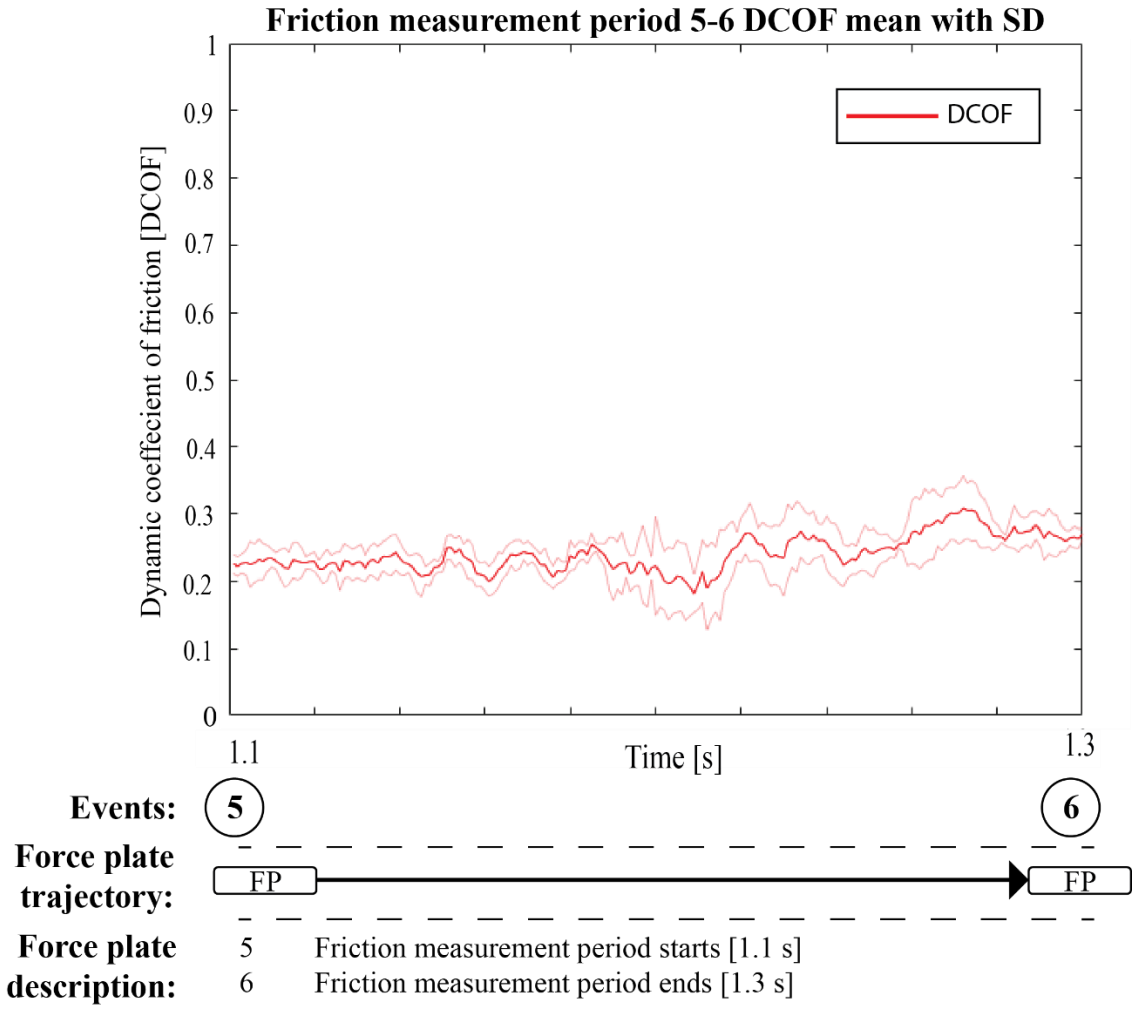

Figure 21 Calculated DCOF as function of time with illustration of force plate trajectory for time interval 5-6 in the measurement cycle. Bold red solid lines are the mean dynamic coeffecients of friction and thin red solid lines are standard deviations. Reused with permission from Study I [67].

The friction measurement results, conducted in Study II, with the three Ecco Xpedition III shoes (Figure 16) constructed of RU, PU and TPU are presented in Figure 22. The highest ACOF was found for the RU shoe sliding on the Eurotile without contaminations (μ = 1.15), whereas the lowest ACOF was found for TPU sliding on steel contaminated with glycerine (μ = 0.12).

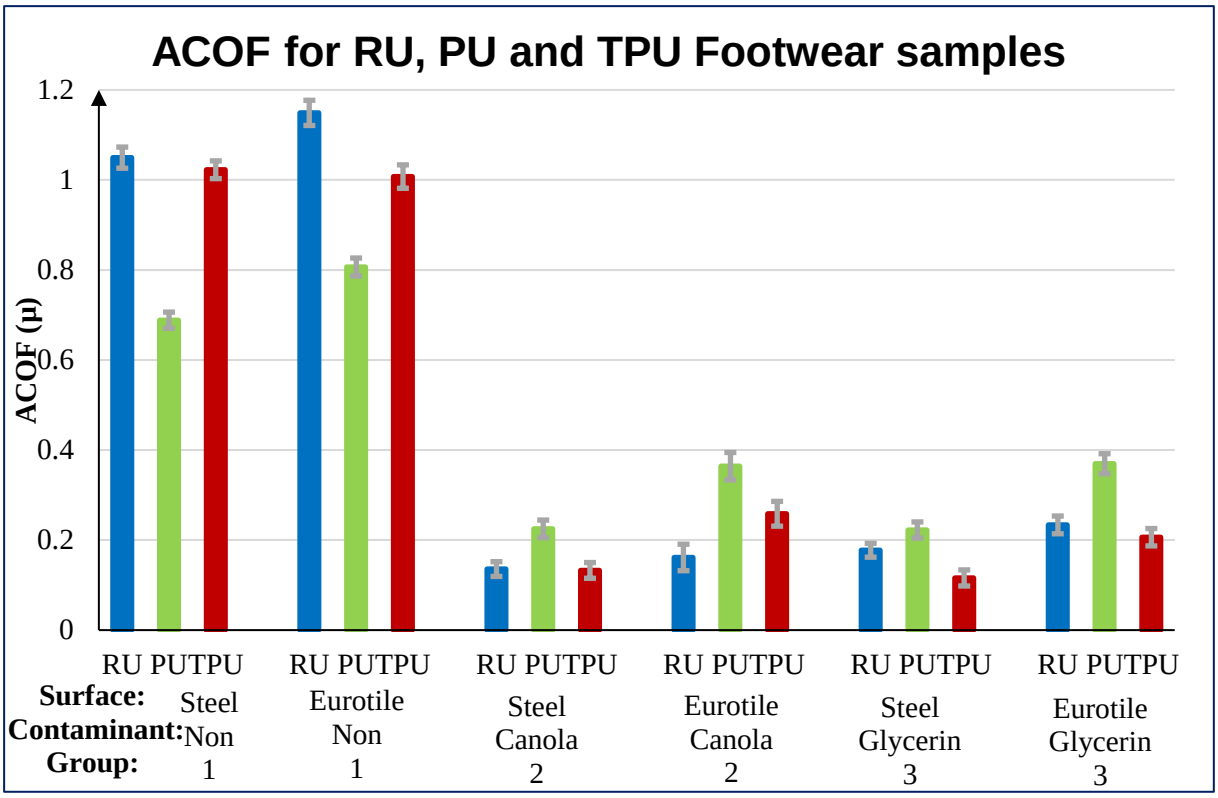

Figure 22 Mean ACOF ± standard deviation for the three Ecco Xpedition III shoes constructed of RU, PU and TPU. Adapted from Study II [68].

The friction measurement results for the five occupational footwear (Figure 17) certified as slip resistant from Study IV is presented in Figure 23 to Figure 27. When the Eurotile was contaminated with SLS, shoe #2 showed the highest ACOF (0.698 ± 0.003) when tested on the robotic test setup, during flat forward slip (Figure 23). Simultaneously, certification data revealed the highest ACOF (0.7) for shoe #3 under the same conditions (Figure 23). All five shoes accommodated the minimum required ACOF of μ ≥ 0.32 indicated by the red line in Figure 23. With the same SLS contaminant and Eurotile surface and an altered shoe/surface angle of 7°, Shoe #2 was also found to have the highest ACOF (0.643 ± 0.003) when tested on the robotic test setup (Figure 24). Nonetheless, certification data showed the highest ACOF (0.6) for shoe #3 under the same conditions. All five shoes accommodated the minimum required ACOF of μ ≥ 0.28 indicated by the red line in Figure 24. When the steel surface was contaminated with glycerin Shoe #2 showed the highest ACOF (0.543 ± 0.002) on the robotic test setup with a flat forward testing condition (Figure 25). External certification data showed the highest ACOF (0.67) for shoe #3 (Figure 25). Shoe #1, shoe #4 and shoe #5 did not pass the minimum required level of friction of μ ≥ 0.18 when tested on the robotic test setup. However, based on certification data all five shoes accommodated the minimum level of friction. With the same glycerin contaminant and steel surface and an altered shoe/surface angle of 7°, Shoe #3 showed the highest ACOF (0.495 ± 0.002) when tested on the robotic test setup. Certification data also showed the highest ACOF (0.5) for Shoe #3. All five shoes accommodated the minimum required ACOF of μ ≥ 0.13 indicated by the red line in Figure 26.

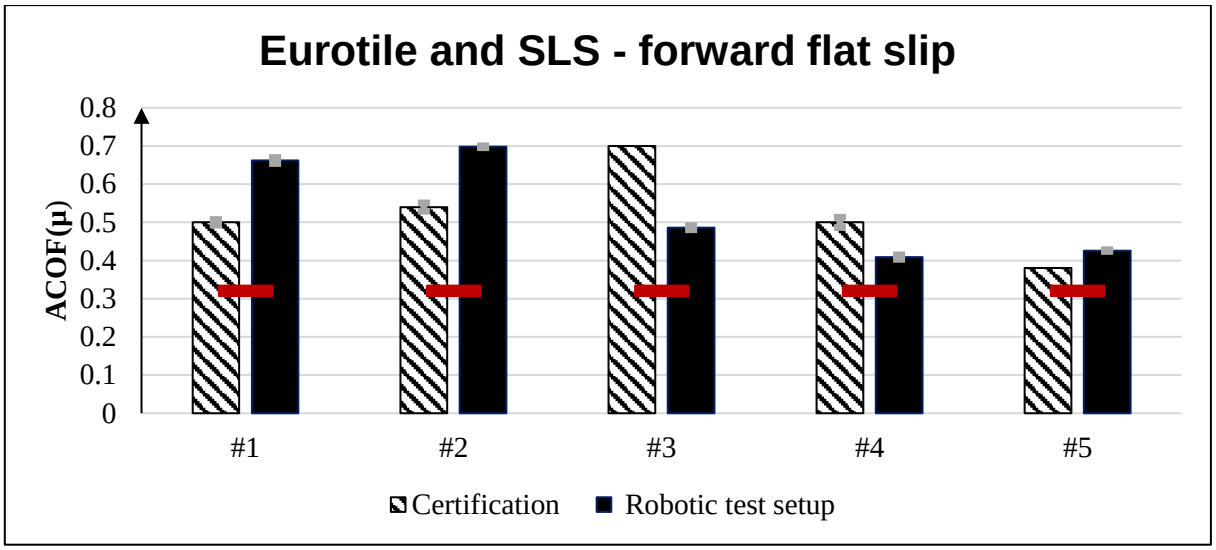

Figure 23. Certification and robotic test setup measurements on Eurotile surface contaminated with SLS during the forward flat slip. The red line represents the minimum ACOF required to meet ISO 20347 certification (μ ≥ 0.32). The error bars represent ± standard deviation for five measurements and are presented when available. Adapted from Study IV.

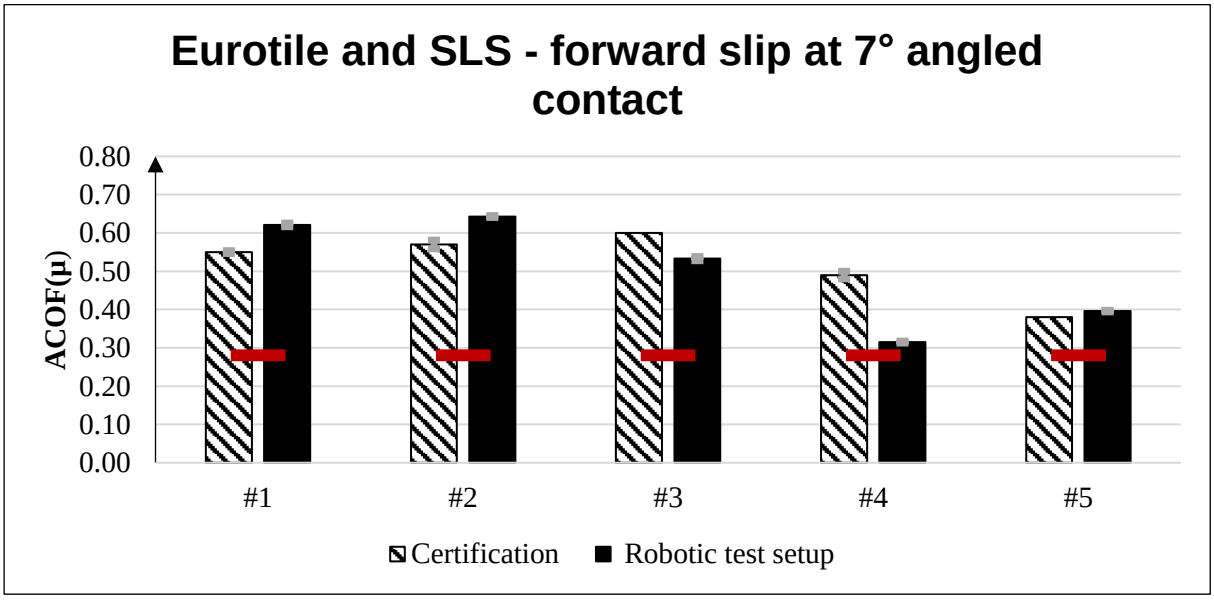

Figure 24 Certification and robotic test setup measurements on Eurotile surface contaminated with SLS during the 7° forward heel slip. The red line represents the minimum ACOF required to meet ISO 20347 certification (μ ≥ 0.28). The error bars represent ± standard deviation for five measurements and are presented when available. Adapted from Study IV.

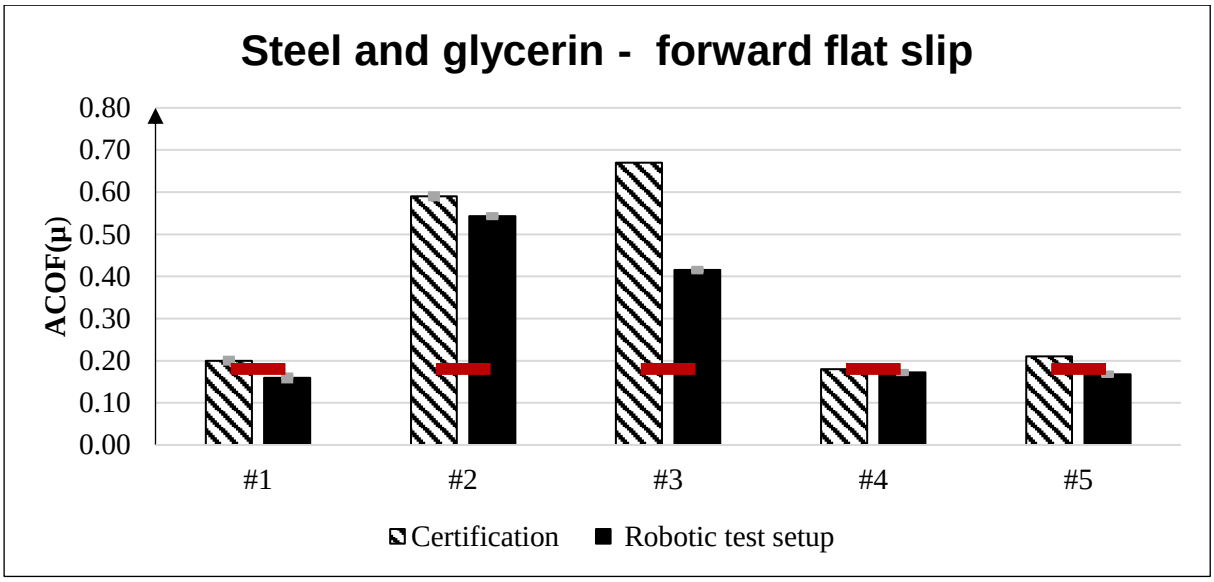

Figure 25 Certification and robotic test setup measurements on steel surface contaminated with glycerin during the forward flat slip. The red line represents the minimum ACOF required to meet ISO 20347 certification (μ ≥ 0.18). The error bars represent ± standard deviation for five measurements and are presented when available. Adapted from Study IV.

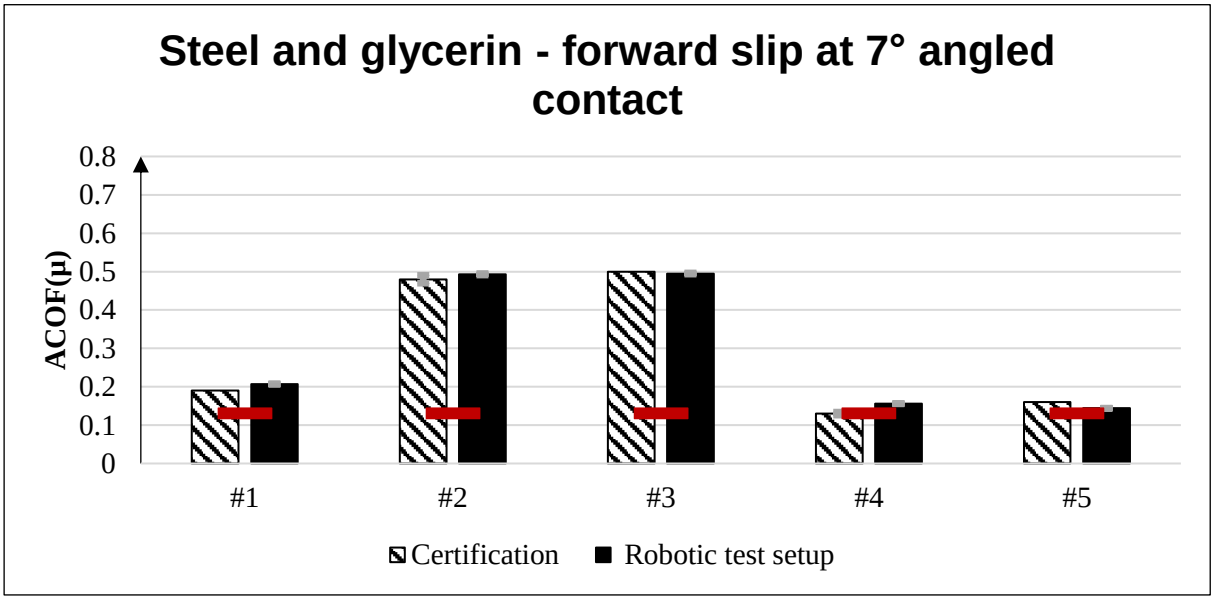

Figure 26 Certification and robotic test setup measurements on steel surface contaminated with glycerin during the 7° forward heel slip. The red line represents the minimum ACOF required to meet ISO 20347 certification (μ ≥ 0.28). The error bars represent ± standard deviation for five measurements and are presented when available. Adapted from Study IV.

When testing conditions were altered to be biofidelic and tested on the robotic test setup equipped with the steel surface and contaminated with glycerin, Shoe #2 had the highest ACOF (0.478 ± 0.003) (Figure 27). Compared to the condition with 7° forward flat slip on steel surface contaminated with glycerin (Figure 26), all shoes showed lower ACOF with biofidelic altered testing parameters.

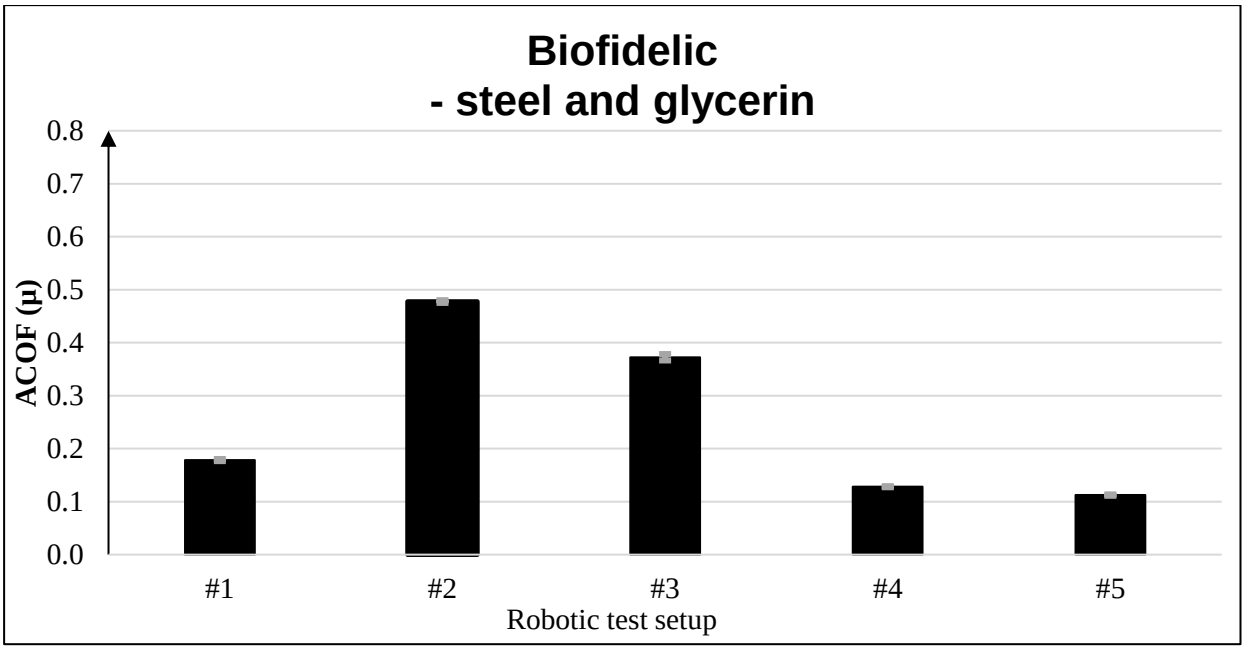

Figure 27 Biofidelic measurements from robotic test setup. The error bars represent ± standard deviation for five measurements. Adapted from Study IV.

DISCUSSION

4.1. SUMMARY

This thesis investigated the slip resistance and friction properties of footwear and outsole materials. This was conducted with both an application-oriented research approach and with a more fundamental research approach of elastomer block friction. The main findings are as follows:

Study I presented a robotic test setup able to determine footwear ACOF in relation to ISO 13287 and able to accommodate biofidelic optimized testing parameters. The repeatability of the robotic test setup was considered good with standard deviations comparable to another slip resistance test devices [33]. Therefore, the robotic test setup was assessed suitable for conducting additional research experiments with whole footwear samples.

Additional slip resistance experiments with whole footwear samples were done in Study II, where the exact same shoe model was constructed with three different outsole materials, namely RU, PU and TPU. The three shoes underwent slip resistance measurements on the robotic test setup from Study I in accordance with the ISO 13287 test standard. On glycerine and canola oil contaminated tile and steel surfaces, the PU sole showed the highest ACOF compared to RU and TPU outsoles. However, on dry tile and steel surfaces the RU outsole revealed the highest ACOF.

In prolongation to Study II, the same three materials were studied in Study III, when constructed as square blocks and subjected to friction experiments on ice surfaces, under biofidelic loading conditions. At -10 °C the RU material had the highest DCOF. At warmer temperatures (close to freezing point), the DCOF difference between the three materials was not particularly pronounced. However, the SCOF for the PU material was substantially higher when the temperature was close to freezing point, compared to the other two materials.

Moreover, slip resistance experiments were also conducted on the robotic test setup, with occupational footwear, certified as slip resistant in Study IV. Certification data was received for five shoes, which also underwent slip resistance experiments in relation to ISO 13287 and experiments with biofidelic optimized testing parameters on the robotic test setup from Study I. From certification data, Shoe #3 consistently ranked as the most slip-resistant shoe. However, Shoe #2 appeared as the most slip resistant model from the experiments performed on the robotic test setup in accordance to ISO 13287 and when testing parameters were altered for biofidelic testing parameters.

In Study V the PU, TPU and RU materials were studied as square blocks, when subjected to friction measurements on the same tile and steel surface as used in Studies I, II and IV. Especially the TPU material revealed higher DCOF compared to the other two materials at high sliding velocities.

4.2. DISCUSSION – ELASTOMER BLOCK FRICTION RESEARCH

Studies III and Study V dealt with elastomer block friction research. Hence, the materials were thoroughly characterized and square blocks were subjected to friction experiments on ice and dry tile and steel surfaces.

From Study III it it was found that at cold temperatures (-10 °C and -5 °C) the RU material revealed highest DCOF compared to the PU and TPU material blocks. The difference was however most pronounced at slower sliding velocities (0.3 – 1 m/s). With increased ambient temperatures (-2 °C and 0 °C) the PU material exhibited highest DCOF. The relatively higher DCOF and SCOF measurements for PU at higher temperatures (-2 C° to 0 C°) can possible be explained by its porous nature and viscoelastic contribution to friction. The porous PU enables the ability to absorb a small amount of water and therefore it is likely that ice sintering is formed between the ice surface and the PU pores. This was further supported by the findings in Study V, where the PU material showed the highest viscoelastic

friction contribution. Higher viscoelastic friction contribution increases the overall friction, when fluids are present [70], indicating that the PU material may have higher friction on contaminated/wet surfaces. This was in fact also the case in Study III when the PU slide over ice surface at -2 °C and 0 °C, where a water film is expected and also the case in Study II where fluid contaminants were present.

Based on the surface energy measurements conducted in Study III, the RU revealed the lowest wettability (Table 1) and is thereby the most hydrophobic material. Increased hydrophobicity for sliders decreases the coefficient of friction over ice surface, when temperatures are close to the melting point [71] and is therefore another possible contributor to the lower SCOF for RU at warmer ice temperatures.

In contrast, the findings from Study V showed that the TPU had superior DCOF compared to the PU and RU materials on dry steel and tile surfaces. In addition, the DCOF generally increased as function of sliding velocity on dry steel and tile surfaces for all three materials. A possible explanation is that the TPU material behaves like a viscous fluid at low frequencies and high temperatures. In this dry sliding condition and at high sliding velocities, the material temperature is expected to increase rapidly and may cause increased friction. The calculated viscoelastic friction contribution for the RU, PU and TPU elastomer block materials (Figure 19 C,D) was generally low, relative to the total measured friction (Figure 19 A,B). Hence, the adhesive friction component had a much greater role in the total measured friction and is likely caused by low surface roughness and dry sliding condition. The steel and tile surfaces have relatively low roughness, which has previously been found to increase the adhesive friction component, compared to surfaces with higher roughness [72]. In addition, lubricants have also been found to lower the adhesive component for elastomers [73].

The results from Study III generally indicated the opposite effect of sliding velocity compared to Study V. Increased sliding velocity and temperature on ice surfaces caused a decreased DCOF, which is in accordance with previous friction experiments conducted with rubber on ice surface [74]–[76]. The film formation caused by meltwater is argued to increase with increased sliding velocity and ambient temperature and thus creating a water layer separating the elastomer blocks and the ice surface, which ultimately decreases the DCOF [74]. In prolongation, at the lower ambient temperatures, the ice surface is solid-like with a more rough surface topography. When the surface topography is rougher, the elastic modulus of the elastomer is theoretically important, since a softer material will be able to better comply with the surface asperities and ultimately increase the DCOF. The DMA (see Figure 9) measurements showed a low elastic modulus at high frequencies (E5-E15 Hz) for the RU material compared to PU and TPU and possibly contributed to a higher DCOF on ice surfaces (at 0.3 m/s at -10 C° and -5 C°), since the RU is hypothetically able to better comply with the surface asperities. Furthermore, the (tan(δ)) (material damping property) is also found to affect the DCOF [16]. Tan(δ) is higher for RU at high frequencies compared to PU and TPU and supposedly more pronounced at low temperatures, which will shift the frequency curve to the left (Figure 9).

4.3. DISCUSSION - APPLICATION-ORIENTED RESEARCH OF FOOTWEAR SLIP RESISTANCE

Force actuated robotic test setup

The force actuated robotic test setup from Study I was evaluated in relation to the ISO 13287 and found suitable for determining footwear slip resistance in accordance with the ISO 13287. This was further supported by Studies II and IV, where the robotic test setup was used for conducting footwear slip resistance measurements comparable to similar research conducted on footwear slip resistance [18]. Study IV did however reveal differences between measurements conducted on the robotic test setup and certification measurements externally provided. The reason for this is not clear. However, a possible explanation for this could be attributed difference in wear of the tile surface used with the robotic test setup and the tile surface used for external certification measurements, since wear has been found to affect its friction properties [77].

Furthermore, the robotic test setup testing parameters and conditions used in Study II may not be the most representative for real slipping events. The shoes were subjected to a flat forward sliding motion as specified in the ISO 13287. Previous research has however found that the initial heel contact phase constitutes the highest risk of slipping [78] and thus a heel/surface angle is arguably more valid. Moreover, testing parameters such as normal load of 400 N [31], sliding velocity between 0.5–1 m/s [30], static contact time between 0–250 ms [79] and shoe/surface contact angle of 13-17° [15], [80], [81], are argued to be more representative for slipping events. With a large degree of flexibility, the robotic test setup could accommodate these testing parameters. This set the foundation for the testing parameters referred to as biofidelic in Figure 17 and were implied in Study IV, when studying slip resistance of commercially footwear. When testing under biofidelic conditions (Figure 27), the ACOF was consistently lower compared to testing conditions in accordance with the ISO 13287 (Figure 26), despite the same surface and contaminant. This supports previous research findings that the ISO 13287 overestimates footwear slip resistance [30]. This phenomena may be explained by increased sliding velocity, which is found to reduce footwear slip resistance, when contaminants are present [82]. Furthermore, increased heel/surface contact angle may lead to reduced contact area and thus lower ACOF [83]. The latter is also linked to an increase in contact pressure, due to the reduced contact area. This can ultimately lead to reduced COF for polymer materials [84]. It should be noted that when the sliding velocity was increased (as for biofidelic measurements), the friction measurement period was decreased, due to the total robotic platform displacement distance of 120 mm in this setup. Hence, the number of data points between events 5-6 (Figure 15 bottom) was reduced, leading to a larger degree of measurement uncertainty.

Slip resistance of RU, PU and TPU

The slip resistance of three geometrically identical shoes constructed of RU, PU and TPU was evaluated in relation to ISO 13287 with the robotic test setup in Study II. The ACOF measurements for the three shoes were comparable to research with footwear with similar hardness, contaminations and surfaces [83], [85], [86]. In addition, the finding that PU materials are more slip resistant than other common outsole materials on contaminated surfaces is supported by previous research [47], [48], [87]. Furthermore, the PU was also the softest of the three elastomers, which also previously has been linked to higher slip resistance [88]. It should however be noted that PU outsoles may wear out faster [89] and require a more frequent replacement. Since it was not possible to control for hardness, it is unknown whether the material choice or the hardness difference had the greatest impact on the slip resistance. Future studies should ideally control for hardness across materials.

In prolongation to Study II, the same three materials (RU, PU and TPU) were also subject to friction experiments on ice surface in Study III. It was found that RU had the highest DCOF at cold (-10 °C) temperatures and is in accordance with research by Gao and colleagues, who also found higher DCOF for rubber materials compared to polyurethane materials [17]. Even though Study III is considered as more fundamental elastomer friction research, since square blocks were used instead of whole shoes, the testing parameters were still aspired to be biofidelic. DCOF between 0.1-0.3 is associated with an increased risk of slipping [28], why it can be assumed that the three materials will not be particularly slip resistant on ice. Especially not at temperatures above -10 °C nor at sliding velocities above 1 m/s, which are not unlikely to happen in usage conditions [66]. Study III did also determine SCOF, which revealed much higher values for PU at warm ice (0 °C). It is however debated whether SCOF or DCOF are the best measure of slip resistance [9], [36]. When high SCOF values may prevent the initiation of a slip for walking subjects anticipating slippery surfaces [27], a high DCOF is related to slip probability [15], [28], [37]. Therefore, increased DCOF and SCOF could arguably improve footwear slip resistance [90]. Due to this, it can be speculated whether hybrid outsoles consisting of multiple materials are preferred to accommodate slip resistance on various ice temperatures. Hybrid outsoles constructed with embedded fibers [91] and smooth/rough surfaces [92] have already shown to be effective solutions for improved slip resistance on ice surface. It is also worth looking into potential slip resistance improvements caused by a hybrid outsole constructed of different elastomer materials.

Slip resistance of commercial footwear certified as slip resistant

When Study II controlled for outsole geometry, Study IV used commercially available shoes certified as slip resistant and focused on identifying footwear parameters, which in previous studies have been linked to friction/slip properties. Generally, shoe #2 and #3 revealed the highest ACOF. However, measurements conducted on the robotic test setup and external certification measurements found disagreement, whether shoe #2 or #3 had the highest ACOF. Nonetheless, based on previous studies, possible explanations why these ranked the highest can be related to thread patterns, outsole materials, outsole hardness, outsole shape and mid/outsole foam thickness. These will be discussed in the following.

Footwear outsoles with a high concentration of small thread blocks, and thus a high concentration of fluid drainage channels, have previously revealed high ACOF measurements under contaminated conditions [18], [83]. Shoe #2 and #3 likewise have numerous small thread blocks, which therefore are expected to contribute to the higher ACOF values. Another outsole shape factor affecting the ACOF is angled or beveled heel, which has been found to affect footwear slip resistance [45]. More specifically, an increased heel beveling positively affects footwear slip resistance. Shoe #2 has a pronounced sagittal heel angle compared to the other shoes, which may partly explain why it exhibits the highest ACOF under biofidelic testing conditions (Figure 27). In addition, lower outsole hardness has long been associated with higher slip resistance under contaminated conditions [50]. Shoe #2 has the second lowest hardness (shore A 62) among the five shoes tested and may therefore also contribute to its high ACOF measurements. Lastly, Shoe #2 had a thick midsole compared to the other shoes and may contribute the higher ACOF measurements. A study by Moriyasu and colleagues found that elastomer blocks with a thick EVA foam layer above a uniform layer of rubber resulted in higher friction compared to equal sized blocks with thinner EVA foam layer and thicker rubber layer [21].

4.1. LIMITATIONS

This thesis has some limitations in relation to the different studies and will be mentioned in the following.

The RU, PU and TPU materials used in Studies II, III and V were provided by an external polymer supplier. The exact material compositions are unknown and numerous material combinations of the materials may exist. Whether different material compositions of the materials would reveal different friction properties is unknown. Therefore, assuming that the findings for the three materials hold true for other material compositions of RU, PU and TPU materials should be done with caution. In addition, the three materials have different hardness levels and the material factor is not entirely isolated. Therefore, studies should idealy control for hardness, when evaluating the effect of outsole materials.

In general, the more fundamental studies (Studies III and V) conducted with elastomer block samples did not represent a realistic reproduction of a complete shoe. Complete shoes have complex geometries in terms of e.g. midsole foam [21] and outsole geometries [20], which also affect the friction/slip resistance properties. Nontheless, when studying the friction properties of elastomer blocks, the tribosystem complexity decreases and isolating factores become more easy. With this in mind, human specific parameters such as e.g. foot motion and slip anticipation were not taken into account. However, loading conditions (normal load/pressure, sliding velocity and static contact time) were incorporated to represent slipping events.

Lastly, the robotic test setup developed within this thesis (Study I) also has some limitations, which should be mentioned. The test setup is expensive, and the construction has a few practical limitations: Measurements with sliding velocities above 0.5 m/s are unreliable. The maintaince of the hydraulics has an annual cost of approximately 2300 USD. Furthermore, the hydraulic actuated platform is integrated in the floor. The oil supply generates considerable heat and noise and should be taken into account when the installation location is chosen.

4.2. IMPLEMENTATION AND FUTURE RESEARCH

This PhD thesis contributed with research of the elastomer block friction research and applied research in relation to footwear slip resistance. In this chapter, future research suggestions and implementation obstacles are discussed.

As described in the introduction, specific research related to slipping and the role of footwear has been studied for decades. Nonetheless, research findings and modern technologies have implementation obstacles [11]. Beschorner recently described some of these implementation obstacles and attributed the complex shoe/surface friction mechanisms as one of the major challenges. As illustrated in Figure 3 several factors affect the footwear friction/slip resistance, why it is highly oversimplified to stamp footwear as slip resistant across various use scenarios. This statement is also backed up by the results from this thesis, indicating that outsole materials (RU, PU and TPU), individually outperformed each other in indifferent environments and under different loading conditions. Hence, it is comprehensible that footwear manufactures struggle with this challenge and simultaneously must address other footwear requirements, such as comfort, fit, breathability, cost etc. In addition, footwear designers may not possess the necessary background, relevant to apply the engineering tools and knowledge [11]. However, Iraqi and colleagues presented a "toolbox" of different apparatuses as indicators of footwear slip resistance, which ranges from expensive and advanced to cheap and easy to use [83]. The majority of these apparatuses were also used in this thesis and include (listed from simple to advanced); visual observation, calliper/ruler, shore A durometer, stylus profilometer, surface energy measurement and dynamic mechanical analysis. Tools such as calliper/ruler and shore A durometer can be used for determining outsole pattern depth/width and hardness and are fairly easy to use and cheap to purchase. In contrast, stylus profilometer, surface energy measurement and dynamic mechanical analysis are more advanced and expensive, why these methods also require more specialised knowledge and economical bandwidth to include. Hence, it is suggested that industrial safety responsible staff and minor footwear manufactures are educated in using the cheap and simple tools, whereas the more advanced and thus expensive tools are reserved for larger footwear manufactures, specialised outsole manufactures and academic researchers in the field.

In relation to the latter, there might be an opportunity to extend the research area of footwear, with more in depth focuses on the viscoelastic properties. As already discussed in the chapter 1.3.2, the hysteresis contribution to elastomer friction has been studied in relation to the tire/road contact mechanism and included the dynamic mechanical analysis tool. One of the main differences between footwear and tire friction could however be related to the difference in sliding velocity. For tires the sliding velocity is much lower, due to the anti-lock braking system (ABS) [93], compared to the footwear sliding, where the kinetic sliding velocity is often much higher [66]. Therefore, the viscoelastic characteristics should supposedly be different, as well and outsole rubber compounds should ideally be developed specifically to accommodate the loading conditions from slipping.

Lastly, the importance of researchers collaborating with footwear manufactures is emphasized. Conducting research on actual footwear when controlling for individual footwear parameters is of high value in order to obtain realistic research in relation to the complex slipping phenomena. During collaborations, it becomes possible for the footwear manufactures to acquire highly specialised knowledge, access to biomechanical laboratory facilities and stay up to date with research. On the other hand, researchers may gain valuable insight into the manufacturing processes of footwear/outsoles, which may be considered when conducting research on prototypes and extrapolating findings onto footwear ready for serial production. Collaborations and joint projects between industry and academia are therefore encouraged to help bridging the gap between these parties.

CONCLUSION

This PhD thesis investigated elastomer friction from a footwear application and outsole elastomer block level. This included the development of a highly flexible robotic test setup in Study I, which was able to conduct footwear slip resistance measurements in relation to ISO 13287 and alter biofidelic testing parameters. The setup revealed good repeatability with low standard deviations and was considered applicable for footwear slip resistance determination. This robotic test setup was used to quantify the slip resistance of footwear samples in Study II and Study IV, whereas Study III and Study V were considered as more fundamental elastomer friction research, conducted with elastomer material blocks on other tribometers.

From Studies II, III and V, it is clear that the three outsole materials (RU, PU and TPU) have different friction properties, which are much affected by the counter surface, contaminants and sliding velocity. In fact, all three materials outperformed each other, however under different circumstances. The PU had the highest static friction on warm ice and highest dynamic friction on glycerine and canola oil contaminated tile and steel surfaces. The RU had the highest dynamic friction on cold ice. However, whether the RU or the TPU have the highest friction on dry steel is conflicting from Study II and Study V. The RU showed a DCOF of 1.05 in Study II and a DCOF of 1.02 in Study V when sliding on dry steel with 0.3 m/s. However, the TPU showed a DCOF of 1.02 in Study II and a DCOF of 1.65 in Study V when sliding on dry steel with 0.3 m/s. Hence, a difference of 61,8 %. This suggests that there exists no single material, which provides the best slip resistance in all environments. Therefore, materials should be carefully chosen by their intended application, and possible disadvantages should be considered.

From Study IV, it was concluded that testing conditions and footwear design influenced the ACOF measurements. Specifically, it was found that biofidelic testing parameters lowered the ACOF measurements compared to testing parameters in accordance with ISO 13287. In addition, it was argued that small outsole tread pattern increased heel beveling, and midsole thickness increased footwear slip resistance.

Lastly, future research should ideally focus on optimizing slip resistant footwear to accommodate area- and industry-specific environments. Simultaneously, attention should be given to the knowledge gap between the academic research in slip resistance and the industrial stakeholders in the footwear industry.

LITERATURE LIST

[1] Arbejdstilsynet, "Arbejdstilsynets Årsopgørelse 2021 - Anmeldte Arbejdsulykker 2016-2021," 2021. [Online]. Available: https://at.dk/media/7413/arbejdsulykker-aarsopgoerelse-2021-bilag-b.pdf.

[2] Beskæftigelsesministeriet, "Et nyt og forbedret arbejdsmiljø - Bilagsrapport, Bind 1," 2018.

[3] Sundhedsstyrelsen, "Sygdomsbyrden i Danmark, Ulykker, Selvskade og Selvmord 2016," Copenhagen S, 2016. Accessed: May 02, 2019. [Online]. Available: www.sst.dk.

[4] C. Gao and J. Abeysekera, "A systems perspective of slip and fall accidents on icy and snowy surfaces," *Ergonomics*, vol. 47, no. 5, pp. 573–598, 2004, doi: 10.1080/00140130410081658718.

[5] "Statistics Norway. Fall vanligste arbeidsulykke," 2021. https://www.ssb.no/helse/helseforhold-og-levevaner/statistikk/arbeidsulykker/artikler/fall-vanligste-arbeidsulykke (accessed Jan. 20, 2022).

[6] Bureau of Labor Statistics, "National Census of Fatal Occupational Injuries in 2020," 2021. Accessed: Aug. 15, 2022. [Online]. Available: www.bls.gov/iif/oshwc/cfoi/cfoi_rates_2020hb.xlsx.

[7] Acting Medical Officer of Health, "Preventing Injuries from Wintertime Slips and Falls in Toronto," 2016. Accessed: Sep. 02, 2022. [Online]. Available: http://app.toronto.ca/tmmis/viewAgendaItemHistory.do?item=2015.HL7.3.

[8] T. K. Courtney, G. S. Sorock, D. P. Manning, J. W. Collins, and M. A. Holbein-Jenny, "Occupational slip, trip, and fall-related injuries can the contribution of slipperiness be isolated?," *Ergonomics*, vol. 44, no. 13, pp. 1118–1137, Oct. 2001, doi: 10.1080/00140130110085538.

[9] M. Tisserand, "Progress in the prevention of falls caused by slipping," *Ergonomics*, vol. 28, no. 7, pp. 1027–1042, 1985, doi: 10.1080/00140138508963225.

[10] ASTM F3445-21, "Standard Specification for Performance Requirements when Evaluating Slip Resistance of Protective (Safety) Footwear using ASTM F2913 Whole Shoe Test Method," 2021. Accessed: Aug. 30, 2022. [Online]. Available: https://www.astm.org/f3445-21.html.

[11] K. E. Beschorner, "The Future of Footwear Friction," *Proc. 21st Congr. Int. Ergon. Assoc.* , vol. 223, 2021, Accessed: Aug. 02, 2022. [Online]. Available: http://www.springer.com/series/15179.

[12] R. Ding, A. Gujrati, M. M. Pendolino, K. E. Beschorner, and T. D. B. Jacobs, "Going Beyond Traditional Roughness Metrics for Floor Tiles : Measuring Topography Down to the Nanoscale," *Tribol. Lett.*, vol. 69, p. 92, 2021, doi: 10.1007/s11249-021-01460-8.

[13] C. G. J. Baker, *Handbook of food factory design*. 2013.

[14] W. Chang *et al.*, "The role of friction in the measurement of slipperiness, Part 2: Survey of friction measurement devices," *Ergonomics*, vol. 44, no. 13, pp. 1233–1261, 2001, doi: 10.1080/00140130110085583.

[15] A. Iraqi, R. Cham, M. S. Redfern, and K. E. Beschorner, "Coefficient of friction testing parameters influence the prediction of human slips," *Appl. Ergon.*, vol. 70, no. July 2017, pp. 118–126, 2018, doi: 10.1016/j.apergo.2018.02.017.

[16] B. N. J. Persson, “Theory of rubber friction and contact mechanics,” *J. Chem. Phys.*, 2001, doi: 10.1063/1.1388626.

[17] C. Gao, J. Abeysekera, M. Hirvonen, and R. Grönqvist, “Slip resistant properties of footwear on ice,” *Ergonomics*, vol. 47, no. 6, 2004, doi: 10.1080/00140130410001658673.

[18] T. Jones, A. Iraqi, and K. Beschorner, “Performance testing of work shoes labeled as slip resistant,” *Appl. Ergon.*, vol. 68, pp. 304–312, 2018, doi: 10.1016/j.apergo.2017.12.008.

[19] J. Hale, R. Lewis, and M. J. Carré, “Rubber friction and the effect of shape,” *Tribol. Int.*, vol. 141, 2020, doi: 10.1016/j.triboint.2019.105911.

[20] T. Yamaguchi, Y. Katsurashima, and K. Hokkirigawa, “Effect of rubber block height and orientation on the coefficients of friction against smooth steel surface lubricated with glycerol solution,” *Tribol. Int.*, vol. 110, 2017, doi: 10.1016/j.triboint.2017.02.015.

[21] K. Moriyasu, T. Nishiwaki, K. Shibata, T. Yamaguchi, and K. Hokkirigawa, “Friction control of a resin foam/rubber laminated block material,” *Tribol. Int.*, vol. 136, 2019, doi: 10.1016/j.triboint.2019.04.024.

[22] M. G. Blanchette and C. M. Powers, “The influence of footwear tread groove parameters on available friction,” *Appl. Ergon.*, vol. 50, pp. 237–241, Sep. 2015, doi: 10.1016/j.apergo.2015.03.018.

[23] R. Grönqvist *et al.*, “Measurement of slipperiness : fundamental concepts and definitions,” *Ergonomics*, vol. 44, no. 13, p. 1117, 2001, doi: 10.1080/00140130110085552.

[24] D. H. Richie, *Pathomechanics of Common Foot Disorders*. Oakland: Springer, 2021.

[25] L. Strandberg and H. Lanshammar, “The dynamics of slipping accidents,” *J. Occup. Accid.*, vol. 3, pp. 153–162, 1981, Accessed: May 24, 2019. [Online]. Available: http://production.datastore.cvt.dk/filestore?oid=5332b62094c29b73349fc1c7&targetid=5332b62094c29b73349fc1cb.

[26] D. E. Anderson, C. T. Franck, and M. L. Madigan, “Age differences in the required coefficient of friction during level walking do not exist when experimentally-controlling speed and step length,” *J. Appl. Biomech.*, vol. 30, no. 4, 2014, doi: 10.1123/jab.2013-0275.

[27] R. Cham and M. S. Redfern, “Changes in gait when anticipating slippery floors,” *Gait Posture*, vol. 15, no. 2, pp. 159–171, Apr. 2002, doi: 10.1016/S0966-6362(01)00150-3.

[28] J. P. Hanson, M. S. Redfern, and M. Mazumdar, “Predicting slips and falls considering required and available friction,” *Ergonomics*, vol. 42, no. 12, pp. 1619–1633, Dec. 1999, doi: 10.1080/001401399184712.

[29] I. Standard, “Personal protective equipment – Footwear – Test method for slip resistance (ISO 13287:2019),” 2019.

[30] G. Hunwin, S. Thorpe, and K. Hallas, “Improvements to the EN slip resistance test for footwear,” *Contemp. Ergon. Hum. Factors 2010*, vol. Proceeding, pp. 471–479, 2010.

[31] M. G. Blanchette and C. M. Powers, “Slip Prediction Accuracy and Bias of the SATRA STM 603 Whole Shoe Tester,” *J. Test. Eval.*, vol. 43, no. 3, p. 20130308, 2015, doi: 10.1520/JTE20130308.

[32] K. E. Beschorner, A. Chanda, B. E. Moyer, A. Reasinger, S. C. Griffin, and I. J. M., “Validating

the ability of a portable shoe-floor friction testing device, NextSTEPS, to predict human slips," *Appl. Ergon.*, 2022, doi: https://doi.org/10.1016/j.apergo.2022.103854.

[33] C. Aschan, M. Hirvonen, T. Mannelin, and E. Rajamäki, "Development and validation of a novel portable slip simulator," *Appl. Ergon.*, vol. 36, no. 5, pp. 585–593, 2005, doi: 10.1016/j.apergo.2005.01.015.

[34] S. R. Lewis, K. Hallas, B. Keen, G. Hunwin, R. Shaw, and M. J. Carré, "Development of a new shoe/floor slip resistance test rig," *Tribol. Int.*, vol. 151, 2020, doi: 10.1016/j.triboint.2020.106500.

[35] J. Clarke, M. J. Carré, L. Damm, and S. Dixon, "The development of an apparatus to understand the traction developed at the shoe-surface interface in tennis," *Proc. Inst. Mech. Eng. Part P J. Sport. Eng. Technol.*, 2013, doi: 10.1177/1754337112469500.

[36] T. Yamaguchi, S. Hatanaka, and K. Hokkirigawa, "Effect of Step Length and Walking Speed on Traction Coefficient and Slip between Shoe Sole and Walkway," *Tribol. Online*, vol. 3, no. 2, 2008, doi: 10.2474/trol.3.59.

[37] J. M. Burnfield and C. M. Powers, "Prediction of slips: an evaluation of utilized coefficient of friction and available slip resistance," *Ergonomics*, vol. 49, no. 10, pp. 982–995, Aug. 2006, doi: 10.1080/00140130600665687.

[38] K. W. Li, H. H. Wu, and Y.-C. Lin, "The effect of shoe sole tread groove depth on the friction coefficient with different tread groove widths, floors and contaminants," *Appl. Ergon.*, vol. 37, pp. 743–748, 2006, doi: 10.1016/j.apergo.2005.11.007.

[39] K. W. Li and J. C. Chin, "Effects of tread groove orientation and width of the footwear pads on measured friction coefficients," in *Safety Science*, 2005, vol. 43, no. 7, doi: 10.1016/j.ssci.2005.08.006.

[40] K. W. Li and C. J. Chen, "The effect of shoe soling tread groove width on the coefficient of friction with different sole materials, floors, and contaminants," *Appl. Ergon.*, vol. 35, pp. 499–507, 2004, doi: 10.1016/j.apergo.2004.06.010.

[41] J. Hale, A. O'connell, R. Lewis, M. J. Carré, and J. A. Rongong, "An Evaluation of Shoe Tread Parameters using FEM," *Tribol. Int.*, vol. 153, p. 106570, 2021, doi: 10.1016/j.triboint.2020.106570.

[42] S. L. Hemler *et al.*, "Changes in under-shoe traction and fluid drainage for progressively worn shoe tread," 2019, doi: 10.1016/j.apergo.2019.04.014.

[43] V. H. Sundaram, S. L. Hemler, A. Chanda, J. M. Haight, M. S. Redfern, and K. E. Beschorner, "Worn region size of shoe outsole impacts human slips: Testing a mechanistic model," *J. Biomech.*, vol. 105, 2020, doi: 10.1016/j.jbiomech.2020.109797.

[44] S. M. Reza Moghaddam, S. L. Hemler, M. S. Redfern, T. D. Jacobs, and K. E. Beschorner, "Computational model of shoe wear progression: Comparison with experimental results," 2019, doi: 10.1016/j.wear.2019.01.070.

[45] D. Lloyd and M. G. Stevenson, "Measurement of slip resistance of shoes on floor surfaces. Part 2: Effect of a bevelled heel," *J. Occup. Heal. Saf. - Aust. New Zeal.*, vol. 5, no. 3, 1989.

[46] D. P. Manning and C. Jones, "The effect of roughness, floor polish, water, oil and ice on underfoot friction: current safety footwear solings are less slip resistant than microcellular polyurethane," *Appl. Ergon.*, vol. 32, pp. 185–196, 2001.

[47] K. Beschorner *et al.*, “Modeling mixed-lubrication of a shoe-floor interface applied to a pin-on-disk apparatus,” *Tribol. Trans.*, vol. 52, no. 4, pp. 560–568, 2009, doi: 10.1080/10402000902825705.

[48] C. M. Strobel, P. L. Menezes, M. R. Lovell, and K. E. Beschorner, “Analysis of the contribution of adhesion and hysteresis to shoe-floor lubricated friction in the boundary lubrication regime,” *Tribol. Lett.*, vol. 47, no. 3, pp. 341–347, Sep. 2012, doi: 10.1007/s11249-012-9989-5.

[49] Y. J. Tsai and C. M. Powers, “The influence of footwear sole hardness on slip initiation in young adults,” *J. Forensic Sci.*, vol. 53, no. 4, pp. 884–888, 2008, doi: 10.1111/j.1556-4029.2008.00739.x.

[50] R. Grönqvist, “Mechanisms of friction and assessment of slip resistance of new and used footwear soles on contaminated floors,” *Ergonomics*, vol. 38, no. 2, pp. 224–241, 1995, doi: 10.1080/00140139508925100.

[51] L. Strandberg, “The effect of conditions underfoot on falling and overexertion accidents,” *Ergonomics*, vol. 28, no. 1, pp. 131–147, 1985, doi: 10.1080/00140138508963123.

[52] D. F. Moore, “The friction and lubrication of elastomers,” *Pergamon*, vol. 9, 1972.

[53] B. Lorenz, Y. R. Oh, S. K. Nam, S. H. Jeon, and B. N. J. Persson, “Rubber friction on road surfaces: Experiment and theory for low sliding speeds,” *J. Chem. Phys.*, vol. 142, no. 19, 2015, doi: 10.1063/1.4919221.

[54] K. Menard and N. Menard, *Dynamic Mechanical Analysis*, 3rd ed. Boca Raton: CRC Press, 2020.

[55] B. N. J. Persson, O. Albohr, U. Tartaglino, A. I. Volokitin, and E. Tosatti, “On the nature of surface roughness with application to contact mechanics, sealing, rubber friction and adhesion,” *J. Phys. Condens. Matter*, vol. 17, no. 1, 2005, doi: 10.1088/0953-8984/17/1/R01.

[56] M. Mahboob Kanafi, “Rocky road – surface roughness impactson rubber friction,” 2017.

[57] M. Mahboob Kanafi, A. J. Tuononen, L. Dorogin, and B. N. J. Persson, “Rubber friction on 3D-printed randomly rough surfaces at low and high sliding speeds,” *Wear*, vol. 376–377, 2017, doi: 10.1016/j.wear.2017.01.092.

[58] Y.-X. Wang, J.-H. Ma, L.-Q. Zhang, and Y.-P. Wu, “Material Properties Revisiting the correlations between wet skid resistance and viscoelasticity of rubber composites via comparing carbon black and silica fillers,” *j. Polym. Test.*, vol. 30, pp. 557–562, 2011, doi: 10.1016/j.polymertesting.2011.04.009.

[59] D. Ura and M. Carré, “Development of a Novel Portable Test Device to Measure the Tribological Behaviour of Shoe Interactions with Tennis Courts,” 2016, doi: 10.1016/j.proeng.2016.06.237.

[60] S. B. Auganæs, A. F. Buene, and A. Klein-Paste, “Laboratory testing of cross-country skis – Investigating tribometer precision on laboratory-grown dendritic snow,” *Tribol. Int.*, vol. 168, no. January, 2022, doi: 10.1016/j.triboint.2022.107451.

[61] A. Tiwari, N. Miyashita, and B. N. J. Persson, “Rubber Wear and the Role of Transfer Films on Rubber Friction on Hard Rough Substrates,” *Tribol. Lett.*, vol. 69, no. 2, 2021, doi: 10.1007/s11249-021-01410-4.

[62] L. Jakobsen, S. B. Auganæs, A. F. Buene, I. M. Sivebaek, and A. Klein-Paste, “Dynamic and Static Friction Measurements of Elastomer Footwear Blocks on Ice Surface,” *Tribol. Int.*, p. 108064, Nov. 2022, doi: 10.1016/J.TRIBOINT.2022.108064.

[63] G. Carbone, B. Lorenz, B. N. J. Persson, and A. Wohlers, “Contact mechanics and rubber friction for randomly rough surfaces with anisotropic statistical properties,” *Eur. Phys. J. E*, vol. 29, no. 3, 2009, doi: 10.1140/epje/i2009-10484-8.

[64] A. Tiwari, N. Miyashita, N. Espallargas, and B. N. J. Persson, “Rubber friction: The contribution from the area of real contact,” *J. Chem. Phys.*, vol. 148, no. 22, 2018, doi: 10.1063/1.5037136.

[65] L. Jakobsen, F. Lysdal, Gertz, and I. M. Sivebæk, “Tribosystem for determination of footwear slip resistance under high sliding velocities,” *Nord. Symp. Tribol. Nord. 2022.*, 2022.

[66] W. Chang *et al.*, “The role of friction in the measurement of slipperiness, Part 1: Friction mechanisms and definition of test conditions The role of friction in the measurement of slipperiness, Part 1: Friction mechanisms and definition of test conditions,” *Ergonomics*, vol. 44, no. 13, 2001, doi: 10.1080/00140130110085574.

[67] L. Jakobsen, F. G. Lysdal, T. Bagehorn, U. G. Kersting, and I. M. Sivebaek, “Evaluation of an actuated force plate-based robotic test setup to assess the slip resistance of footwear,” *Int. J. Ind. Ergon.*, vol. 88, p. 103253, Mar. 2022, doi: 10.1016/J.ERGON.2021.103253.

[68] L. Jakobsen, F. Lysdal, Gertz, T. Bagehorn, U. Kersting, and I. Sivebaek, Marius, “The Effect of Footwear Outsole Material on Slip Resistance on Dry and Contaminated Surfaces with Geometrically Controlled Outsoles,” *Ergonomics*, 2022, doi: https://doi.org/10.1080/00140139.2022.2081364.

[69] ISO, “Personal protective equipment - Footwear - Test method for slip resistance (ISO 13287:2019),” *CEN, Eur. Comm. Stand.*, vol. 13287, 2019.

[70] M. J. H. Cowap, S. R. M. Moghaddam, P. L. Menezes, and K. E. Beschorner, “Contributions of adhesion and hysteresis to coefficient of friction between shoe and floor surfaces: Effects of floor roughness and sliding speed,” *Tribol. - Mater. Surfaces Interfaces*, vol. 9, no. 2, 2015, doi: 10.1179/1751584X15Y.0000000005.

[71] A. M. Kietzig, S. G. Hatzikiriakos, and P. Englezos, “Ice friction: The effects of surface roughness, structure, and hydrophobicity,” *J. Appl. Phys.*, vol. 106, no. 2, 2009, doi: 10.1063/1.3173346.

[72] M. J. H. Cowap, S. R. M. Moghaddam, P. L. Menezes, and K. E. Beschorner, “Contributions of adhesion and hysteresis to CoF between shoe and floor surfaces: Effects of floor roughness and sliding speed.,” *Tribology*, vol. 9, no. 2, pp. 77–84, 2015.

[73] Caitlin Moore Strobel • Pradeep L. Menezes • *et al.*, “Analysis of the Contribution of Adhesion and Hysteresis to Shoe-Floor Lubricated Friction in the Boundary Lubrication Regime,” *Tribol Lett*, no. 341–347, pp. 341–347, 2012, doi: 10.1007/s11249-012-9989-5.

[74] O. Lahayne *et al.*, “Rubber Friction on Ice: Experiments and Modeling,” *Tribol. Lett.*, vol. 62, no. 2, 2016, doi: 10.1007/s11249-016-0665-z.

[75] G. Skouvaklis, J. R. Blackford, and V. Koutsos, “Friction of rubber on ice: A new machine, influence of rubber properties and sliding parameters,” *Tribol. Int.*, vol. 49, 2012, doi: 10.1016/j.triboint.2011.12.015.

[76] A. J. Tuononen, A. Kriston, and B. Persson, “Multiscale physics of rubber-ice friction,” *J. Chem. Phys.*, vol. 145, no. 11, 2016, doi: 10.1063/1.4962576.

[77] M. Engels, “Recerence Materials - UK Slip Resistance Group,” 2018. [Online]. Available: https://www.ukslipresistance.org.uk/wp-content/uploads/2018/07/Marcel-Engels-Presentation-

Reference-materials-final.pdf.

[78] L. Strandberg, “On accident analysis and slip-resistance measurement,” *Ergonomics*, vol. 26, no. 1, pp. 11–32, 1983, doi: 10.1080/00140138308963309.

[79] R. Grönqvist, S. Matz, and M. Hirvonen, “Assessment of shoe-floor slipperiness with respect to contact-time-related variation in friction during heel strike,” *Occup. Ergon.*, vol. 3, no. 4, pp. 197–208, Nov. 2003, doi: 10.3233/OER-2003-3402.

[80] D. Albert, B. Moyer, and K. E. Beschorner, “Three-Dimensional Shoe Kinematics During Unexpected Slips: Implications for Shoe–Floor Friction Testing,” *IISE Trans. Occup. Ergon. Hum. Factors*, vol. 5, no. 1, pp. 1–11, 2017, doi: 10.1080/21577323.2016.1241963.

[81] K. E. Beschorner, A. Iraqi, M. S. Redfern, R. Cham, and Y. Li, “Predicting slips based on the STM 603 whole-footwear tribometer under different coefficient of friction testing conditions,” 2019, doi: 10.1080/00140139.2019.1567828.

[82] K. E. Beschorner, M. S. Redfern, W. L. Porter, and R. E. Debski, “Effects of slip testing parameters on measured coefficient of friction,” *Appl. Ergon.*, vol. 38, no. 6, pp. 773–780, Nov. 2007, doi: 10.1016/j.apergo.2006.10.005.

[83] A. Iraqi, N. S. Vidic, M. S. Redfern, and K. E. Beschorner, “Prediction of coefficient of friction based on footwear outsole features,” *Appl. Ergon.*, vol. 82, p. 102963, 2020, doi: 10.1016/j.apergo.2019.102963.

[84] B. J. Briscoe and D. Tabor, “The effect of pressure on the frictional properties of polymers,” *Wear*, vol. 34, pp. 29–38, 1975, doi: https://dx.doi.org/10.1016/0043-1648(75)90306-3.

[85] S. R. M. Moghaddam, A. Acharya, M. S. Redfern, and K. E. Beschorner, “Predictive multiscale computational model of shoe-floor coefficient of friction,” *J. Biomech.*, vol. 66, pp. 145–152, 2018, doi: 10.1016/j.jbiomech.2017.11.009.

[86] P. J. Walter, C. M. Tushak, S. L. Hemler, and K. E. Beschorner, “Effect of tread design and hardness on interfacial fluid force and friction in artificially worn shoes,” *Footwear Sci.*, vol. 13, no. 3, pp. 245–254, 2021, doi: 10.1080/19424280.2021.1950214.

[87] D. P. Manning and C. Jones, “The effect of roughness, foor polish, water, oil and ice on underfoot friction: current safety footwear solings are less slip resistant than microcellular polyurethane,” *Appl. Ergon.*, vol. 32, pp. 185–196, 2001.

[88] R. Grönqvist and M. Hirvonen, “Slipperiness of footwear and mechanisms of walking friction on icy surfaces,” *Int. J. Ind. Ergon.*, vol. 16, no. 3, 1995, doi: 10.1016/0169-8141(94)00095-K.

[89] I. J. Kim, “Identifying shoe wear mechanisms and associated tribological characteristics: Importance for slip resistance evaluation,” *Wear*, vol. 360–361, pp. 77–86, 2016, doi: 10.1016/j.wear.2016.04.020.

[90] T. Yamaguchi *et al.*, “Development of new footwear sole surface pattern for prevention of slip-related falls,” *Saf. Sci.*, vol. 50, no. 4, 2012, doi: 10.1016/j.ssci.2011.12.017.

[91] Z. Shaghayegh Bagheri, A. Anwer, G. Fernie, H. E. Naguib, and T. Dutta, “Effects of multi-functional surface-texturing on the ice friction and abrasion characteristics of hybrid composite materials for footwear,” *Wear*, vol. 418–419, 2019, doi: 10.1016/j.wear.2018.11.030.

[92] T. Yamaguchi, J. Hsu, Y. Li, and B. E. Maki, “Efficacy of a rubber outsole with a hybrid surface pattern for preventing slips on icy surfaces,” *Appl. Ergon.*, vol. 51, 2015, doi:

10.1016/j.apergo.2015.04.001.

[93] S. Hemette, “Rubber-Ice Friction A Multi-Scale and Multi-Physical Approach,” 2019.

APPENDED JOURNAL ARTICLES

Lasse Jakobsen[a]*, Filip Gertz Lysdal[a], Timo Bagehorn[b], Uwe G. Kersting[b,c] and Ion Marius Sivebaek[a]

[a]*Department of Mechanical Engineering, Technical University of Denmark, Copenhagen, Denmark;*

[b]*Department of Health Science and Technology, Aalborg University, Denmark*

[c]*Institute of Biomechanics and Orthopaedics, German Sport University Cologne*

*Lasse Jakobsen, lasjak@mek.dtu.dk, Phone: 004520406213

Adress:

Produktionstorvet, 425,

2800 Kgs. Lyngby, Denmark

Evaluation of a force plate-based robotic test setup to assess the slip resistance of footwear

Abstract

Slipping accidents are a frequent cause of occupational related accidents. This is often due to an insufficient available coefficient of friction (ACOF) of footwear. The aim of this study was to present a footwear ACOF test setup, and to evaluate it based on device requirements presented in the ISO 13287 test standard. One left Airtox TX2 shoe underwent slip resistance measurements under three test modes (Forward flat slip, backward slip on the forefoot at angled contact and forward heel slip at angled contact), with six contaminant conditions (dry steel, dry tile, glycerine on steel, glycerine on tile, canola oil on steel and canola oil on tile). The test setup was successfully able to measure ACOF in close accordance to the ISO 13287 test standard with a good repeatability. Furthermore, the test setup can alter biomechanical and tribophysical testing conditions, which may provide more valid footwear ACOF measurements in the future.

Relevance to industry: The setup can accommodate biomechanical and tribophysical testing conditions, hence the setup can be a tool for accessing more valid ACOF measurements - closer to real world slip events. Footwear manufactures or researchers, with the goal of improving footwear slip resistance, can implement the setup.

Keywords: Friction; Traction; Footwear; Slipping; Testing

Introduction

Fall accidents on the same level account for 22.4% of all serious work related accidents, reported in the period 2012-2016 in Denmark (Arbejdstilsynet, 2017). Annually, injuries attributed to falling accounts for expenditures of approximately 3.9 billion DKK in lost production costs (Sundhedsstyrelsen, 2016). The same challenge is present in other western countries, including the UK, USA and Sweden, where especially the aging part of the work force is at risk (Chang et al., 2016; Courtney et al., 2001). When

many work related injuries are decreasing, the amount of fall accidents are increasing (Chang et al., 2016). In fact, the Liberty Mutual Workplace Safety Index showed that the direct cost of disabling workplace injuries, related to falls on the same level was US$9.19 billion in 2012 (Liberty Mutual Workplace Safety Index 2012). In 2021 the cost has increased to US$10.58 billion (Liberty Mutual Workplace Safety Index 2021). Slipping is acknowledged as the most significant cause of fall accidents (Courtney et al., 2001) and therefore prevention of slipping has a great potential to reduce the occurrence of occupational accidents (Beschorner and Singh, 2012).

The occurrence of a slip becomes less likely to occur when the available coefficient of friction (ACOF) exceeds the required coefficient of friction (RCOF) (Hanson et al., 1999). Here, the RCOF can be determined by dividing the horizontal force with the vertical force, during walking across a force plate under slippery conditions (Beschorner et al., 2016; Cham and Redfern, 2002; Yamaguchi and Masani, 2015). In contrast, the ACOF is commonly determined by mechanical testing during which a footwear sample is dragged across a floor surface (Iraqi et al., 2020, 2018a).

Measurement results for ACOF differ substantially dependent on the test setup and test conditions (Chang et al., 2001). To accommodate these variations, the "ISO 13287:2019 - Personal protective equipment – Footwear – Test method for slip resistance" was established (ISO 13287, 2019). Commercially available test devices, such as the STM 603 (Satra Technology, Kettering, Great Britain) and the DW9530 (Fanyuan Instrument, Hefei, China) can operate in accordance with the ISO 13287:2019 test standard. Both devices are designed with a force transducer positioned above a shoe last. In biomechanics, however, a force plate is considered the golden standard to evaluate the acting forces between footwear and floor (McLaughlin, 2013). A test device incorporating this established method for the assessment of ACOF in footwear is

therefore expected to provide the highest "transmissibility" to RCOF, where this same equipment is already used.

Overall, this leads to the aim of this study which was to design a force plate-based ACOF test setup, and evaluate it based on device and setup requirements presented in the ISO 13287 test standard.

Method

With the aim of designing a force plate-based ACOF test setup, we instrumented a force plate atop of a robotic hydraulic platform (van Doornik and Sinkjaer, 2007). Testing parameters and device requirements was performed in accordance to the ISO 13287 standard (Table 1) (*ISO 13287*, 2019).

	Requirements according to ISO 13287
1	Normal force 400-500 ± 25 N
2	Accuracy of device for friction measurement of 2% or better
3	Sliding velocity of 0.30 ± 0.03 m/s
4	Static contact time between initial contact and start of movement of ≤1.0 s.
5	Measurement period shall start within 0.3 s of achieving the full normal force and end 0.6 s after start of movement.
6	Shoe contact angle at 0 and 7.0 ± 0.5°
7	Measurement period shall start within 0.3 s of achieving the full normal force.
8	Able to include wet contaminants
9	Able to apply tile (Eurotile 2) and steel surface (Rz between 1.6 µm and 2.5 µm)

Table 1 Test setup requirements

Device description

The experimental setup consisted of a steel frame (Figure 1 E) designed to maintain a fixed position of a shoe (Figure 1 A) above a force plate (Figure 1 B) (AMTI-OPT464508HF-1000, Advanced Mechanical Technology, Inc. Watertown MA, USA).

The manufacturer states a measurement accuracy of ±0.1% of the applied load (up to 4448 N) (Advanced Mechanical Technology Inc., Platform datasheet). The force plate was mounted atop of a hydraulic platform (Serman-Tipsmark, Brønderslev, Denmark), able to move along the vertical and horizontal axes (Figure 1 Z and Y) at velocities ranging from 0-1 m/s (van Doornik & Sinkjaer, 2007). The hydraulic platform was movement and velocity controlled in Mr. Kick (Mr. Kick version 3.0, Aalborg, Denmark). Additionally, a retroreflective marker was placed on the hydraulic platform to capture platform movements using an eight-camera motion capture system (Qualisys Oqus 3+ and QTM 2019 software, Qualisys Gothenburg, Sweden). Force plate and movement data were recorded with a 1000 Hz and 500 Hz sample rate, respectively.

A plastic shoe-last size 43 EU (Framas, Pirmasens, Germany) was fixed directly under a vertical lead (Figure 1 G), which was able to move in the vertical direction. Normal load was applied to the vertical lead through a vertical force distributer using standard weight plates (Figure 1 F). Non-restricted vertical movement of the lead was ensured by applying PTFE foil on the surfaces of the vertical lead and the inner support frame, which maintain the horizontal position of the shoe. Additionally, a PTFE based oil (Kema Oil, PTFE TRI-17) was applied to the PTFE surfaces to allow for smooth and low friction contact.

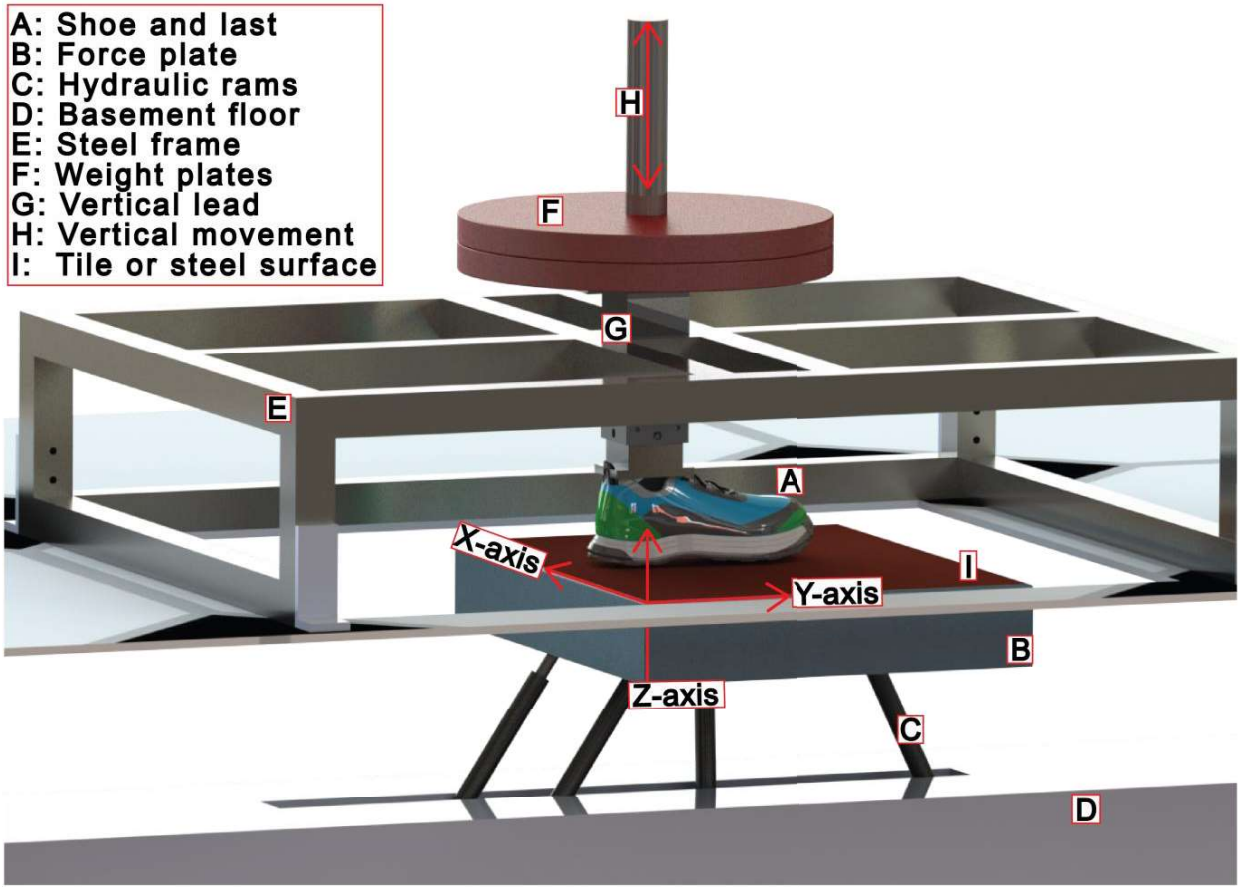

Figure 1 Illustration of test setup

Preparation and cleaning

The procedure of the test and preparation of footwear and floor was in accordance to the specification of ISO 13287. Hence, the shoe was sanded with 400 grit paper, cleaned using an ethanol solution, scrubbed with a clean medium stiff brush, washed with demineralized water and dried using clean dry compressed air and then at ambient temperature (23 ± 2 °C). Surfaces were cleaned with an ethanol solution, scrubbed gently with a clean medium stiff brush, rinsed with demineralized water and dried using clean dry compressed air and then at ambient temperature.

Surfaces

Two surfaces were used in the setup. One ceramic tile (Euro tile 2 specified in ISO 13287) and a steel plate number 1.4301 with a mean roughness (Rz) of 1.65 µm. The steel plate roughness is measured using a surtronic 25 profilometer (Taylor Hobson, Leicester, United Kingdom) in accordance with the specifications from ISO 13287, which implies 10 measurements at different locations in the direction of sliding movement. The mean roughness (Rz) must be between 1.6 µm and 2.5 µm according to ISO 13287. The 10 measurements were measured in accordance with ISO 4287 (ISO, 1997).

Footwear

The left shoe from a pair of size EU 43 Airtox TX2 (Airtox, Virum, Denmark) safety footwear was used for evaluation of the test setup.

Testing Conditions

The shoe was exposed to three different test modes (Figure 2) (Forward flat slip, backward slip on the forefoot at angled contact and forward heel slip at angled contact), with six contaminant and surface combinations (dry steel, dry tile, glycerine on steel, glycerine on tile, canola oil on steel and canola oil on tile). A 7° aluminium wedge was

constructed in accordance with the specifications of ISO 13287, to control shoe/surface contact angle before testing.

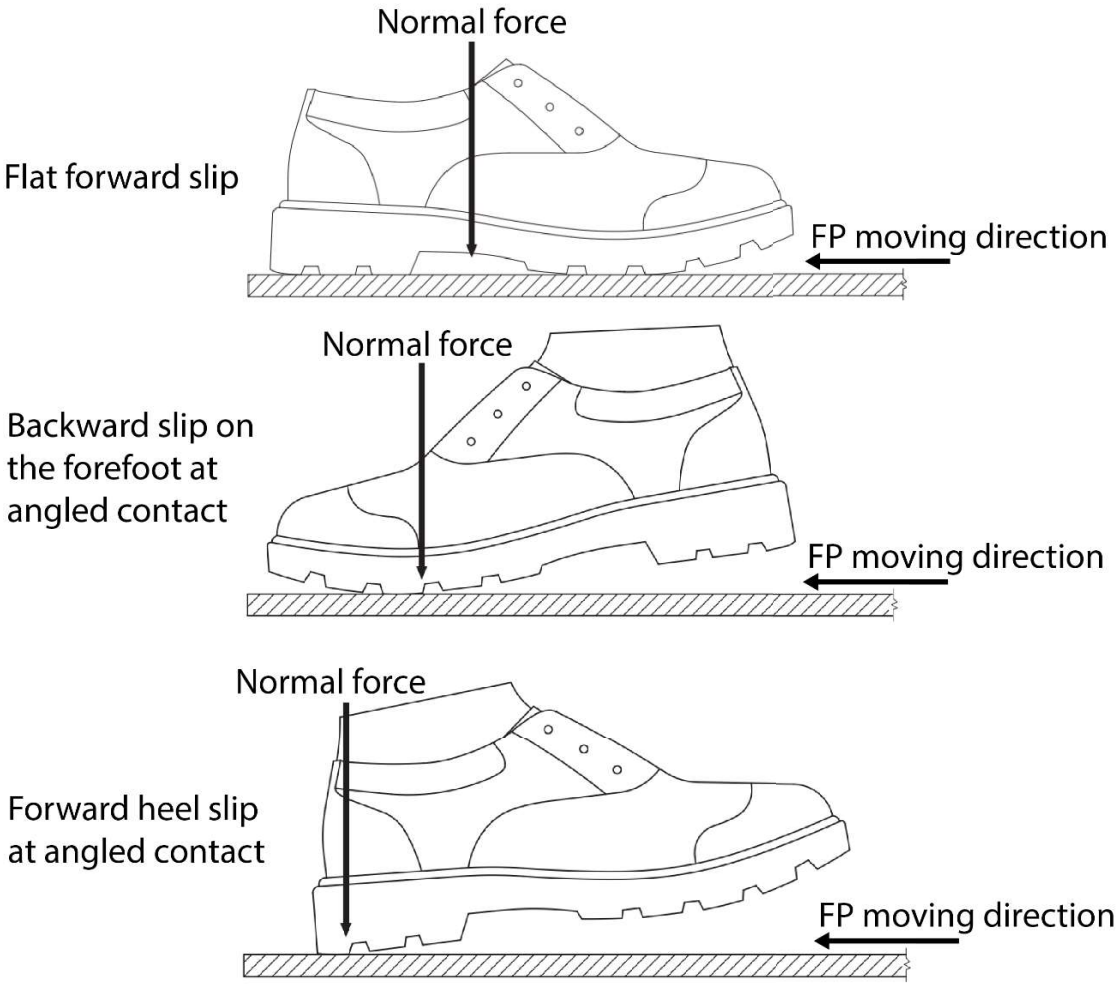

Figure 2. Footwear orientation and force plate (FP) sliding direction. Adapted from ISO 13287 with permission from Danish Standards (ISO 13287, 2019)

In total, this sums up to 18 different conditions. Five slip resistance measurements were taken for all test conditions, leading to 90 measurements in total. Five measurement repetitions for each condition in accordance with the ISO 13287.

Test procedure

The platform was resting in the starting position between 0.0 s and 0.5 s and no external forces acted on the force plate (Figure 3, event 1). At 0.5 s the platform moved upwards in the vertical direction and initial contact between shoe and surface was reached (Figure 3 event 2). At 0.8 s the shoe was resting statically on the surface (i.e., full normal load reached) (Figure 3 event 4). After 1.0 s the platform started moving in the horizontal direction (from forfoot to heel) with a constant velocity of 0.298 ± 0.01 m/s (Figure 3 event 5). The friction measurement period started at 1.1 s and ended at 1.3 s (Figure 3 event 5-6). The horizontal movement ended at 1.35 s and corresponded to a moving distance of 120 mm (Figure 3 event 7). From 1.35 s to 2.2 s the platform was static (Figure 3 event 8). In the time interval 2.2 to 2.5 s the robotic platform moved horizontally (heel to forefoot) in the horizontal direction to prevent overshooting of the hydraulic rams (Figure 3 event 9). After 2.5 s the platform moved back towards the starting point.

All dry (non-contaminated) measurements were performed first. Surface and shoe were wiped with isopropyl alcohol after every five measurements under dry conditions. During contaminated conditions, the surfaces were wiped clean for every five measurements and fresh contaminants were reapplied. Shoe and surfaces were thoroughly cleaned with soap and rinsing water when changing between glycerin and canola oil contaminants.

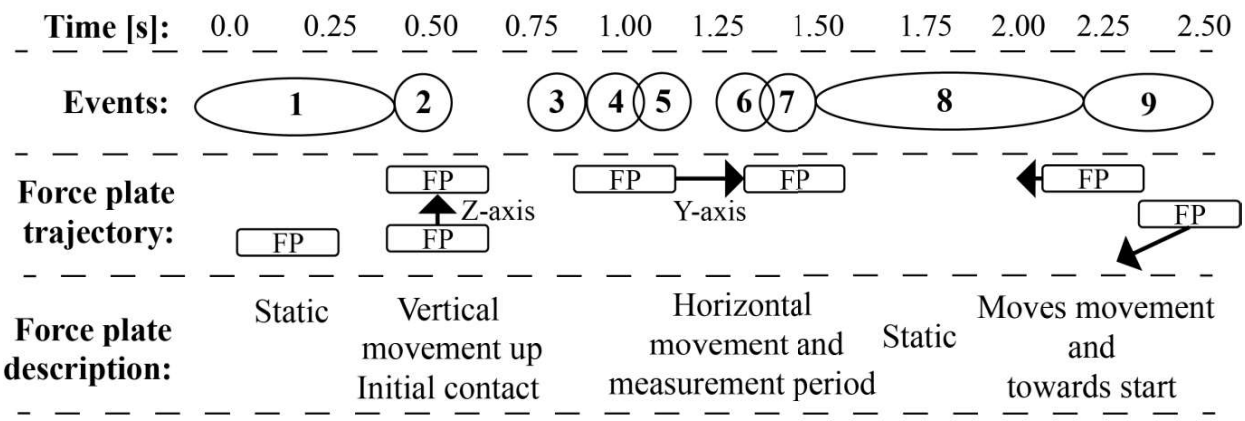

1 Force plate is static [0.0 - 0.5 s]
2 Force plate moves up / initial contact [0.5 s]
3 Full normal load (500 N) is reached [0.8 s]
4 Force plate horizontal movement starts [1.0 s]
5 Friction measurement period starts [1.1 s]
6 Friction measurement period ends [1.3 s]
7 Force plate horizontal movement ends[1.35 s]
8 Force plate is static [1.35 - 2.2 s]
9 Force plate moves down and contact ceases [2.2 - 2.5 s]

Figure 3 Illustration and description of platform movement cycle.

Data Processing

Force and movement data were imported into MATLAB version R2020b (MathWorks, Massachusetts, USA) and processed in a customized script. Force and movement data were filtered with a second order low pass filter with a cut-off frequency of 20 Hz and 10 Hz, respectively. Force and movement data were synchronized by calculating the cross covariance and aligning data via circular shift. Beforehand 10 platform cycles were performed without shoe contact for both the steel and tile surface mounted atop. These 10 platform movements without shoe contact were averaged and subtracted from the friction measurements. This was done to account for the inertia generated when the force plate was accelerated (Oliveira et al., 2017). The dynamic coefficient of friction

(DCOF) was calculated by dividing the horizontal reaction forces, F_x and F_y (friction forces) with the vertical reaction force F_z (normal force) (Equation 1).

$$\mathrm{DCOF} = \sqrt{\frac{F_x^2 + F_y^2}{F_z^2}} \quad 1$$

The mean DCOF for five measurements was calculated as function of time. Lastly, the corresponding mean DCOF in the measurement period (Figure 3 event 5-6) was calculated and presented as an average and standard deviation.

Results

An entire movement cycle of the robotic platform generated three force components (Figure 4). Bold solid lines are the mean reaction forces (blue = vertical force Z-axis; green = horizontal force Y-axis; red = horizontal force X-axis) and thin solid lines are the corrosponding standard deviations. No contact forces were present between 0.0 s and 0.5 s (Figure 4 event 1). Both the hozitontal force components (Figure 4 green and red) and the vertical force component (Figure 4 blue) fluctuates at 0.5 s, when the robitic plateform started moving. At 0.6 s a peak appeares in all three force components due to the rapid contact between shoe and surface. The force componenets stabilizes at 0.8 s at ~500 N (Figure 4 event 3).

When the horizontal movement started at 1.0 s (Figure 4 event 4) the horizontal Y and X force components rises, with the Y component being the dominant. Simultaneously, the vertical Z force component fluctuates shortly. All three force components reached a plateau between 1.2 s and 1.3 s. After 1.35 s (Figure 4 event 7) all force components are fluctuating slightly as the platform movement ends.

From 1.35 s to 2.2 s (Figure 4 event 8) the robotic platform was static and the vertical Z force component and the horizontal X force component were static. The horizontal Y force component moves towards 0 as the tension between shoe and surface decreases.

After 2.2 s the robotic platform moved horizontally (heel to forefoot) and the horizontal Y force component changes direction (**Error! Reference source not found.** event 9).

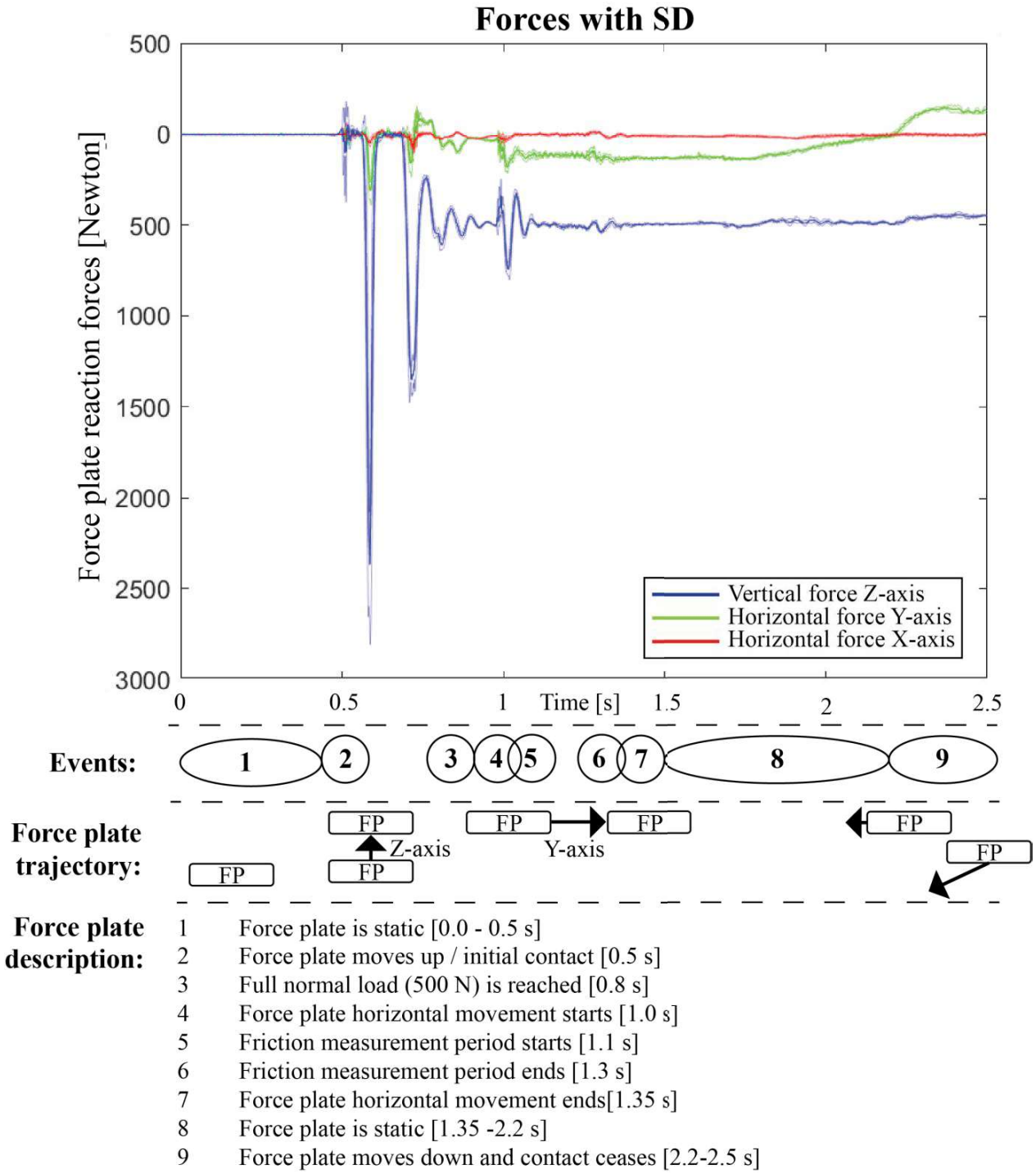

Figure 4 Vertical and Horizontal force components for an entire robotic platform movement cycle. Bold solid lines are the mean reaction forces (blue = vertical force Z-

axis; green = horizontal force Y-axis; red = horizontal force X-axis). The thinner solid lines represent the corresponding standard deviation.

The time period from event 4 to 7 is zoomed and represents the time period when the robotic platform moved horizontally (forefoot to heel) where the coeffecient of friction is calculated from (Figure 5 event 5-6). At 1.1 s the X and Z force components flucturates and reaches a pleteau after 1.2 s.

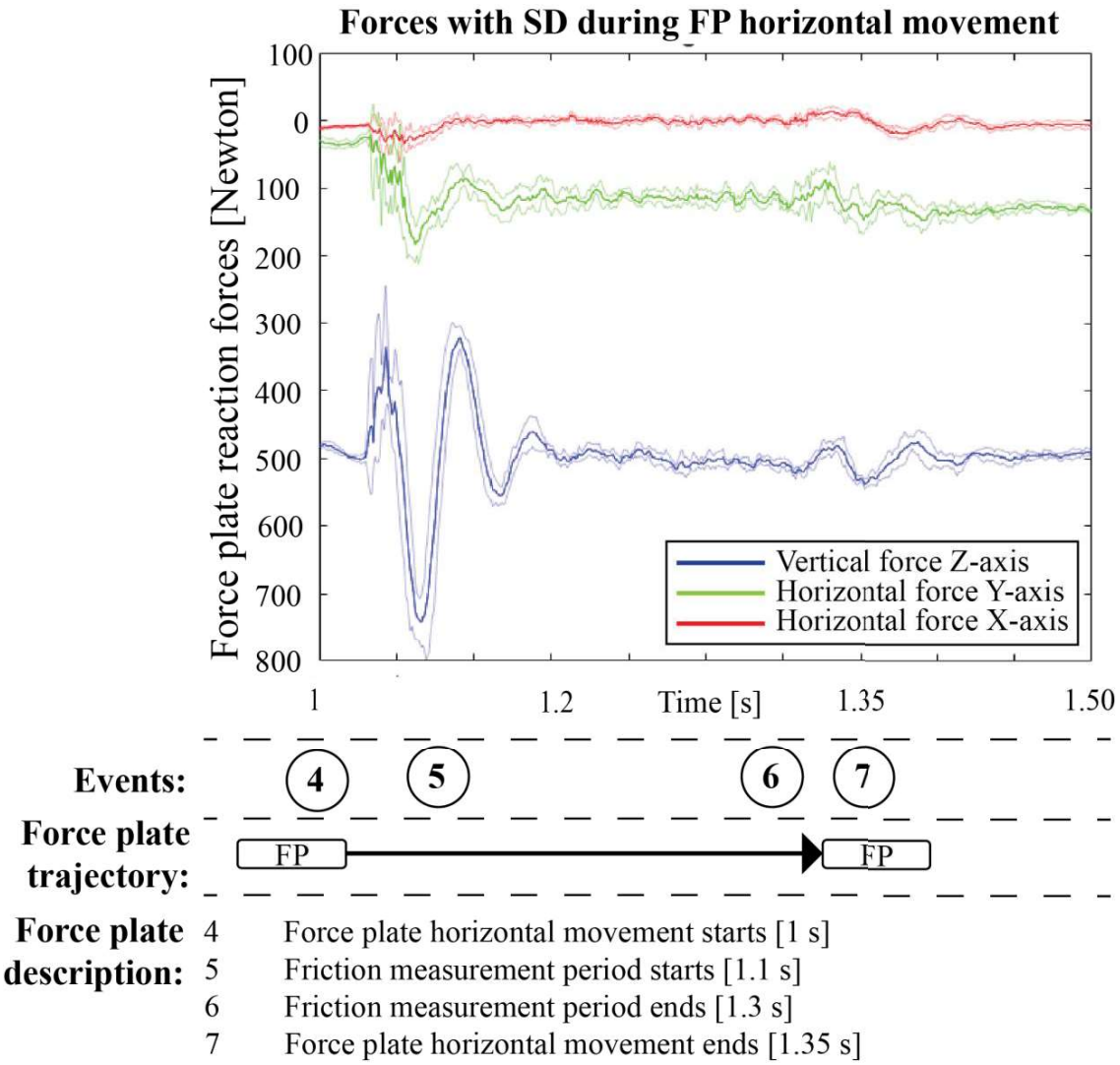

Figure 5 Vertical and Horizontal force components in the time interval 4-7 in the measurement cycle. Bold solid lines are the mean reaction forces (blue = vertical force

Z-axis; green = horizontal force Y-axis; red = horizontal force X-axis). The thinner solid lines represent the corresponding standard deviation.

The calculated DCOF is represented by the solid red line from (Figure 6 event 5-6). The DCOF fluctuates between ~0.2 and ~0.3 in the friction measurement period.

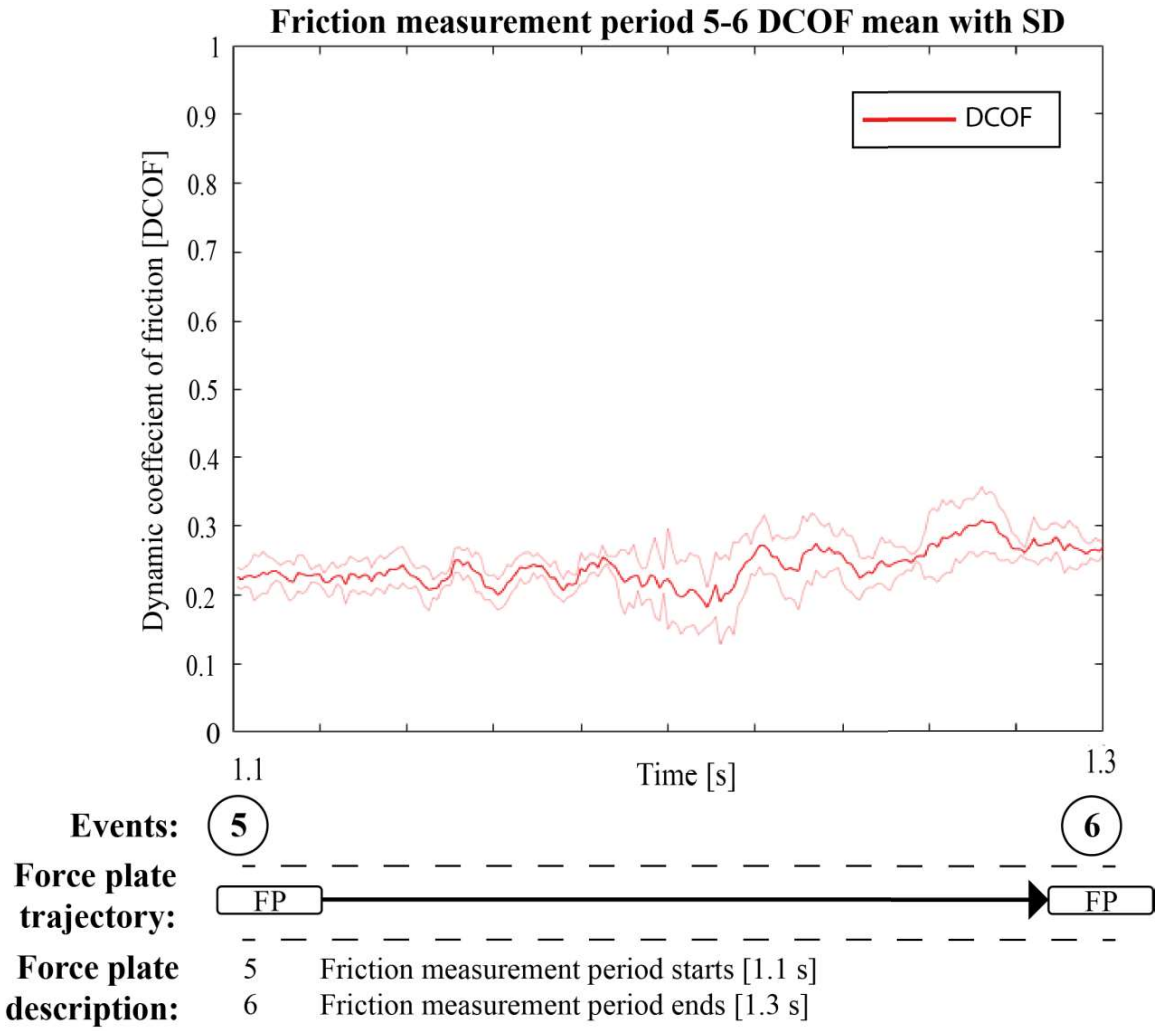

Figure 6 Calculated DCOF as function of time with illustration of force plate trajectory for time interval 5-6 in the measurement cycle. Bold red solid lines are the mean dynamic coeffecients of friction and thin red solid lines are standard deviations.

In general, the conditions without contaminants had higher DCOF compared to the conditions without. The highest DCOF was 0.93 and was found in forward heel slip at angled contact on the steel surface without contaminants. The lowest DCOF was 0.13

found in the backward slip of the forefoot on the steel surface - with glycerin as contaminant (Figure 8; Table A.1). Highest standard deviation (0.03) is found in forward heel slip at angled contact on the steel surface without contaminants. Lowest standard deviation (0.01) is found in backward slip on the forefoot on the Eurotile surface with glycerine as contaminant. Absolute values of mean dynamic coefficient of friction and standard deviation for all tested conditions are shown in appendix (Table A.1).

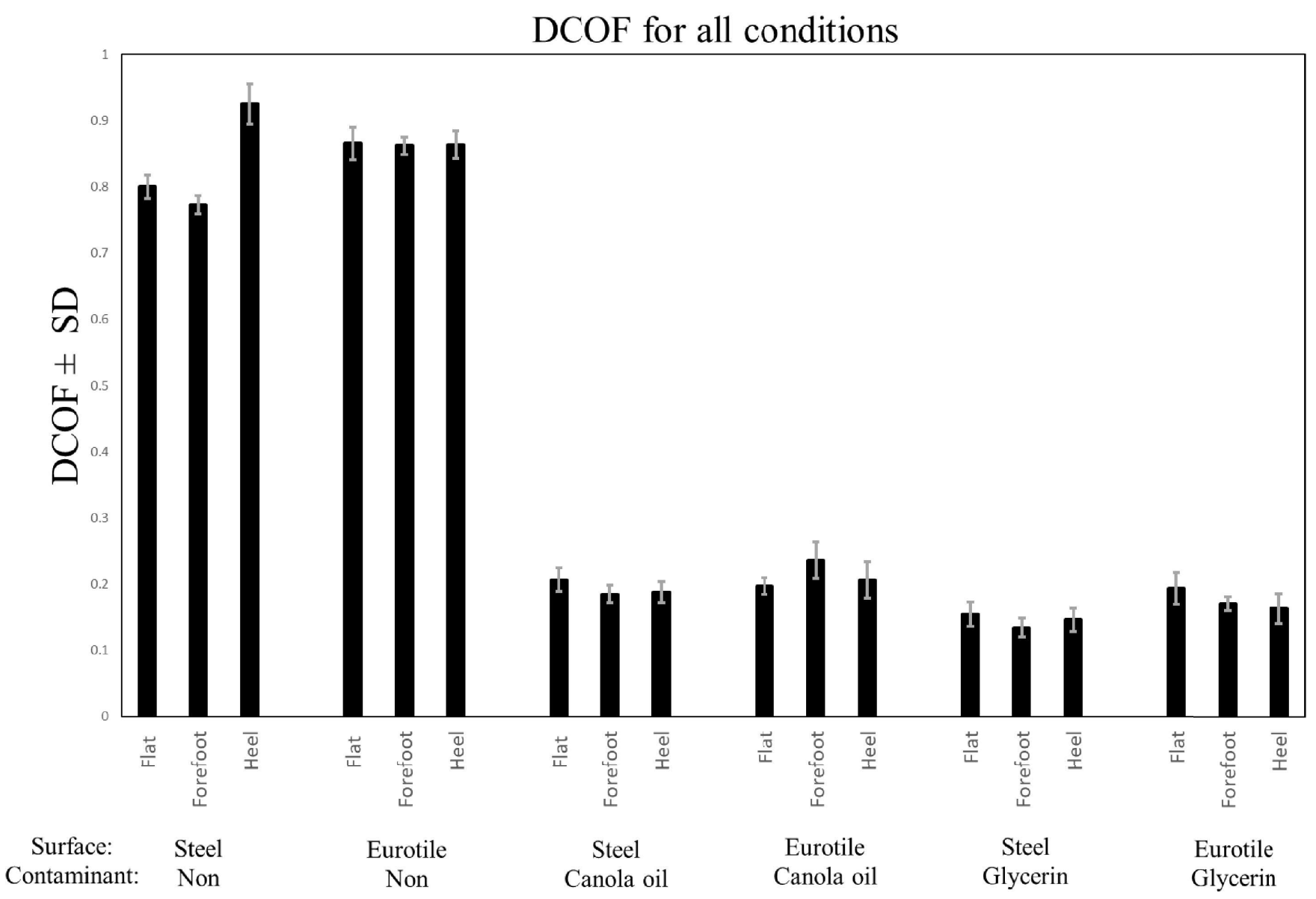
DCOF for all conditions
DCOF ± SD
1
0.9
0.8
0.7
0.6
0.5
0.4
0.3
0.2
0.1
0
Flat
Forefoot
Heel
Surface:
Contaminant:
Steel
Non
Eurotile
Non
Steel
Canola oil
Eurotile
Canola oil
Steel
Glycerin
Eurotile
Glycerin

Figure 7 Mean dynamic coefficient of friction for all tested conditions ± standard deviation.

Discussion

This study presents a new test setup for determining footwear ACOF measurements in close relation to the ISO 13287. The test setup repeatability is considered good with standard deviations below 0.03 (min: 0.01 max: 0.03) for all conditions. The test setup repeatability is similar to other slip resistance test devices presented in the scientific community (Aschan et al., 2005). The coefficient of friction test results on contaminated surfaces from this study are comparable to previous research with commercially available footwear (Grönqvist et al., 2003; Jones et al., 2018; Yamaguchi and Hokkirigawa, 2014).

Even though the presented test setup is assessed capable of performing in close relation to the ISO 13287, the testing parameters from the standard, may not be the most valid for predicting the ACOF (Blanchette and Powers, 2015). In fact, Blanchette and Powers compared ACOF and RCOF in an experiment and found that the setup parameters from the ISO 13287 (500 N normal load, 0.3 m/s sliding velocity and 7° heel contact angle) was only able to predict 35% of slip events. However, by modifying testing parameters to normal load of 400 N, sliding velocity of 0.5 m/s and heel contact angle at 9°, 74 % of slip events were predicted (Blanchette and Powers, 2015). This is supported by other research, which suggests contact pressure between 200-1000 kPa (Chang et al., 2001). Sliding velocity is recommended between 0-1 m/s (Chang et al., 2001) or 0.5-1 m/s (Hunwin et al., 2010). Static contact time is recommended at maximum 600 ms (Chang et al., 2001) or 0-250 ms (Grönqvist et al., 2003). Lastly, shoe/surface angle is recommended at 17° (Iraqi et al., 2018a), 13° (Beschorner et al., 2019) and 14.7° (Albert et al., 2017). Thus, a wide range of relevant testing parameters have been used in the scientific literature, which may be more suitable for predicting the ACOF of footwear.

An obvious advantage of test setup consisting of a movable force plate is the apparent high degree of flexibility. This could potentially allow us to alter biomechanical and tribophysical conditions such as; normal load, sliding velocity, shoe/surface angle, static contact time and different surface/contaminant conditions, which all independently have been shown to change footwear friction behavior (Chang et al., 2001).
The test setup represented in this study should be able to accommodate these alterations, with the velocity- and acceleration-controlled robotic platform (van Doornik and Sinkjaer, 2007). The force platform can tolerate normal load ranges from 250 N to 4448 N, sliding velocity between 0-1 m/s and heel contact angle between 0-45° and static contact time between 0-1 s. It should be noted that with an increasing sliding velocity, a decrease in friction measurement period (Figure 3 event 5-6) would be inevitable, due to the total robotic platform displacement distance of 120 mm in this setup. Modifications to the steel frame has to be made to accommodate the maximal robotic platform displacement distance of 200 mm. However, as long as the vertical and horizontal forces reaches a plateau, the DCOF calculation should be considered acceptable.

Due to the maximal displacement distance of 120 mm, requirement 5 (Measurement period should be between 0.3 s after start of movement and end 0.6 s after start of movement), could not be met. The 120 mm horizontal displacement caused an elapsed movement time of 0.35 s. Thus, a delay of 0.3 s from movement start to the beginning of the measurement period was not possible in this particular setup. This also led to a measurement period of 0.2 s instead of the 0.3 s suggested in the ISO 13287. Nonetheless, this time interval can be argued to be relevant, since slipping events have been shown to start between 30-50 ms after initial heel contact (Iraqi et al., 2018b). Averaging measurement period in the range of 0 ms (representing the instant of slip-

start) to 200 ms is argued to be reasonable (Beschorner et al., 2020). Additionally, the force measurements did reached a plateau in the friction measurement period (event 5-6) making the friction measurement considerably sufficient.

Conclusion

This study presented a new robotic force plate-based footwear slip resistance test setup. The design was largely able to accommodate the footwear friction device requirements stated in the ISO 13287, Personal protective equipment - Footwear - Test method for slip resistance. The test setup showed good repeatability with low standard deviations for all testing conditions. DCOF results were comparable to previous findings and this setup is therefore considered applicable for footwear slip resistance determination. Moreover, the design of this system allowed for a large degree of flexibility to vary the testing conditions. This is relevant then testing footwear slip resistance under biomechanically and tribophysical relevant conditions.

Acknowledgement

This study was funded by the Danish Working Environment Research Fund (grant number: 20195100816). Spraino ApS financed the construction of the frame atop the hydraulic system and lasts for fixation of footwear.

References

Advanced Mechanical Technology Inc., Platform datasheet http://www.a-tech.ca/Product/Series/2324/OPT464508HF_Optima_Force_Platform/?tab=6 [WWW Document]. URL http://www.a-tech.ca/Product/Series/2324/OPT464508HF_Optima_Force_Platform/?tab=6 (accessed 8.27.21).

Albert, D., Moyer, B., Beschorner, K.E., 2017. Three-Dimensional Shoe Kinematics During Unexpected Slips: Implications for Shoe–Floor Friction Testing. IISE Trans. Occup. Ergon. Hum. Factors 5, 1–11. https://doi.org/10.1080/21577323.2016.1241963

Arbejdstilsynet, 2017. Baggrundsnotat om snubleulykker (2017) - Alvorlige arbejdsulykker ved fald, gliden og snublen. Copenhagen.

Aschan, C., Hirvonen, M., Mannelin, T., Rajamäki, E., 2005. Development and validation of a novel portable slip simulator. Appl. Ergon. 36, 585–593. https://doi.org/10.1016/j.apergo.2005.01.015

Beschorner, K.E., Albert, D.L., Redfern, M.S., 2016. Required coefficient of friction during level walking is predictive of slipping. Gait Posture 48, 256–260. https://doi.org/10.1016/j.gaitpost.2016.06.003

Beschorner, K.E., Iraqi, A., Redfern, M.S., Cham, R., Li, Y., 2019. Predicting slips based on the STM 603 whole-footwear tribometer under different coefficient of friction testing conditions. https://doi.org/10.1080/00140139.2019.1567828

Beschorner, K.E., Iraqi, A., Redfern, M.S., Moyer, B.E., Cham, R., 2020. Influence of averaging time-interval on shoe-floor-contaminant available coefficient of friction measurements. Appl. Ergon. 82, 1–6. https://doi.org/10.1016/j.apergo.2019.102959

Beschorner, K.E., Singh, G., 2012. A Novel Method for Evaluating the Effectiveness of Shoe-Tread Designs Relevant to Slip and Fall Accidents. https://doi.org/10.1177/1071181312561560

Blanchette, M.G., Powers, C.M., 2015. Slip Prediction Accuracy and Bias of the SATRA STM 603 Whole Shoe Tester. J. Test. Eval. 43, 20130308. https://doi.org/10.1520/JTE20130308

Cham, R., Redfern, M.S., 2002. Changes in gait when anticipating slippery floors. Gait Posture 15, 159–171. https://doi.org/10.1016/S0966-6362(01)00150-3

Chang, W.R., Grönqvist, R., Leclercq, S., Brungraber, R.J., Mattke, U., Strandberg, L., Thorpe, S.C., Myung, R., Makkonen, L., Courtney, T.K., 2001. The role of friction in the measurement of slipperiness, Part 2: Survey of friction measurement devices. Ergonomics 44, 1233–1261. https://doi.org/10.1080/00140130110085583

Chang, W.R., Leclercq, S., Lockhart, T.E., Haslam, R., 2016. State of science: occupational slips, trips and falls on the same level State of science: occupational slips, trips and falls on the same level. Ergonomics 59, 861–883. https://doi.org/10.1080/00140139.2016.1157214

Courtney, T.K., Sorock, G.S., Manning, D.P., Collins, J.W., Holbein-Jenny, M.A., 2001. Occupational slip, trip, and fall-related injuries - Can the contribution of slipperiness be isolated? Ergonomics 44, 1118–1137. https://doi.org/10.1080/00140130110085538

Grönqvist, R., Matz, S., Hirvonen, M., 2003. Assessment of shoe-floor slipperiness with respect to contact-time-related variation in friction during heel strike. Occup. Ergon. 3, 197–208. https://doi.org/10.3233/OER-2003-3402

Hanson, J.P., Redfern, M.S., Mazumdar, M., 1999. Predicting slips and falls considering required and available friction. Ergonomics 42, 1619–1633. https://doi.org/001401399184712

Hunwin, G., Thorpe, S., Hallas, K., 2010. Improvements to the EN slip resistance test for footwear. Contemp. Ergon. Hum. Factors 2010 Proceeding, 471–479.

Insurance, L.M., 2019. Liberty Mutual Workplace Safety Index. 2019. Hopkinton, Massachusetts.

Iraqi, A., Cham, R., Redfern, M.S., Beschorner, K.E., 2018a. Coefficient of friction testing parameters influence the prediction of human slips. Appl. Ergon. 70, 118–126. https://doi.org/10.1016/j.apergo.2018.02.017

Iraqi, A., Cham, R., Redfern, M.S., Vidic, N.S., Beschorner, K.E., 2018b. Kinematics and kinetics of the shoe during human slips. J. Biomech. J. 74, 57–63. https://doi.org/10.1016/j.jbiomech.2018.04.018

Iraqi, A., Vidic, N.S., Redfern, M.S., Beschorner, K.E., 2020. Prediction of coefficient of friction based on footwear outsole features. Appl. Ergon. 82, 102963.

https://doi.org/10.1016/j.apergo.2019.102963
ISO, 1997. ISO 4287:1997 - Geometrical Product Specifications (GPS) — Surface texture: Profile method — Terms, definitions and surface texture parameters.
Jones, T., Iraqi, A., Beschorner, K., 2018. Performance testing of work shoes labeled as slip resistant. Appl. Ergon. 68, 304–312. https://doi.org/10.1016/j.apergo.2017.12.008
Liberty Mutual Workplace Safety Index 2012, n.d. . Hopkington, Massachusetts.
McLaughlin, P., 2013. Testing agreement between a new method and the gold standard—How do we test? | Elsevier Enhanced Reader. J. Biomech. 46, 2757–2760.
Oliveira, A.S., Silva, P.B., Lund, M.E., Farina, D., Kersting, U.G., 2017. Balance Training Enhances Motor Coordination During a Perturbed Sidestep Cutting Task. https://doi.org/10.2519/jospt.2017.6980 47, 853–862. https://doi.org/10.2519/JOSPT.2017.6980
Standard, I., 2019. Personal protective equipment – Footwear – Test method for slip resistance (ISO 13287:2019).
Sundhedsstyrelsen, 2016. Sygdomsbyrden i Danmark, Ulykker, Selvskade og Selvmord 2016. Copenhagen S.
van Doornik, J., Sinkjaer, T., 2007. Robotic Platform for Human Gait Analysis. IEEE Trans. Biomed. Eng. 54, 1696–1702. https://doi.org/10.1109/TBME.2007.894949
Yamaguchi, T., Hokkirigawa, K., 2014. Development of a High Slip-resistant Footwear Outsole Using a Hybrid Rubber Surface Pattern. Ind. Health 52, 414–423. https://doi.org/10.2486/indhealth.2014-0105
Yamaguchi, T., Masani, K., 2015. Contribution of center of mass-center of pressure angle tangent to the required coefficient of friction in the sagittal plane during straight walking. Biotribology 5, 16–22. https://doi.org/10.1016/j.biotri.2015.12.002

Appendix

Contaminant/Surface	Test modes	**DCOF** (±SD)
None/Steel	Flat	0.80 (0.01)
	Forefoot	0.77 (0.01)
	Heel	0.92 (0.03)
None/Eurotile	Flat	0.87 (0.02)
	Forefoot	0.86 (0.01)
	Heel	0.86 (0.02)
Canola oil/Steel	Flat	0.21 (0.02)
	Forefoot	0.18 (0.01)
	Heel	0.19 (0.02)
Canola oil/Eurotile	Flat	0.20 (0.01)
	Forefoot	0.24 (0.03)
	Heel	0.20 (0.03)
Glycerin/Steel	Flat	0.15 (0.02)
	Forefoot	0.13 (0.01)
	Heel	0.15 (0.02)
Glycerin/Eurotile	Flat	0.19 (0.02)
	Forefoot	0.17 (0.01)
	Heel	0.16 (0.02)

Table A.1 Mean DCOF ± SD for all conditions.

Ergonomics

ISSN: (Print) (Online) Journal homepage: https://www.tandfonline.com/loi/terg20

The Effect of Footwear Outsole Material on Slip Resistance on Dry and Contaminated Surfaces with Geometrically Controlled Outsoles

Lasse Jakobsen, Filip Gertz Lysdal, Timo Bagehorn, Uwe G. Kersting & Ion Marius Sivebaek

To cite this article: Lasse Jakobsen, Filip Gertz Lysdal, Timo Bagehorn, Uwe G. Kersting & Ion Marius Sivebaek (2022): The Effect of Footwear Outsole Material on Slip Resistance on Dry and Contaminated Surfaces with Geometrically Controlled Outsoles, Ergonomics, DOI: 10.1080/00140139.2022.2081364

To link to this article: https://doi.org/10.1080/00140139.2022.2081364

Lasse Jakobsen[a]*, Filip Gertz Lysdal[a], Timo Bagehorn[b], Uwe G. Kersting[b,c] and Ion Marius Sivebaek[a]

[a]*Department of Mechanical Engineering, Technical University of Denmark, Copenhagen, Denmark;*

[b]*Department of Health Science and Technology, Aalborg University, Denmark*

[c]*Institute of Biomechanics and Orthopaedics, German Sport University Cologne*

*Lasse Jakobsen, lasjak@mek.dtu.dk, corresponding author

Phone: 004520406213

Produktionstorvet, 425, 2800 Kgs. Lyngby, Denmark

The Effect of Footwear Outsole Material on Slip Resistance on Dry and Contaminated Surfaces with Geometrically Controlled Outsoles

Abstract

Previous studies have compared slip resistance of commercially available footwear, however, often lacking the ability to isolate factors such as material and surface properties, or/and geometry. The aim of this study was to compare slip resistance of geometrically identical shoes with varying outsole materials. Three left Ecco Xpedition III shoes were constructed out of three different outsole materials: polyurethane (PU), thermoplastic polyurethane (TPU) and vulcanized rubber (RU). The shoes were tested for dynamic coefficient of friction (DCOF) on a steel and a tile surface, without contamination and with glycerine and canola oil as contaminants. The shoes were significantly ($p<0.001$) different from each other across all surface/contaminant conditions/combinations, with the PU having a significantly 61-125% ($p<0.001$) higher DCOF on contaminated surfaces compared to the RU outsole.

Keywords: Friction; Footwear; Traction; Slips, trips and falls

Practitioner Summary: Previous research has suggested the importance of studying individual parameters separately of footwear in relation to slip resistance. In this study, we managed to construct geometrically identical shoes and compare the slip resistance between three different outsole materials. We found that the polyurethane outsole was the least slippery choice of material for this specific footwear model on contaminated surfaces.

Introduction

Falling accidents caused by slipping in work environments are a major concern and one of the leading causes of absence from work (Arbejdstilsynet, 2017; U.S. Department of Labor- Bureau of Labor Statistics, 2019). Insufficient friction between surface and footwear outsole has long been recognized as a direct risk factor for such slip accidents

to occur (Tisserand, 1985). This entails that either the surface, or the footwear outsole are factors that can be modified to improve slip resistance (Grönqvist et al., 2001).

One obvious way to optimize the friction properties is by changing the surface or surface roughness (Chang et al., 2001; Kim et al., 2013). However, branches such as food industry require high levels of hygiene standards, which limits the ability to increase surface roughness (Baker, 2013). Optimizing the friction properties of the footwear outsoles is therefore of superior relevance for the attempt to prevent slipping accidents.

Previous research has consequently primarily focused on footwear outsole materials and geometry, such as groove/thread pattern design and the associated slip resistance (Li and Chen, 2004). Footwear outsoles are typically constructed of different materials such as polyurethane (PU) (Gauvin et al., 2015), polyvinyl chloride (PVC) (Beschorner et al., 2009), ethylene vinyl acetate (EVA), natural rubber (Gauvin et al., 2015), neolite (Li and Chen, 2004) and thermoplastic polyurethane (TPU) (Sato et al., 2020) among others. Hence, a variety of different outsole materials exists and suits different uses, manufacturing processes and costs. Research, which controls for individual parameters (e.g., outsole geometry and materials and material properties) is needed to accurately study the effect of specific parameters (Gao and Abeysekera, 2004; Jones et al., 2018). Nonetheless, footwear used in scientific investigations are often prototypes and may undergo substantially alterations in the ramp up process before serial production.

This led to the purpose of this study, which was to investigate the mechanical slip resistance of three geometrically identical footwear samples, produced with three different outsole materials to the exact specifications by the manufacturer, as if they were for retail.

Method

Footwear

Three types of commercially available and commonly used outsole materials were used in the production of three complete shoes (Figure 1) of the same footwear model (Xpedition III, ECCO A/S, Bredebro, Denmark). These three materials require a different and specific manufacturing process, namely: low pressure injection of polyurethane (PU), injection moulding of a thermoplastic polyurethane (TPU) and vulcanization of rubber (RU), which also is the original commercially available version. The shoe soles were constructed using the same mould, and the shoes were thus identical in appearance, size and geometry, but varied in the choice of outsole material. The hardness of the three materials was measured statically through the use of a shore A durometer, with five separate measurements performed on the heel of each shoe. The TPU was the hardest material with an average shore A hardness score of 79.6 (SD: 1.14), followed by RU with an average Shore A of 68.4 (SD: 1.14), and PU with 56.4 (SD: 0.89).

Figure 1: Testing prototypes/shoes constructed of RU (left – note the red part in the forefoot is also RU), PU (middle) and TPU (right).

Surfaces and contaminants

Two surfaces were used in the setup. One ceramic tile (Eurotile 2 specified in ISO 13287:2019 Footwear – test method for slip resistance) and a steel plate (number 1.4301). The roughness was measured using a Surtronic 25 profilometer (Taylor Hobson, Leicester, United Kingdom) in accordance with the specification from ISO 13287. According to the ISO 13287, the average of 10 Rz measurements on the steel surface at different locations shall be between 1.6 µm and 2.5 µm. The average of 10 Rz measurements was 1.65 µm for the steel surface. The average of 10 Rz measurements conducted on the Eurotile was 20.00 µm and should be between 20.00 µm and 26.00 µm. Cutoff length for the roughness measurements was 0.25 mm for the steel plate and 2.5 mm for the Eurotile. The two surfaces were attached on top of the force plate with double-sided tape to ensure fixation. Eighty-five percent glycerine solution (85% glycerol and 15% water by volume solution with a viscosity of 110 cP at 20 °C) (GP Association, 1963), as used in the ISO 13287 and Canola oil (65 cP at 20°C) (Jones et al., 2018) was used as surface contaminants. 50 ml contamination was used and distributed with a brush over an area of 10 by 40 cm, to ensure full contamination of the entire area between shoe and surface. Contaminants were removed and replenished when changing shoe or surface.

Slip resistance measurements

The three shoes were tested for slip resistance with a modified robotic platform developed for human gait analysis (van Doornik and Sinkjaer, 2007). A detailed description of the slip resistance measurement system has been previously described (Jakobsen et al., 2022). A steel frame was designed to maintain a fixed position of a shoe and last above a force plate (AMTI- OPT464508HF-1000, Advanced Mechanical Technology, Inc. Watertown MA, USA). The force plate was mounted atop of a

hydraulic platform (Serman-Tipsmark, Brønderslev, Denmark), able to move along the vertical and horizontal axes. Sliding velocity was set to 0.3 m/s and normal force set to 500 N in accordance with the ISO 13287. Shoe cleaning/preparation, surface roughness measurements and contaminant concentrations followed the guidelines specified in ISO 13287. Thus, the shoes were sanded with 400 grit sandpaper, cleaned using an ethanol solution, scrubbed with a clean medium stiff brush, washed with demineralized water, dried using clean dry compressed air, and then rested at the room temperature. Surfaces were washed with an ethanol solution, scrubbed gently with a clean medium stiff brush, rinsed with demineralized water and dried using clean dry compressed air and then at ambient temperature.

The shoes were oriented/aligned with the sole in parallel with forward moving direction, hence the platform moved from forefoot to heel (Figure 2). Five slip resistance measurements were performed for each of six different surface/contaminant combinations. All non-contaminant measurements were carried out prior to the contaminated measurements. Measurements with glycerine contamination were carried out secondly and canola oil contaminant measurements were performed last. Surfaces and shoes were thoroughly cleaned with soap and rinsing water between contaminant conditions.

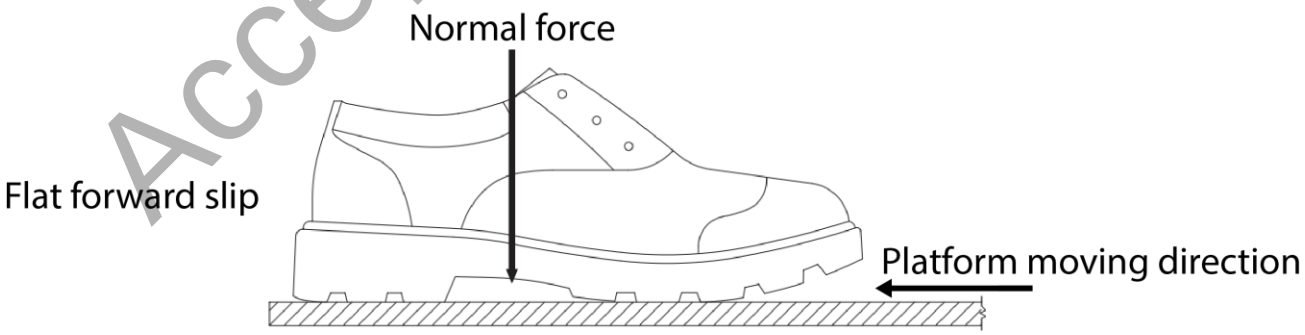

Figure 2 Testing mode: flat forward. Adapted from ISO 13287 with permission from Danish Standards (ISO 13287, 2019).

Data processing and statistical analysis

The dynamic coefficient of friction (DCOF) was used as a measure of slip resistance and was calculated using a customize script in MATLAB version R2020b (MathWorks, Massachusetts, USA) by dividing the sum of the horizontal reaction forces, F_x and F_y (friction forces) with the vertical reaction force F_z (normal force) (Jakobsen et al., 2022) A one-way ANOVA was performed in Minitab version 19.2020.1 (Minitab, Pennsylvania, USA) to compare the effect of outsole materials on DCOF means within each of the six surface/contaminant combinations. A Tukey post-hoc test analysis was performed to detect significant difference between shoes within each surface/contaminant combinations, with RU used as reference in the reporting.

Results

Steel surface without contaminations

There was a statistically significant difference among the three shoes on the steel surface when no contaminates were present as determined by one-way ANOVA ($F(2,12) = 2884.82$, $p< 0.0001$). The post hoc test revealed a significant difference in DCOF for TPU ($P <0.0001$, 95% C.I = [-0.04103; -0.01279]), which is 2.86% lower than RU (Table 1 and Figure 3). PU was also significantly different ($P <0.0001$, 95% C.I = [(0.34702; 0.37526)]) with 33.33% lower DCOF compared to RU (Table 1 and Figure 3).

Eurotile surface without contaminations

There was a statistically significant difference among the three shoes on the Eurotile surface when no contaminates were present as determined by one-way ANOVA ($F(2,12) = 1391.14$, $p< 0.0001$). The post hoc test revealed a significant difference in

DCOF for TPU (P <0.0001, 95% C.I = [-0,15887; -0,12408]), which is 13.04% lower than RU (Table 1 and Figure 3). PU was also significantly different (P <0.0001, 95% C.I = [(0,32504; 0,35983)]) with 29.57% lower DCOF compared to RU (Table 1 and Figure 3).

Steel surface with canola oil contamination

There was a statistically significant difference among the three shoes on the steel surface when canola oil contaminates were present as determined by one-way ANOVA ($F(2,12) = 6316.40$, $p< 0.0001$). The Tukey post hoc test revealed a significant difference in DCOF for TPU (P = 0.0166, 95% C.I = [-0.005558; -0.000580]), which is 7.14% lower than RU (Table 1 and Figure 3). PU was also significantly different (P <0.0001, 95% C.I = [-0.091795; -0.086817]) with 64.29% higher DCOF compared to RU (Table 1 and Figure 3).

Eurotile surface with canola oil contamination

There was a statistically significant difference among the three shoes on the Eurotile surface when canola oil contaminates were present as determined by one-way ANOVA ($F(2,12) = 3437.62$, $p< 0.0001$). The Tukey post hoc test revealed a significant difference in DCOF for TPU ($P \leq 0.0001$, 95% C.I = [0.09055; 0.10359]), which is 62.5% higher than RU (Table 1 and Figure 3). PU was also significantly different (P <0.0001, 95% C.I = [-0.20932; -0.19628]) with 125% higher DCOF compared to RU (Table 1 and Figure 3).

Steel surface with glycerine contamination

There was a statistically significant difference among the three shoes on the steel surface when glycerine contaminates were present as determined by one-way ANOVA

(F(2,12) = 5217.03, p< 0.0001). The Tukey post hoc test revealed a significant difference in DCOF for TPU (P ≤ 0.0001, 95% C.I = [-0.06440; -0.05881]), which is 33.33% lower than RU (Table 1 and Figure 3). PU was also significantly different (P <0.0001, 95% C.I = [-0.04774; -0.04215]) with 22.22% higher DCOF compared to RU (Table 1 and Figure 3).

Eurotile surface with glycerine contamination

There was a statistically significant difference among the three shoes on the Eurotile surface when glycerine contaminates were present as determined by one-way ANOVA (F(2,12) = 5373.39, p< 0.0001). The Tukey post hoc test revealed a significant difference in DCOF for TPU (P ≤ 0.0001, 95% C.I = [-0.03191; -0.02291]), which is 8.7% lower than RU (Table 1 and Figure 3). PU was also significantly different (P <0.0001, 95% C.I = [-0.14046; -0.13147]) with 60.87% higher DCOF compared to RU (Table 1 and Figure 3).

Contaminant	**Surface**	**Shoes**	**DCOF μ** (±SD)	**Relative difference**
non	steel	RU	1.05 (0.02)	Original
non	steel	PU	0.70 (0.02)*	-33.33%
non	steel	TPU	1.02 (0.02)*	-2.86%
non	Eurotile	RU	1.15 (0.03)	Original
non	Eurotile	PU	0.81 (0.02)*	-29.57%
non	Eurotile	TPU	1.00 (0.03)*	-13.04%
canola oil	steel	RU	0.14 (0.02)	Original
canola oil	steel	PU	0.23 (0.02)*	64.29%
canola oil	steel	TPU	0.13 (0.02)*	-7.14%
canola oil	Eurotile	RU	0.16 (0.03)	Original
canola oil	Eurotile	PU	0.36 (0.03)*	125.00%
canola oil	Eurotile	TPU	0.26 (0.03)*	62.50%
glycerine	steel	RU	0.18 (0.02)	Original
glycerine	steel	PU	0.22 (0.02)*	22.22%

glycerine	steel	TPU	0.12 (0.02)*	-33.33%
glycerine	Eurotile	RU	0.23 (0.02)	Original
glycerine	Eurotile	PU	0.37 (0.02)*	60.87%
glycerine	Eurotile	TPU	0.21 (0.01)*	-8.70%

Table 1 Mean DCOF ± standard deviation and relative difference compared to the original RU version. * represents significant difference ($p<0.05$) from the original RU within each surface/contaminant combination.

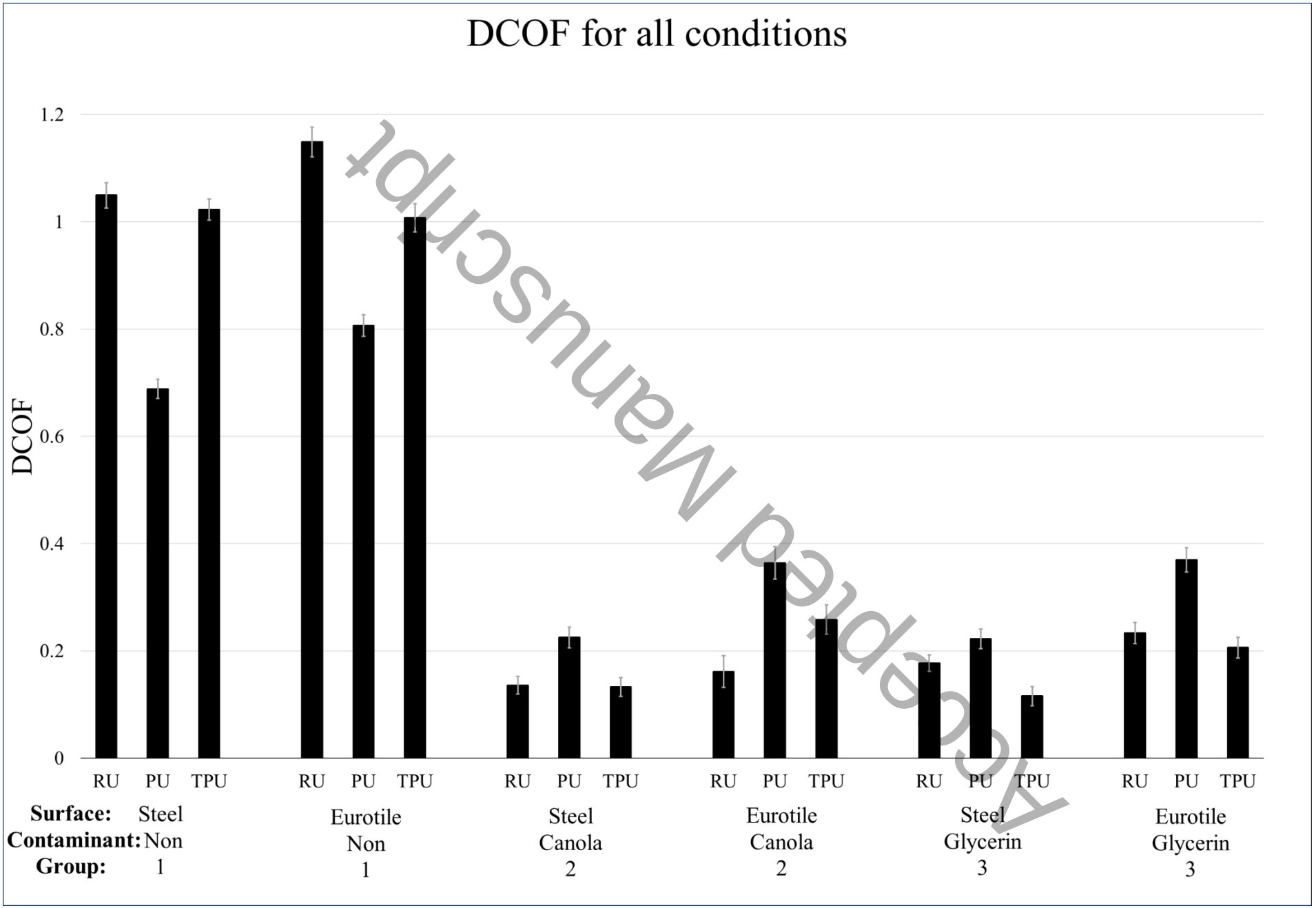

Figure 3 Mean DCOF plot for all shoes and conditions ± standard deviation.

Discussion

In this study, the slip resistance of geometrically identical shoes with three different outsole materials and two different contaminants were tested systematically. The RU sole had the highest DCOF on both the steel and Eurotile surface, when no contaminants were present. The PU sole had the highest DCOF on both the steel and the Eurotile surfaces with both canola oil and glycerine as contaminants. The lowest DCOF was found for the TPU sole on the steel surface with glycerine as contaminant.

The results from this study are somewhat comparable to previous research with comparable footwear, hardness, contaminations and surfaces (Iraqi et al., 2020; Moghaddam et al., 2018; Walter et al., 2021). Walter and colleagues measured the DCOF of rubber soles with three different outsole designs and different hardness levels (shore A 66-71) on a glycerine-contaminated tile and found the DCOF ranging from ~0.06 - ~0.37. The findings for the rubber outsole in our study is within this range with a DCOF of 0.23 on the Eurotile surface contaminated with glycerine. Moghaddam and colleagues compared slip resistance of shoes with different material properties and identical geometry on a canola oil contaminated tile and found DCOF ranging from ~0.1-0.5. This range is also comparable to our DCOF measurement range (0.13-0.36) on the Eurotile contaminated with canola oil. Lastly, Iraqi et al., 2020 used geometrically identical soles with different hardness (shore A 54, 60, 63) on two tile types, contaminated with canola oil and found DCOF ranging from ~0.3-0.6. These findings are comparable to the soft PU (shore A 56) used in this study with a DCOF of 0.36 on the canola oil contaminated Eurotile.

Previous research has outlined the importance of choosing the right footwear material for the intended environments for optimal slip resistance (Beschorner et al., 2009;

Manning & Jones, 2001; Strobel et al., 2012). Thus, the results from this study support previous findings of PU materials being more slip resistant than other common outsole materials on contaminated surfaces. Even though PU outsoles outperform rubber outsoles in slip resistance, they have also been found to wear out faster (Kim, 2016), leading to a more rapid decrease in slip resistance. This characteristic is especially evident on contaminated surfaces, where the draining abilities of an outsole is reduced as the wear and tear increases (Hemler et al., 2021). The use of PU would therefore arguably require a more frequent replacement of the footwear to maintain an adequate protection from slipping. In addition, the low DCOF found for the PU sole under dry conditions may be due to its low hardness. It has previously been shown that elastomer tread block deformation reduces the contact area, resulting in low adhesion friction under dry condition (Moriyasu et al., 2019). This deformation purportedly also leads to high contact pressure at the front corner edges of the tread pattern. This edge contact and high contact pressure can prevent infiltration of the contaminating fluids, which may increase adhesion friction under contaminated conditions (Yamaguchi et al., 2017). Since the surfaces used in this study have relatively low roughness, the adhesive friction contribution is important (Persson and Volokitin, 2006). This might also explain why the harder rubber sole has a lower DCOF when contaminated, due to its lower stress concentration at the front corner edges.

Material properties, such as hardness, has previously been found to affect slip resistance. Therefore, softer materials may be considered more slip resistant than harder materials, in particular when contaminations are present (Grönqvist, 1995). Nonetheless, a pilot study from the present research group, suggests that dynamic mechanical analysis (DMA) can extend the traditional static hardness material characterization of PU and RU soles and have shown that the stiffness of outsoles is

highly dependent on load frequency (Jakobsen et al., 2021 A). A theory for rubber friction predicts the friction coefficient based on the surface roughness, sliding velocity, the storage and loss modulus, temperature, nominal contact pressure and Poisson's ratio (Persson, 2001) in which the storage and loss modulus can be determined with a DMA (Menard and Menard, 2020). It is unknown if this theory is also valid for other viscoelastic materials (such as TPU and PU). Hence, future studies need to focus on the dynamic material properties of outsole materials rather than static hardness measurements in the attempt to optimize outsole materials to accommodate the biomechanical and tribophysical conditions from real slipping events.

It should be noted that the testing parameters from the ISO 13287 may not be most valid for replicating the biomechanical conditions from slipping accidents (Blanchette and Powers, 2015). In fact, sliding velocities, normal loads and heel/floor angles could be altered to accommodate more valid testing parameters (Beschorner et al., 2019; Chang et al., 2001; Hunwin et al., 2010; Iraqi et al., 2018). Thus, these parameters should arguably be altered to test whether any tested outsoles still meet the RCOF limit.

Limitations

It is emphasized that the shoes were identical in geometry and constructed of materials applicable in a real shoe manufacturing line. Even though the shoes were identical in geometry, we were not able to normalise outsole hardness, with the PU sole being the softest, followed by the RU and TPU soles respectively. Hardness has previously been found to affect footwear slip resistance, with softer outsoles being more slip resistant when contaminants are present (Grönqvist, 1995). Future studies related to selection of slip resistant outsole materials should also control for hardness across materials.

The shoes were tested on a flat forward condition as specified in the ISO 13287. However, this condition may not be the most biomechanically relevant representation of

a slip event, since the highest risk of slipping is at the initial heel contact phase (Strandberg, 1983). Additional measurements with focus on the heel part should be conducted in future studies, as this may vary the obtained slip resistance.

Furthermore, we only tested one sample of each shoe, with a potential risk of a carry-over effect of contaminations between testing conditions. To accommodate this risk, all non-contaminated measurements were performed first, followed by glycerine and canola oil contaminated measurements, in the same order. Moreover, the shoe samples were thoroughly cleaned by abrasion, brushing, washing, ethanol wiping and dried with compressed air.

We did not assess or control for outsole surface roughness. We assumed that the surface roughness of the shoe soles was identical between samples, due to the use of the same mould in the manufacturing process, as well as the same pre-testing preparation procedure using 400 Grit sandpaper.

Lastly, since we only compared one outsole tread pattern, it is not possible to extrapolate the findings from this study to other outsole patterns, and it remains unknown if the differences between the three outsole materials would be similar for other outsole patterns.

Conclusion

The findings from this study suggest that outsole materials play an important role in the complete footwear/surface tribosystem, and also suggests that the choice of outsole materials is dependent on the present surfaces and contaminants in the given environment. We found that the PU outsole with shore A 56.4 hardness had better slip resistance compared to the TPU with shore A 79.6 and the RU with shore A 68.4 on contaminated surfaces.

This study adds to the growing body of evidence suggesting that PU outsole is a good material candidate for slip resistant outsoles in contaminated environments. However, various material compositions of each material exist, why it is also unclear which material formulation may form the most slip resistant outsole. Further studies controlling for, e.g., outsole hardness and material compositions are needed to conclude that PU outsoles are more slip resistant under certain contaminated surface conditions, than other materials.

Acknowledgment and conflicts

This study was funded by the Danish Working Environment Research Fund (grant number: 20195100816). ECCO Shoes A/S manufactured the shoes used in this study, but had no role in the interpretation and presentation of the results. The authors want to thank Sophia Sachse from ECCO A/S for her extensive help and very fast execution. The authors have no conflict of interest to declare.

References

Arbejdstilsynet, 2017. Baggrundsnotat om snuble ulykker (2017).

Baker, C.G.J., 2013. Handbook of food factory design, Handbook of Food Factory Design. https://doi.org/10.1007/978-1-4614-7450-0

Beschorner, K., Lovell, M., Higgs, C.F., Redfern, M.S., Beschorner, K., Lovell, M., Fred Higgs Iii, C., Redfern, M.S., Fred Higgs Iii, C., 2009. Modeling mixed-lubrication of a shoe-floor interface applied to a pin-on-disk apparatus. Tribol. Trans. 52, 560–568. https://doi.org/10.1080/10402000902825705

Beschorner, K.E., Iraqi, A., Redfern, M.S., Cham, R., Li, Y., 2019. Predicting slips

based on the STM 603 whole-footwear tribometer under different coefficient of friction testing conditions. https://doi.org/10.1080/00140139.2019.1567828

Blanchette, M.G., Powers, C.M., 2015. Slip Prediction Accuracy and Bias of the SATRA STM 603 Whole Shoe Tester. J. Test. Eval. 43, 20130308. https://doi.org/10.1520/JTE20130308

Chang, W.-R., Grönqvist, R., Leclercq, S., Myung, R., Makkonen, L., Strandberg, L., Brungraber, R.J., Mattke, U., Thorpe, S.C., 2001. The role of friction in the measurement of slipperiness, Part 1: Friction mechanisms and definition of test conditions The role of friction in the measurement of slipperiness, Part 1: Friction mechanisms and definition of test conditions. Ergonomics 44. https://doi.org/10.1080/00140130110085574

Chang, W.R., Kim, I.J., Manning, D.P., Bunterngchit, Y., 2001. The role of surface roughness in the measurement of slipperiness, in: Ergonomics. https://doi.org/10.1080/00140130110085565

Gao, C., Abeysekera, J., 2004. A systems perspective of slip and fall accidents on icy and snowy surfaces. Ergonomics 47, 573–598. https://doi.org/10.1080/00140130410081658718

Gauvin, C., Pearsall, D., Damavandi, M., Michaud-Paquette, Y., Farbos, B., Imbeau, D., 2015. Risk Factors for Slip Accidents among Police Officers and School Crossing Guards . Montréal, Québec.

GP Association, 1963. Physical properties of glycerol and its solutions. Glycerine Prod. Assoc. 1–27.

Grönqvist, R., 1995. Mechanisms of friction and assessment of slip resistance of new and used footwear soles on contaminated floors. Ergonomics 38, 224–241. https://doi.org/10.1080/00140139508925100

Grönqvist, R., Chang, W., Courtney, T.K., Leamon, T.B., Redfern, M.S., K, T., B, T., S, M., 2001. Measurement of slipperiness : fundamental concepts and definitions. Ergonomics 44, 1117. https://doi.org/10.1080/00140130110085552

Hemler, S.L., Pliner, E.M., Redfern, M.S., Haight, J.M., Beschorner, K.E., 2021. Effects of natural shoe wear on traction performance: a longitudinal study. Footwear Sci. 1–12.

Hunwin, G., Thorpe, S., Hallas, K., 2010. Improvements to the EN slip resistance test for footwear. Contemp. Ergon. Hum. Factors 2010 Proceeding, 471–479.

Iraqi, A., Cham, R., Redfern, M.S., Beschorner, K.E., 2018. Coefficient of friction testing parameters influence the prediction of human slips. Appl. Ergon. 70, 118–126. https://doi.org/10.1016/j.apergo.2018.02.017

Iraqi, A., Vidic, N.S., Redfern, M.S., Beschorner, K.E., 2020. Prediction of coefficient of friction based on footwear outsole features. Appl. Ergon. 82, 102963. https://doi.org/10.1016/j.apergo.2019.102963

Jakobsen, L., Lysdal, F.G., Bagehorn, T., Kersting, U.G., Sivebaek, I.M., 2022. Evaluation of an actuated force plate-based robotic test setup to assess the slip resistance of footwear. Int. J. Ind. Ergon. 88, 103253. https://doi.org/10.1016/J.ERGON.2021.103253

Jakobsen, L., Lysdal, F.G., Sivebaek, I.M., 2021. Dynamic mechanical analysis as a

predictor for slip resistance and traction in footwear. Footwear Sci. 13, S57–S58. https://doi.org/10.1080/19424280.2021.1917680

Jones, T., Iraqi, A., Beschorner, K., 2018. Performance testing of work shoes labeled as slip resistant. Appl. Ergon. 68, 304–312. https://doi.org/10.1016/j.apergo.2017.12.008

Kim, I.-J., Hsiao, H., Simeonov, P., 2013. Functional levels of floor surface roughness for the prevention of slips and falls: Clean-and-dry and soapsuds-covered wet surfaces. Appl. Ergon. 44, 58–64. https://doi.org/10.1016/j.apergo.2012.04.010

Kim, I.J., 2016. Identifying shoe wear mechanisms and associated tribological characteristics: Importance for slip resistance evaluation. Wear 360–361, 77–86. https://doi.org/10.1016/j.wear.2016.04.020

Li, K.W., Chen, C.J., 2004. The effect of shoe soling tread groove width on the coefficient of friction with different sole materials, floors, and contaminants. Appl. Ergon. 35, 499–507. https://doi.org/10.1016/j.apergo.2004.06.010

Manning, D.P., Jones, C., 2001. The effect of roughness, foor polish, water, oil and ice on underfoot friction: current safety footwear solings are less slip resistant than microcellular polyurethane. Appl. Ergon. 32, 185–196.

Menard, K., Menard, N., 2020. Dynamic Mechanical Analysis, 3rd ed. CRC Press, Boca Raton. https://doi.org/10.1007/978-3-540-29805-2_1224

Moghaddam, S.R.M., Acharya, A., Redfern, M.S., Beschorner, K.E., 2018. Predictive multiscale computational model of shoe-floor coefficient of friction. J. Biomech. 66, 145–152. https://doi.org/10.1016/j.jbiomech.2017.11.009

Moriyasu, K., Nishiwaki, T., Shibata, K., Yamaguchi, T., Hokkirigawa, K., 2019. Friction control of a resin foam/rubber laminated block material. Tribol. Int. 136. https://doi.org/10.1016/j.triboint.2019.04.024

Persson, B.N.J., 2001. Theory of rubber friction and contact mechanics. J. Chem. Phys. https://doi.org/10.1063/1.1388626

Persson, B.N.J., Volokitin, A.I., 2006. Rubber friction on smooth surfaces. Eur. Phys. J. E 21. https://doi.org/10.1140/epje/i2006-10045-9

Sato, S., Yamaguchi, T., Shibata, K., Nishi, T., Moriyasu, K., Harano, K., Hokkirigawa, K., 2020. Dry sliding friction and Wear behavior of thermoplastic polyurethane against abrasive paper. Biotribology 23. https://doi.org/10.1016/j.biotri.2020.100130

Standard, I., 2019. Personal protective equipment – Footwear – Test method for slip resistance (ISO 13287:2019).

Strandberg, L., 1983. On accident analysis and slip-resistance measurement. Ergonomics 26, 11–32. https://doi.org/10.1080/00140138308963309

Strobel, C.M., Menezes, P.L., Lovell, M.R., Beschorner, K.E., 2012. Analysis of the contribution of adhesion and hysteresis to shoe-floor lubricated friction in the boundary lubrication regime. Tribol. Lett. 47, 341–347. https://doi.org/10.1007/s11249-012-9989-5

Tisserand, M., 1985. Progress in the prevention of falls caused by slipping. Ergonomics 28, 1027–1042. https://doi.org/10.1080/00140138508963225

U.S. Department of Labor- Bureau of Labor Statistics, 2019. TABLE R4. Number of

Nonfatal Occupational Injuries and Illnesses Involving Days Away from Work by Industry and Selected Events or Exposures Leading to Injury or Illness, vol. 2019.

van Doornik, J., Sinkjaer, T., 2007. Robotic Platform for Human Gait Analysis. IEEE Trans. Biomed. Eng. 54, 1696–1702. https://doi.org/10.1109/TBME.2007.894949

Walter, P.J., Tushak, C.M., Hemler, S.L., Beschorner, K.E., 2021. Effect of tread design and hardness on interfacial fluid force and friction in artificially worn shoes. Footwear Sci. 13, 245–254. https://doi.org/10.1080/19424280.2021.1950214

Yamaguchi, T., Katsurashima, Y., Hokkirigawa, K., 2017. Effect of rubber block height and orientation on the coefficients of friction against smooth steel surface lubricated with glycerol solution. Tribol. Int. 110. https://doi.org/10.1016/j.triboint.2017.02.015

Dynamic and Static Friction Measurements of Elastomer Footwear Blocks on Ice Surface

***Lasse Jakobsen[a], Sondre Bergtun Auganæs[b], Audun Formo Buene[b], Ion Marius Sivebaek[a] & Alex Klein-Paste[b]**

[a] Department of Mechanical Engineering, Technical University of Denmark, Copenhagen, Denmark,

*Corresponding author: lasjak@mek.dtu.dk

[b] Department of Civil and Environmental Engineering, Norwegian University of Science and Technology, Trondheim, Norway

Abstract

This study conducted friction experiments of three elastomer block materials on ice (low pressure injection of polyurethane (PU), injection moulding of a thermoplastic polyurethane (TPU) and vulcanization of rubber (RU)), with a linear tribometer operating under four different ambient air temperatures (-10 °C to 0 °C) and six different sliding velocities (0.3 to 5 m/s). At low temperatures (-10 °C and -5 °C), the RU material showed the highest dynamic and static friction. However, at high temperatures (-2 °C and 0 °C) the PU revealed the highest dynamic friction and highest static friction at 0 °C. We discuss the physical phenomena's of elastomer friction on ice and in relation to the application of footwear slipping on ice.

Keywords

Footwear; Slip resistance; Elastomer friction, Ice,

1. Introduction

Rubber and elastomer friction on ice surfaces is of great importance in relation to skid resistance of winter tires and slip resistance of footwear. The latter can lead to falling and serious injury if insufficient friction between footwear and ice exists (Chang et al., 2010; Grönqvist & Hirvonen, 1995). In Norway, the most frequent cause of work-related injuries in 2020 was due to falls (Statistics Norway, 2021). This challenge is also present in Denmark, with 110,000 reported fall

accidents, where 750 had fatal outcome in 2016 (Sundhedsstyrelsen, 2016). One of the leading causes of falls is due to slipping (Grönqvist et al., 2001; Hanson et al., 1999). In the Scandinavian countries slippery surfaces is a well-known phenomenon, which often implies snow- and ice-covered roads and walkway pavements. This leads to increased risk of slipping and falling for pedestrians and outdoor workers (Courtney et al., 2001; Gauvin et al., 2015). Therefore, it is important to work on potential strategies to increase slip resistance include spreading sand or salt (Gao & Abeysekera, 2002). The latter is especially an effective dissolver of ice and snow (Wåhlin et al., 2014), which results in increased coefficient of friction between viscoelastic materials and wet pavements (Klein-Paste & Wåhlin, 2013). Footwear outsoles are most often constructed of viscoelastic materials, such as polyurethane (PU) (Gauvin et al., 2015), natural rubber (Gauvin et al., 2015) and thermoplastic polyurethane (TPU) (Sato et al., 2020), and the choice of outsole material affects the slip resistance on ice (Hsu et al., 2016). However, research on footwear slipperiness has primarily been aimed at indoor contaminated surfaces (Jakobsen et al., 2022; Jones et al., 2018; D. Manning et al., 1985; Yamaguchi et al., 2017), where footwear for outdoor occupations has received less attention (Bagheri et al., 2021). Furthermore, it is argued that the most slip resistant footwear materials on contaminated surfaces, may not be the ideal material candidates on icy surfaces (Gao et al., 2004).

For classification and certification purposes, footwear can be tested on ice surfaces in accordance with testing parameters of the ISO 13287 - Personal protective equipment – Test method for slip resistance (ISO 13287:2019 standard). One of the testing parameters implies a sliding velocity of 0.3 m/s. However, slipping events starts when the static friction between the shoe and ice is exceeded. After this, the sliding velocity quickly increases and can be as high as 2.5 m/s (Chang et al., 2001 a). This is an important fact, since the friction properties of viscoelastic outsole

materials are dependent on temperature and load frequency (Persson, 2001), hence also sliding velocity (Jakobsen et al., 2021). Therefore, it is important to conduct static and dynamic friction measurements of viscoelastic materials in a range of sliding velocities and temperatures to obtain realistic application-oriented results. e.g. the tire-ice contact mechanism is an application where the viscoelastic material properties have been found to affect elastomer friction on ice (Klapproth et al., 2016) and is thus also expected to affect the somewhat similar contact mechanism between footwear and ice. Thorough studies of rubber (Lahayne et al., 2016) and polymer (Bäurle et al., 2007) friction on ice, with varying sliding velocities, has been made with both experimental and modelling approaches. However, to the author's knowledge, specific measures performed on elastomer outsole material candidates, during biomechanical relevant loading conditions on ice, has not been reported. Biomechanical loading conditions such as normal load, static contact time and sliding velocity is referred to as biofidelity, whereas the ability to replicate realistic walkway surfaces and contaminants is referred to as environmental fidelity (Chang et al., 2010).

To investigate real-world slipping events, it is crucial to acquire footwear slip resistance measurements with actual footwear outsole materials, obtained under bio- and environmental fidelity conditions. This is the motivation to perform controlled indoor tests on a linear tribometer to determine the friction properties between different elastomer materials used for footwear outsoles on an ice surface.

2. **Methods**

Friction properties between three outsole materials were quantified with a linear tribometer placed in a walk-in freezer. The tribometer is described in details by Giudici and colleagues (Giudici et al., 2017) and evaluated for precision by Auganæs and colleagues (Auganæs et al., 2022).

Footwear material properties, ice surface construction and characteristics, and testing procedure are described in the following sections.

2.1. Footwear outsole material samples

The three materials correspond to three different footwear outsole manufacturing processes, namely: low pressure injection of polyurethane (PU), injection moulding of a thermoplastic polyurethane (TPU) and vulcanization of rubber (RU). The materials were provided as material sheets by ECCO (ECCO A/S, Bredebro, Denmark).

2.1.1. Outsole material mechanical characterization

The materials had a short term (< 10 s) shore A hardness of; PU = 56, TPU = 80 and RU = 68. Dynamic material properties were characterized with Dynamic Mechanical Analysis (DMA) using the time-temperature superposition (TTS) principle (Menard & Menard, 2020). Ø8 mm samples of the three materials were cooled to -130 °C and a thermogram was measured from -130 °C to ~ 300 °C at 1 Hz and 2 °C/min. Frequency sweeps from 10 to 0.1 Hz are done at selected temperatures. TTS master curves were constructed with 23 °C as the reference temperature and are illustrated in Figure 1. Material stiffness (G′) and damping (tan(δ)) corresponding to the selected freezer temperatures (-10, -5, -2 and 0 °C) are presented in Table 1.

Table 1 Material properties obtained with dynamic mechanical analysis at selected freezer temperatures.

	-10 °C		-5 °C		-2 °C		0 °C	
	G' (MPa)	tan(δ)	G' (MPa)	tan(δ)	G' (MPa)	tan(δ)	G' (MPa)	tan(δ)
PU	1.9	0.39	1.65	0.29	1.5	0.26	1.4	0.24
TPU	3.1	0.28	2.95	0.195	2.85	0.16	2.8	0.14
RU	2.2	0.16	1.7	0.185	1.4	0.14	1.2	0.12

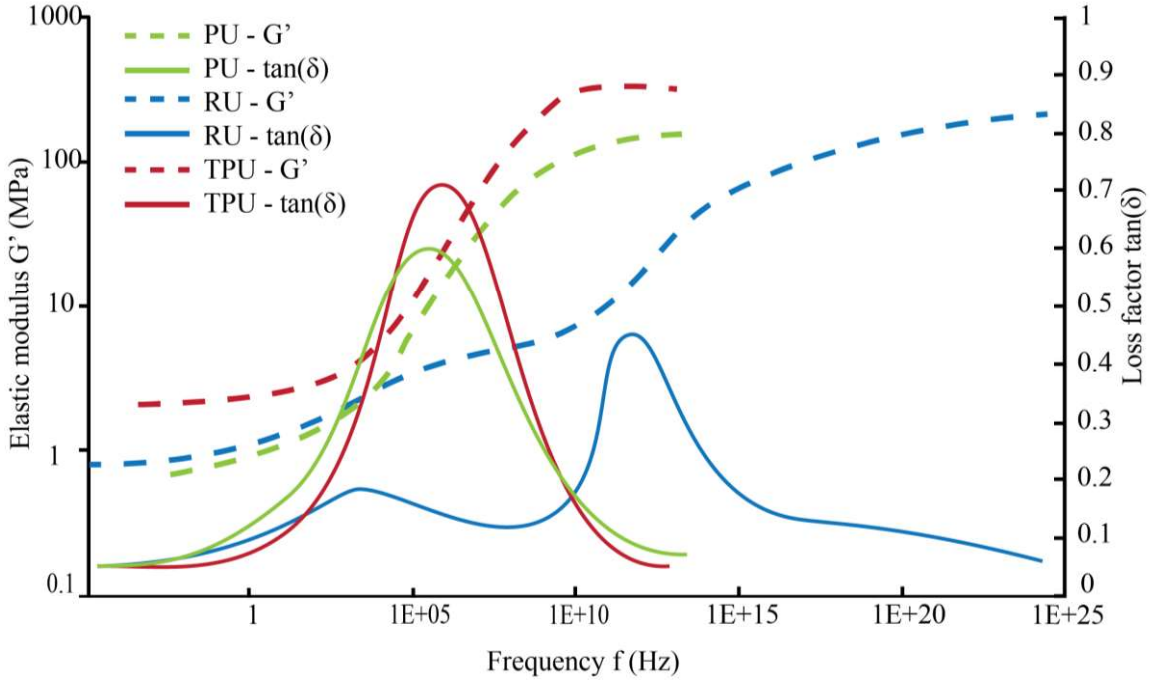

Figure 1 Master curves for the three materials obtained with Dynamic Mechanical Analysis (T 20 °C).

2.1.2. Outsole material surface characterization

The hydrophobicity/wettability of the three materials were identified via surface energy measurements and performed with a Krüss Mobile Surface Analyser (Flexible Liquid) with

distilled water (MilliPore) and diiodomethane (Merck). Due to the high density of diiodomethane (3.32 g/cm3) drops of 1 µL were deposited while for water, 1.5 µL drops were analysed. Five measurements were collected per sample and liquid. The surface free energy (SFE) of the rubbers were calculated with the Owens-Wendt-Rabel-Kaelble model by the Krüss ADVANCE software, yielding the total surface free energy (SFE^{tot}) as well as the dispersive and polar contributions. The surface energy properties are presented in Table 2.

Table 2 Surface energy measurements. CA(H_2O) = contact angle with distilled water; CA(CH_2Cl_2) = contact angle with diiodomethane; SFE_{tot} = total surface free energy; P/D ratio = polar/dispersive ratio.

Sample	CA(H_2O) [°]	CA(CH_2Cl_2) [°]	SFE^{tot} [mN/m]	P/D ratio
PU	97.39 ± 0.67	91.96 ± 2.05	16.65 ± 1.33	0.41
TPU	94.99 ± 0.07	54.46 ± 1.05	32.70 ± 0.67	0.03
RU	109.19 ± 0.18	91.24 ± 0.56	13.46 ± 0.31	0.11

Two square blocks (25 x 25 mm) were cut of each of the three materials and glued to 3D printed mounts as illustrated in Figure 2. The material surface roughness and topography was measured with a non-destructive elastomeric 3D imaging system (GelSight mobile, GelSight, USA), and further analysed using MountainsMap 9.0 software (Digital Surf, France). Roughness parameters (Sa) were calculated according to the ISO 25178 standard (Standard, 2021) with a Robust Gaussian metrological filter of second order (ISO 16610-71) with a cut-off of 2.5 mm. Surface heat map and roughness parameters are presented in Figure 2.

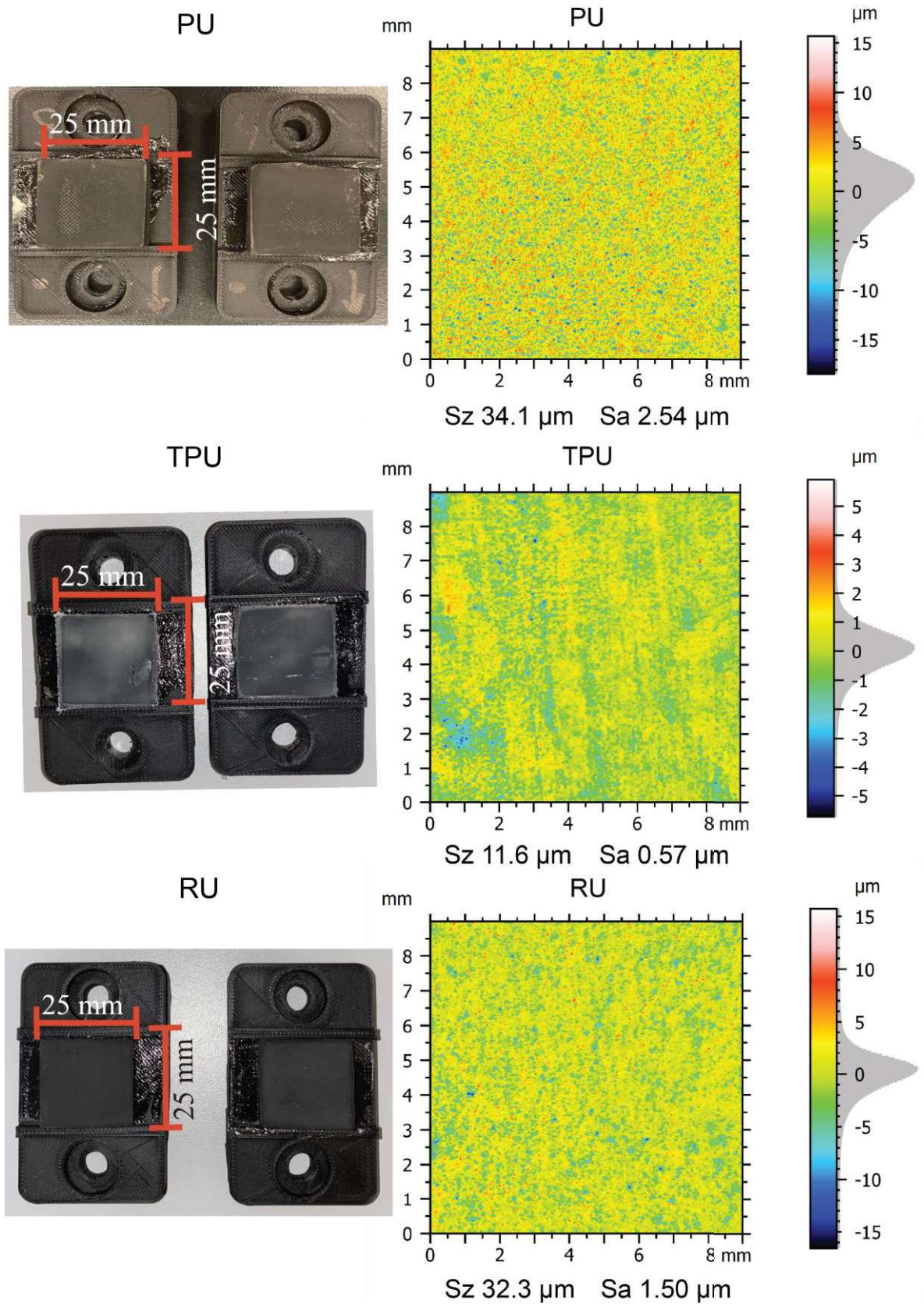

Figure 2 **Visual appearance and surface roughness for the three elastomer material square blocks.**

2.2. Ice surface construction and characterization

The ice surface is presented in Figure 3 and was created in -10 °C by building ice layers on top of a 45 mm hard coarse snow layer. Water holding of 0 °C was first sprayed on to create the base and the last layers were added with a wet rag and levelled by a squeegee until a smooth ice surface of ~5 mm thickness was reached. Next, the ice surface was thermo-polished with an aluminium box, containing 25 °C water. Ice surface roughness and topography was also characterized with the GelSight 3D imaging system and analysed using MountainsMap 9.0 software.

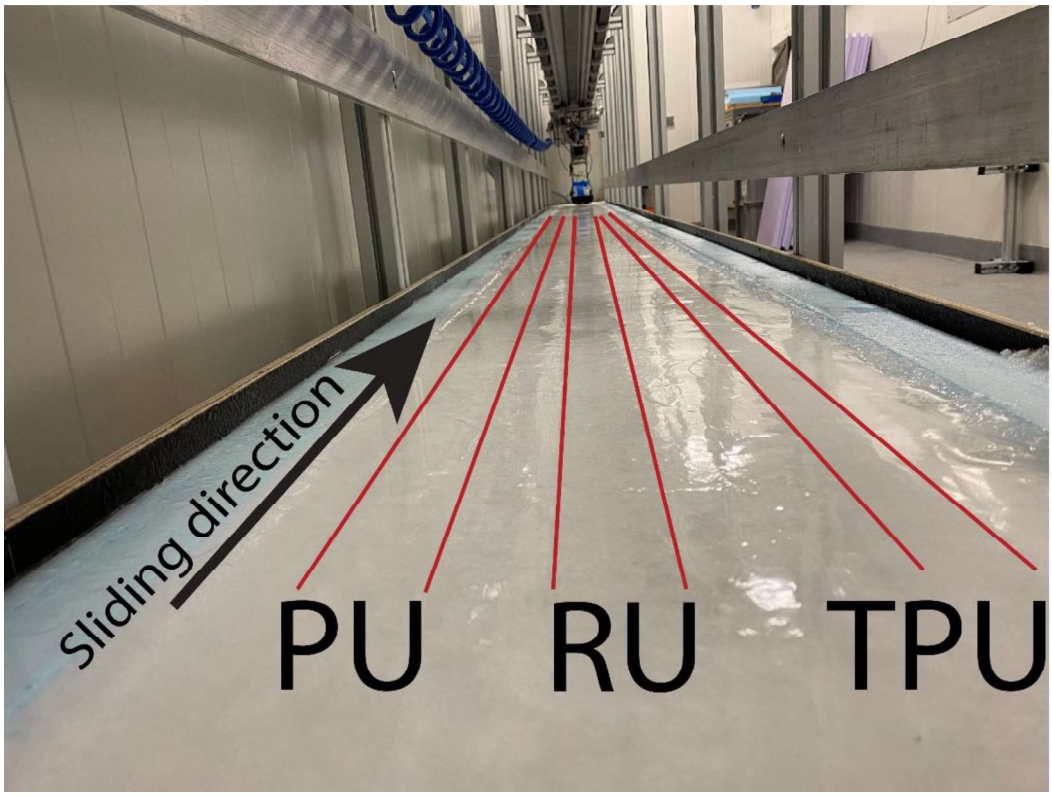

Figure 3 Photo of the ice surface

The ice surface topography is plotted as a heat map (Figure 4), illustrating the ice surface roughness profile for one sliding track (TPU in Figure 3) at 0 °C and -10 °C before and after friction measurements. At 0 °C the average ice surface roughness (Sa) and peak to valley height (Sz) was 0.93 µm and 26.6 µm respectively, before friction measurements, where Sa = 0.65 µm and Sz =

13 µm after friction measurements. At -10 °C, Sa = 1.15 µm and Rz = 22 µm before friction measurements, where Sa = 1.17 µm and Rz = 18.9 µm after friction measurements.

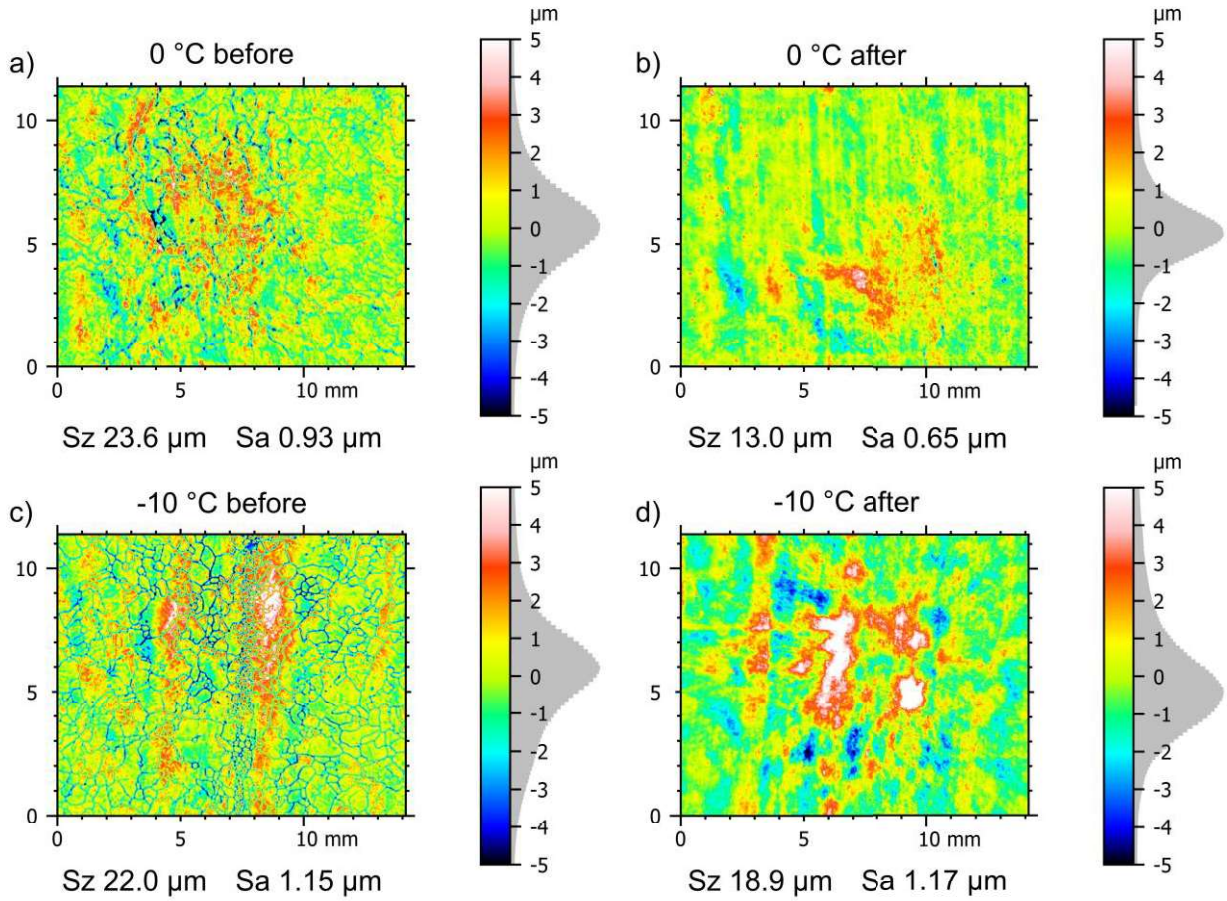

Figure 4 Topography GelSight images at the same approximate location of one ice track (TPU) surface at 0 °C and -10 °C before and after friction measurements (n = 40). The image size is 14 * 12 mm, where the forward sliding direction in the images is vertical upwards.

2.3. Test procedure for friction measurements

A linear tribometer (illustrated in Figure 5), located in the Snowlab at the Norwegian University of Science and Technology, was used to determine friction properties between the three outsole materials and the ice surface.

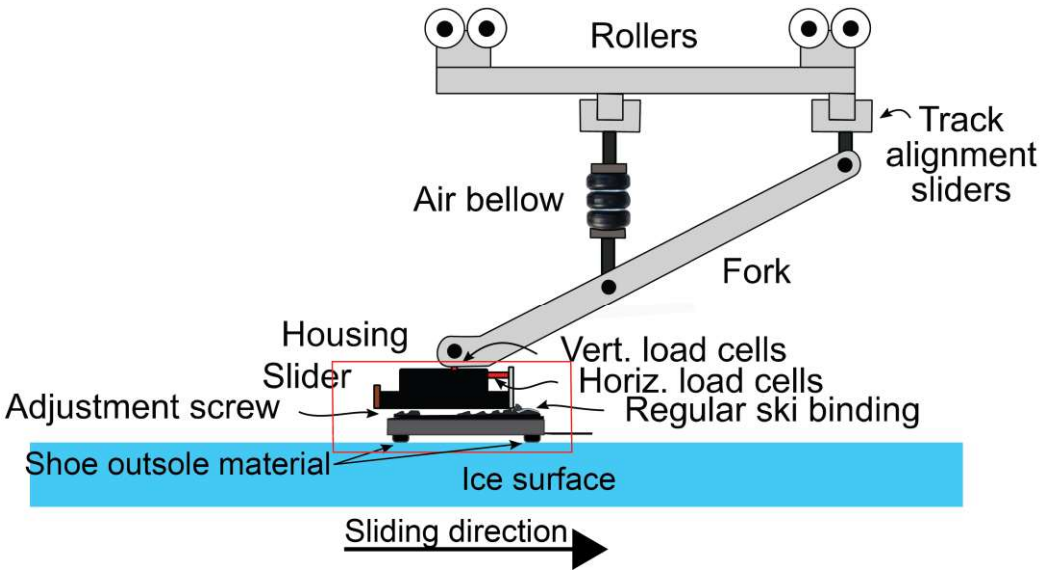

Figure 5 Illustration of the linear tribometer with shoe outsole material specimen sliding on ice surface. Adapted from (Auganæs et al., 2022)

The materials were tested under four different temperatures (-10, -5, -2 and 0 °C). When the temperature was changed, the ice had at least 20 hours to acclimatize, before measurements were performed. Before friction measurements, the outsole material specimens were abraded with 400 grit sandpaper (in compliance with the ISO 13287 - Personal protective equipment – Test method for slip resistance (ISO 13287:2019 standard)), cleaned with water and dried with compressed air and then at the ambient temperature corresponding to the freezer temperature for at least 20 hours. This cleaning procedure was repeated when the freezer temperature was changed.

Two square material blocks were placed 440 mm (center of one block to center of the other block) on an aluminium profile beam, which acted as the interface between a housing slider and the material blocks (see Figure 5). This provided a mechanically stabile configuration, compared to measuring on only one slider block, preventing unwanted oscillations when accelerating the slider.

A normal force of 500 N was applied in the middle of the material blocks, thus a corresponding contact pressure of 0.8 MPa was reached. Pressures in the range of 0.2-1 MPa are previously found

to be realistic, when determining footwear/surface slip resistance (Chang et al., 2001 b). The three material specimens underwent measurements with six different sliding velocities (0.3, 1, 2, 3, 4, 5 m/s) in a randomized order, for each temperature. Each material specimen had its own sliding track as illustrated in Figure 3. Thus, the track alignment slider (Figure 5) was moved laterally when changing materials. Ten run-in measurements for each track were performed for each temperature. Next, five measurements were performed for all sliding velocities, with a custom-made trajectory program. The custom-made trajectory program implied a five-phase program (Figure 6) consisting of I. slow dynamic sliding (0.1 m/s for 20 cm), II. Resting (500 ms), III. acceleration, IV. target sliding velocity (alteration of the six different sliding velocities) and V. deceleration. Hence, all phases were consistent between all measurements, except from phase 4, where the sliding velocity was altered.

The sliding velocity of 0.3 m/s and a static contact time of maximum 1000 ms is in compliance with the ISO 13287 (ISO 13287:2019 standard). 30 seconds waiting period between each measurement was kept consistent throughout all measurements.

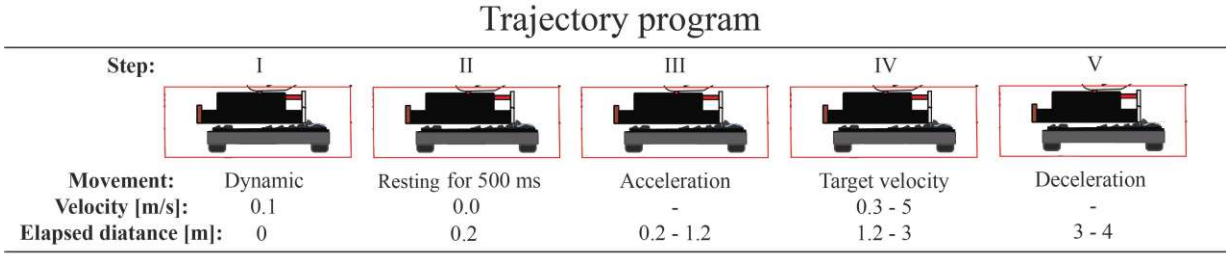

Figure 6 Trajectory program for the tribometer. I. Slow dynamic sliding (0.1 m/s for 20 cm), II. Resting (500 ms), III. Acceleration, IV. Target-sliding velocity (alteration of the six different sliding velocities), V. Deceleration.

2.4. Data processing

Determination of the coefficient of friction was performed by calculating the arithmetic average of five measurements by dividing the horizontal force with the normal force. The dynamic

coefficient of friction is calculated within the measurement region IV (Figure 6). When determining the static coefficient of friction (SCOF), the peak friction coefficient in the position range of II to III (Figure 6) was found and averaged for five measurements.

2.5. **Friction measurements**

An example of the slider trajectory for a typical measurement including I. dynamic movement (0.1 m/s), II. static coefficient of friction, III. acceleration (velocity ramp up), IV. target velocities (0.3 – 5 m/s) and V. deceleration (velocity ramp down) as function of sliding distance, is illustrated in Figure 7a. The dynamic movement period (see Figure 6) is identical for all sliding velocities until the resting pause for 500 ms is reached. The target velocity is achieved after 1 m for velocities 1-5 m/s, however for 0.3 m/s the target velocity is achieved after ~0.2 m sliding distance. For sliding velocities 2-5 m/s the actual sliding velocity is slightly lower than the target velocity, which is due to a discrepancy in tribometer motor control. The return velocity is 1 m/s for all measurements. Figure 7 b illustrates the coefficient of friction as function of sliding distance. The SCOF is

obtained after step II. (500 ms pause). The average DCOF is measured in the green area, where the sliding velocity is steady.

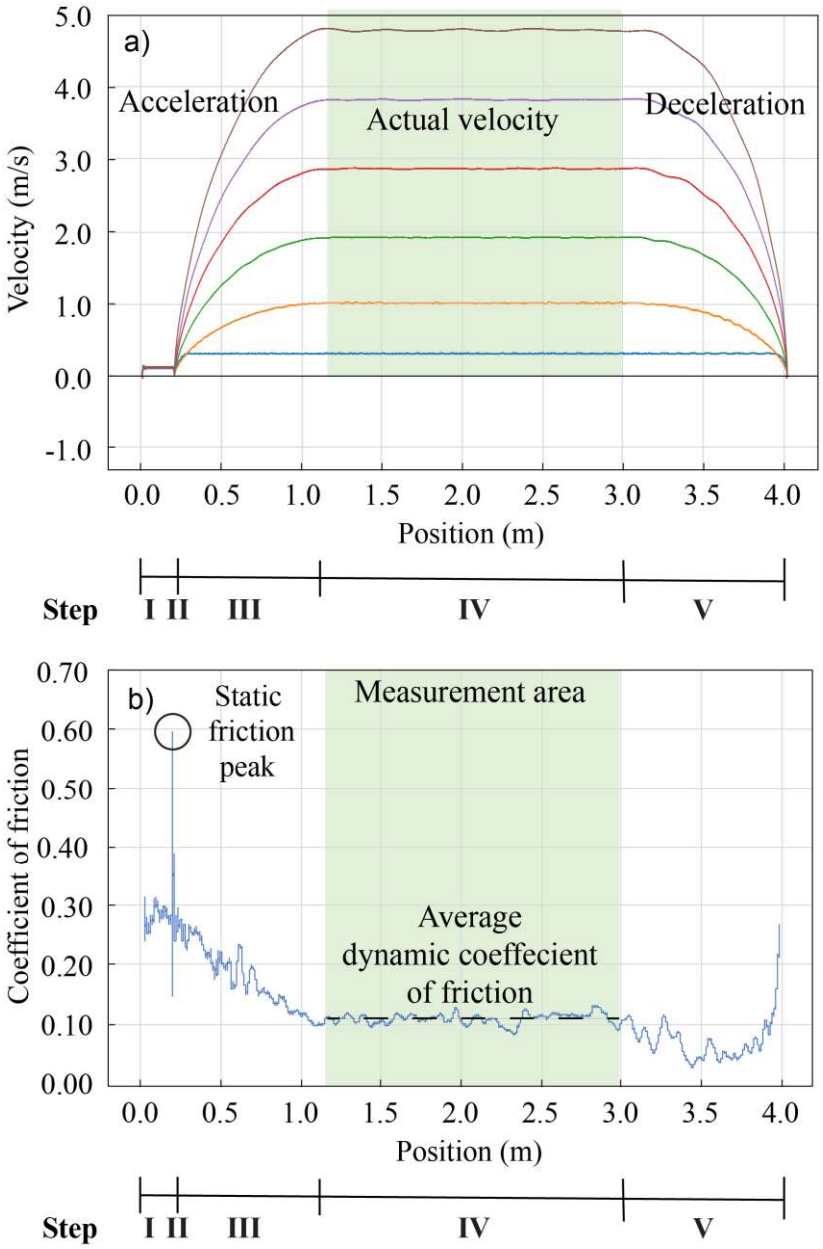

Figure 7 a: Illustration of the velocity as function of sliding distance (m). White areas illustrates the acceleration and deceleration phases and the green area is the actual velocity.

b: Example of static and dynamic friction coefficient as function of sliding distance. Green area illustrates the measurement area for dynamic coefficient of friction. The dashed line is the average DCOF. The example is one measurement for RU at -5 °C with a sliding velocity of 4 m/s.

3. Results

At -10 °C (Figure 8) the DCOF tends to decrease with increasing sliding velocity for all three materials. In addition, the velocity dependency is highest at -10 °C and diminishes as the temperature approaches 0 °C. The RU had the highest DCOF followed by the PU and TPU respectively. At -5 °C (Figure 9) the DCOF tends to decrease with increasing sliding velocity for all three materials. The RU still had the highest DCOF from 0.3 to 1 m/s, but from 2 m/s to 5 m/s the PU had the highest DCOF. At -2 °C (Figure 10) the DCOF tends to decrease with increasing sliding velocity for RU and TPU. The PU had the highest DCOF among the three materials and tends not to systematically decrease with sliding velocity. At -0 °C (Figure 11) the DCOF is less affected by sliding velocity for all three materials, compared to the other temperature measurements. A slight DCOF increase as function of increased sliding velocity appears – most distinctly for the PU.

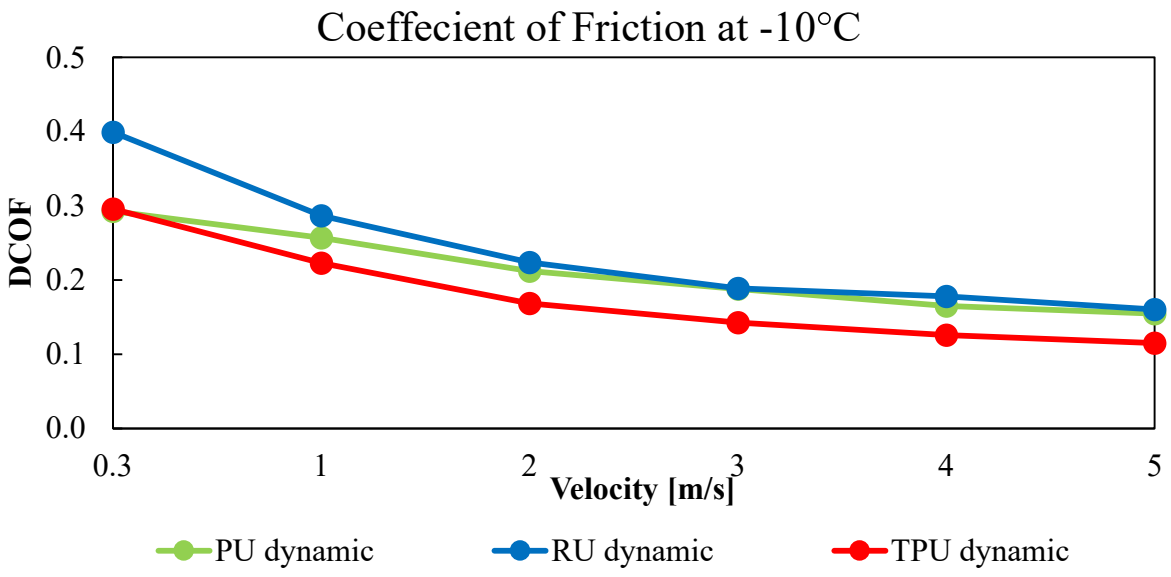

Figure 8 Average dynamic coefficient of friction (DCOF) at – 10 °C as function of sliding velocity. Error bars with ± standard deviations < 0.02 are not visual and left out.

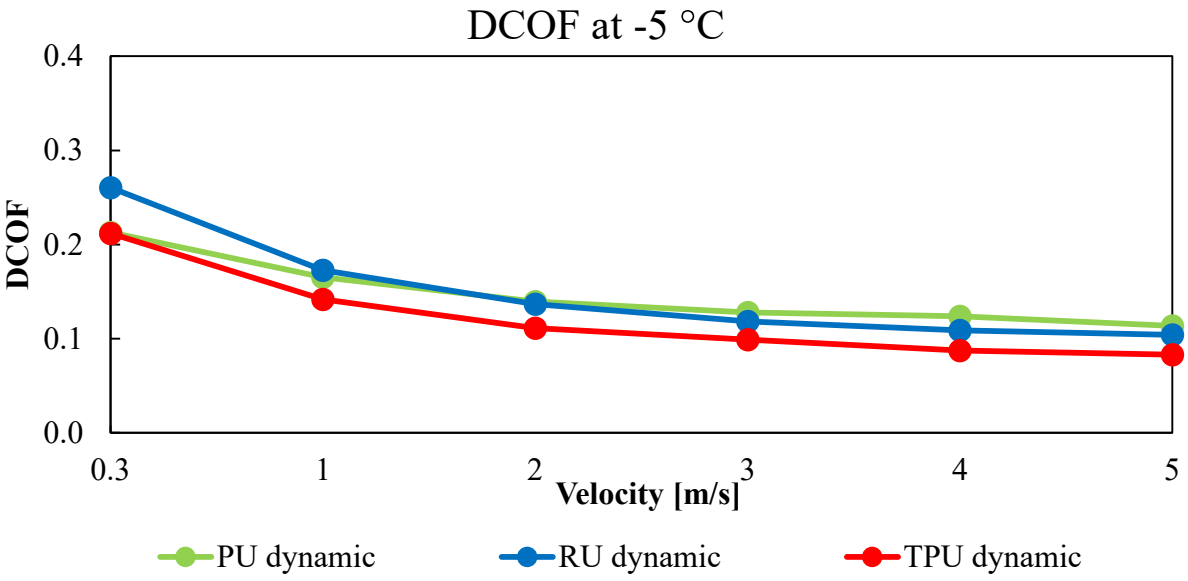

Figure 9 Average dynamic coefficient of friction (DCOF) at -5 °C as function of sliding velocity. Error bars with ± standard deviations < 0.02 are not visual and left out.

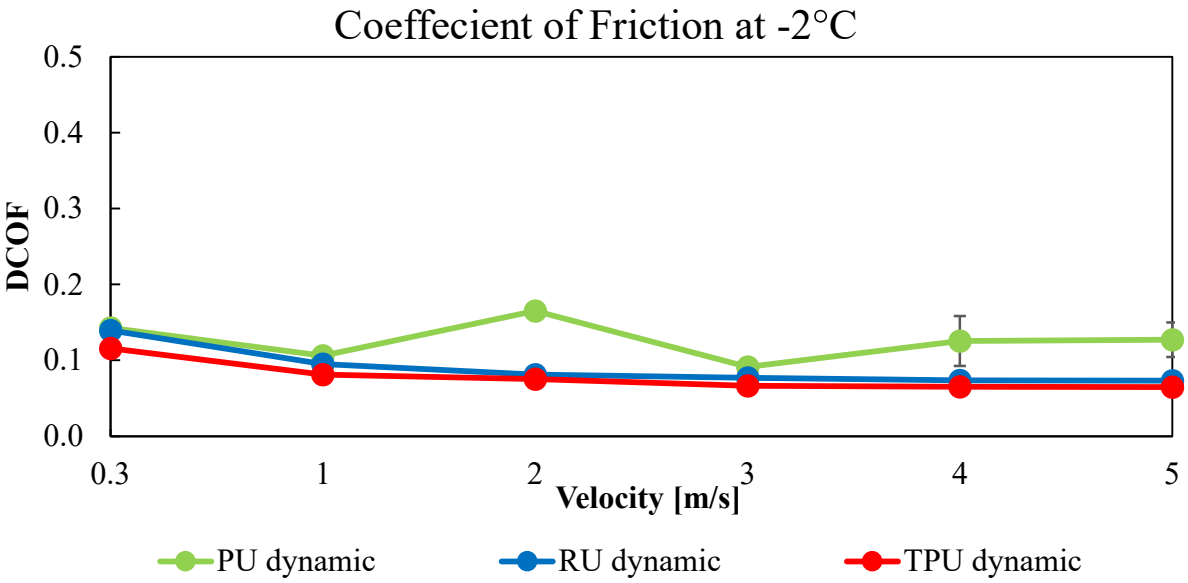

Figure 10 Average dynamic coefficient of friction (DCOF) at -2 °C as function of sliding velocity. Error bars with ± standard deviations < 0.02 are not visual and left out.

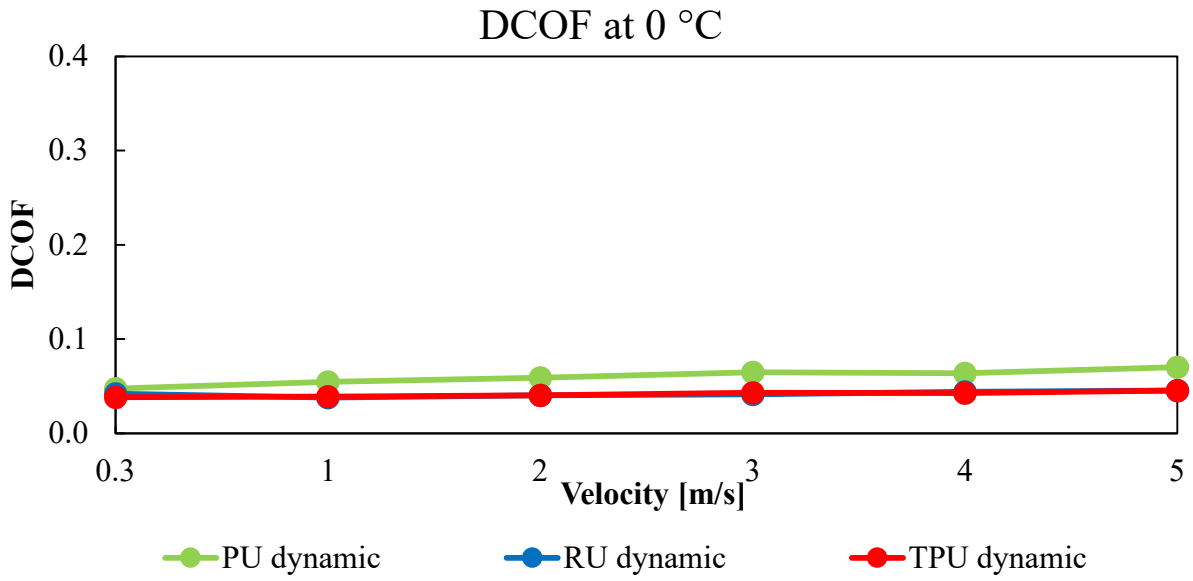

Figure 11 Average dynamic coefficient of friction (DCOF) at 0°C as function of sliding velocity. NOTE – RU and TPU are close related and the TPU curve somewhat overshadows the RU curve. Error bars with ± standard deviations < 0.02 are not visual and left out.

Averaged static coefficient of friction across all sliding velocities from -10 °C to 0 °C for the three outsole materials are presented in Figure 12. The RU material reveals the highest SCOF for -10 °C, -5 °C and -2 °C among the three materials. However, at 0 °C the PU material has the highest SCOF followed by TPU and RU respectively.

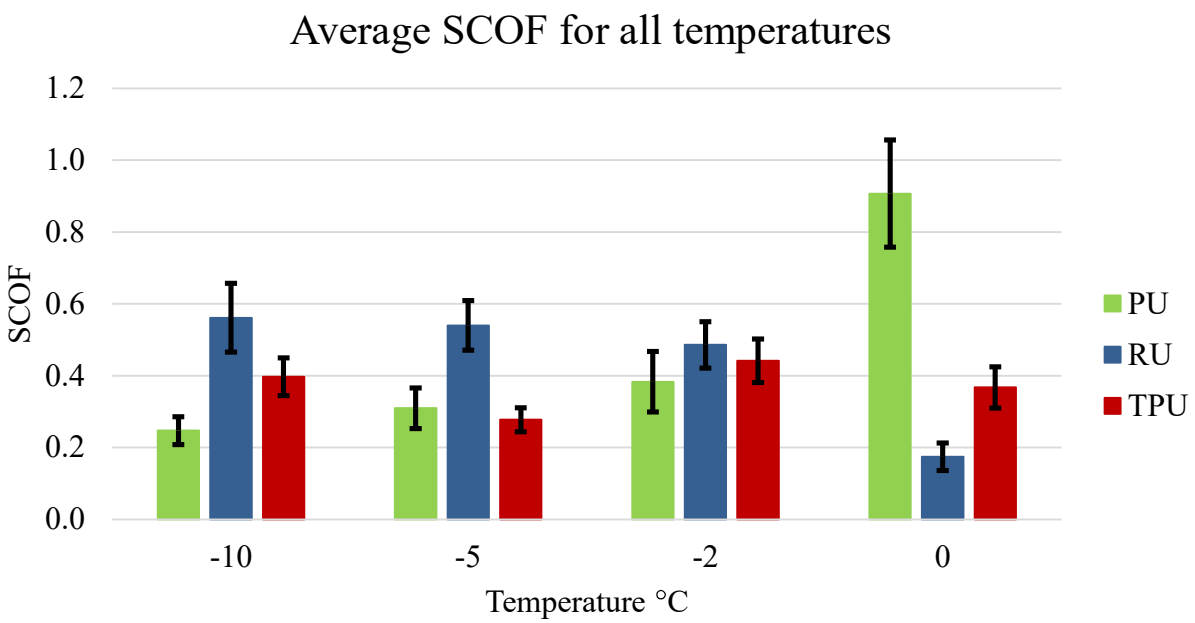

Figure 12 Average static coefficient of friction (SCOF) for all temperatures (0 °C to -10 °C). Average is taken for all 30 measurements conducted for each temperature. Hence, the acceleration varies as illustrated in Figure 7A. Error bars represents ± standard deviation.

4. Discussion

At low temperatures (-10 °C and -5 °C) the vulcanized rubber (RU) showed the highest dynamic friction coefficients at sliding velocities from 0 to 2 m/s, compared to the injection moulded thermoplastic polyurethane (TPU) and the low pressure injected polyurethane (PU). At low temperatures and at sliding velocities from 2 to 5 m/s, the PU showed the highest DCOF. At high temperatures (-2 °C and 0 °C) the PU showed the highest dynamic friction coefficients compared to the TPU and RU materials. At 0 °C, the PU revealed much higher SCOF compared to the TPU and RU materials.

4.1. Elastomer block friction on ice

The observed velocity dependencies in our study are in line with previous research of rubber friction on ice, where DCOF decreased with increased temperatures (Fulop & Isitman, 2020; Lahayne et al., 2016; Skouvaklis et al., 2012) and increased with sliding velocity (Lahayne et al., 2016; Skouvaklis et al., 2012; Tuononen et al., 2016). The decrease in DCOF, as function of increased sliding velocity and increased ambient temperature, is likely due to an increase in meltwater film formation, which separates the elastomer and ice surfaces and acts as a lubrication (Lahayne et al., 2016). At low temperatures, the ice surface is solid-like and the surface is slightly rougher compared to high temperatures. At this solid-like state, the elastomer elastic modulus supposedly has an important role, since a softer material will more easily comply with the roughness of the substrate and thereby increase the friction. Based on the DMA, the RU material has the lowest elastic modulus at high frequencies (E5-E15 Hz). Hence, when the RU slides at 0.3 m/s at -10 C° and -5 C°, it may exhibit vibrations in the range of E5-E15 Hz and this can possibly explain the higher friction at this sliding velocity and temperatures. The damping property (tan(δ)) shown in Figure 1 has also been linked to the coefficient of friction (Persson, 2001) and tan(δ) is

higher for RU at high frequencies than for the other materials. The effect could be more pronounced due the low temperatures, which shift the frequency curve to the left in Figure 1.

In addition, it is more difficult to generate sufficient meltwater through frictional heating at low temperatures. This is supported by the roughness measurements in Figure 4, where the polishing of the ice surface is more pronounced at high temperatures. While this can be explained by both temperature-dependent differences in lubrication mechanism and increased ice abrasion due to reduced hardness of warm ice, we are of the opinion this difference in roughness is caused by the different lubrication regimes at 0 °C and -10 °C. The reason is that more heat is needed to heat the ice to its melting point and the conductive heat fluxes into the ice and the elastomer slider are larger since the temperature gradients are larger (Oksanen & Keinonen, 1982). This leaves less heat to generate a water film at low temperatures. At high temperatures and high sliding velocities above 1 m/s, the formation of meltwater is likely to increase (Southern & Walker, 1972) and makes the elastomer elastic modulus less important. In this stage, friction is mainly determined by the shearing of the meltwater film and the DCOF does not differ much among the three materials. Nonetheless, at 0 °C the effect of sliding velocity tends to change and cause an increase in DCOF as function of increased sliding velocity. This increase in friction at high ice temperatures is likely caused by capillary suction, where the increase in surface meltwater film thickness can cause bridging of water between contact points, which are not load carrying and can cause an increased friction force (Colbeck, 1992). PU is a porous material and it is likely that there will be more of such possible bridge contact points and therefore a higher capillary drag, compared to the other two materials.

The SCOF for PU at 0 °C is distinctly higher compared to the RU and TPU material. The porous PU material has the ability to absorb a small amount of water. Therefore, at 0 °C it is likely that

the PU absorbs water from the surface melt water film, during the resting period of 500 ms (see Figure 6 II) and forms ice sintering between the ice surface and the PU surface pores. Furthermore, the PU has a slightly higher surface roughness compared to the other materials and a greater amount of encapsulated melt water may be present. Hence, breaking the ice bonding at stage III (Figure 6) are likely causing the pronounced SCOF for PU at 0 °C. In addition, the RU has lowest wettability (109.19 ± 0.18° - see Table 2) and therefore is the most hydrophobic material used in this study. At temperatures close to the melting point, increased slider surface hydrophobicity decreases ice friction (Kietzig et al., 2009) and thus may contribute to the low SCOF at 0 °C for RU.

4.2. **Footwear slip resistance on ice**

Rubber outsoles being more slip resistant than PU outsoles at low temperatures is in line with previous research of footwear slip resistance on ice (Gao et al., 2004). The research from Gao and colleagues showed that polyurethane outsoles did not perform better than synthetic rubber, nitrile rubber and natural rubber on pure cold ice (-12 °C). They did however not test at high temperatures closer to zero, where we in the present study, found an opposite tendency, revealing higher dynamic friction for PU soles between -2 and 0 °C and much higher static friction at 0 °C compared to rubber. It should be mentioned, that the exact material compositions for outsoles plays an important role in relation to footwear slip resistance (Manning. & Jones, 1994) and material properties from the present study may differ from the study by Gao et al. 2004.

For the application of footwear slip resistance, sliding velocities above 1 m/s may occur (Chang et al., 2001). Hence, sliding velocities between 0.5-2.5 m/s are probably most relevant in relation to real life slipping accidents. Furthermore, dynamic friction coefficients in the range of 0.1-0.3 is likely to cause slipping (Hanson et al., 1999). Therefore, temperatures above -10 °C is likely to

cause slipping for the three materials investigated in this study. While the DCOF at 0 °C is low for all three materials, it is worth noticing, that the PU showed highest DCOF and considerably higher SCOF compared to the TPU and RU. This is in line with another study conducted on whole footwear constructed of the same three materials, where it was found that the PU outsole revealed higher DCOF on glycerine/canola oil contaminated steel and tile surfaces, compared to the TPU and RU outsoles (Jakobsen et al., 2022).

Both SCOF and DCOF are arguably important and the best frictional measure for preventing slipping is under debate (Tisserand, 1985; Yamaguchi et al., 2008). A high SCOF may prevent slip initiation when a surface is known/expected to be slippery, since walking subjects tend to reduce their heel velocity when anticipating slippery floors (Cham & Redfern, 2002). However, biomechanical studies have demonstrated that if a slip event is initiated, the shoe does not stop sliding (Albert et al., 2017; Iraqi, Cham, Redfern, Vidic, et al., 2018). In prolongation, the available DCOF magnitude is previously found to be related to the probability of slip events (Burnfield & Powers, 2006; Hanson et al., 1999; Iraqi, Cham, Redfern, & Beschorner, 2018). Hence, both SCOF and DCOF is suggested to be evaluated, when determining footwear slip resistance (Yamaguchi et al., 2012). Since the necessary breaking friction force from static to dynamic friction is higher for the PU outsole material at high (close to 0 °C) temperatures compared to TPU and RU, the PU sole may arguably resist the initiation of the dynamic sliding phase. However, due to the low DCOF values at high temperatures the slip probability may still be high. This suggests that one outsole material may not have superior slip resistance on all ice conditions. At low temperatures (-10 °C and - 5 °C) vulcanized rubber may be the better choice, whereas at high temperatures (-2 °C and 0 °C) PU may be a better choice. Recent research have identified that embedding fibers (Anwer et al., 2017; Rizvi et al., 2015) in elastomer material enhances friction on icy surfaces.

Hence, it can be speculated whether a hybrid outsole construction provides a better slip resistance on ice over a wider temperature range. In fact, a hybrid surface pattern outsole for preventing slips on icy surfaces, has already been made with smooth and rough outsole surface pattern (Yamaguchi et al., 2015) and with hybrid composite materials (Shaghayegh Bagheri et al., 2019).

Further studies should potentially aim for investigating hybrid outsole constructions, which combines outsole design concepts, outsole materials and composites to accommodate slip resistance over a wider range of ice surface types and temperatures.

4.3. **Limitations**

This study has some limitations, which should be noted. Despite the fact that the trajectory program for the tribometer included biofidelic testing parameters, it should be noted, that this study lacks validation of human factors. Hence, human specific parameters like e.g. foot motion, normal force build up rate and slip anticipation was not possible to replicate in this study. Furthermore, this study was conducted with elastomer block samples and thus not a realistic reproduction of a common footwear outsole. Outsoles often have more complex geometries, in terms of heel bevelling, outsole pattern and midsole cushioning, which previously has been found to affect the slip resistance (Lloyd & Stevenson, 1989; Moriyasu et al., 2019; Yamaguchi et al., 2017). Lastly, numerous material combinations of RU, PU and TPU may exist and it is not known, whether other material combination may reveal different friction properties. Hence, extrapolation of the findings from this study to other combinations of the materials should be done with caution.

5. **Conclusion**

This study compared friction of three elastomer block materials (low pressure injection of polyurethane (PU), injection moulding of a thermoplastic polyurethane (TPU) and vulcanization

of rubber (RU)), conducted on a linear tribometer operating under four different ambient air temperatures (-10 °C to 0 °C) and six different sliding velocities (0.3 to 5 m/s). A custom-made trajectory program for the tribometer enabled the ability to determine dynamic and static friction coefficients and mimic biofidelic testing parameters relevant for slipping. At low (temperatures -10 °C and -5 °C), the RU material had highest dynamic and static friction. However, at high temperatures (-2 °C and 0 °C) the PU showed highest dynamic friction and higher static friction at 0 °C. The high friction for RU at low temperatures could be explained by the low elastic modulus at high frequencies, making the material comply more with the ice surface during specific sliding velocities, compared with the other materials. The high dynamic and static friction for PU at high temperatures could be explained by its porous nature. Based on these findings we suggest further studies of elastomer friction on ice focused on a hybrid construction based on different materials, design concepts and composite solutions, to potentially accommodate slip resistance over a wider temperature range.

6. ACKNOWLEDGMENTS

This study was funded by the Danish Working Environment Research Fund (grant number: 20195100816). ECCO Shoes A/S provided the material samples used in this study, but had no role in the interpretation and presentation of the results. The authors want to thank Sophia Sachse from ECCO A/S for her extensive help and very fast execution. Lastly, we want to thank Jesper Bøgelund, Senior R&D Engineer at DDS (device delivery & solutions) at Novo Nordisk for providing the DMA measurements. The authors have no conflict of interest to declare.

REFERENCES

Albert, D., Moyer, B., & Beschorner, K. E. (2017). Three-Dimensional Shoe Kinematics During Unexpected Slips: Implications for Shoe–Floor Friction Testing. *IISE Transactions on Occupational Ergonomics and Human Factors*, *5*(1), 1–11. https://doi.org/10.1080/21577323.2016.1241963

Anwer, A., Bagheri, Z. S., Fernie, G., Dutta, T., & Naguib, H. E. (2017). Evolution of the Coefficient of Friction with Surface Wear for Advanced Surface Textured Composites. *Advanced Materials Interfaces*, *4*(6). https://doi.org/10.1002/admi.201600983

Auganæs, S. B., Buene, A. F., & Klein-Paste, A. (2022). Laboratory testing of cross-country skis – Investigating tribometer precision on laboratory-grown dendritic snow. *Tribology International*, *168*(January). https://doi.org/10.1016/j.triboint.2022.107451

Bagheri, Z. S., Beltran, J. D., Holyoke, P., & Dutta, T. (2021). Reducing fall risk for home care workers with slip resistant winter footwear. *Applied Ergonomics*, *90*. https://doi.org/10.1016/j.apergo.2020.103230

Bäurle, L., Kaempfer, T. U., Szabó, D., & Spencer, N. D. (2007). Sliding friction of polyethylene on snow and ice: Contact area and modeling. *Cold Regions Science and Technology*, *47*(3). https://doi.org/10.1016/j.coldregions.2006.10.005

Burnfield, J. M., & Powers, C. M. (2006). Prediction of slips: an evaluation of utilized coefficient of friction and available slip resistance. *Ergonomics*, *49*(10), 982–995. https://doi.org/10.1080/00140130600665687

Cham, R., & Redfern, M. S. (2002). Changes in gait when anticipating slippery floors. *Gait & Posture*, *15*(2), 159–171. https://doi.org/10.1016/S0966-6362(01)00150-3

Chang, W.-R., Courtney, T. K., Grönqvist, R., & Redfern, M. (2010). Measuring slipperiness—discussions on the state of the art and future research. In *Measuring Slipperiness* (pp. 165–172). Taylor & Francis. https://doi.org/10.4324/9780203301913_chapter_8

Chang, W., Grönqvist, R., Leclercq, S., Brungraber, R. J., Mattke, U., Strandberg, L., Thorpe, S. C., Myung, R., Makkonen, L., & Courtney, T. K. (2001). The role of friction in the measurement of slipperiness, Part 2: Survey of friction measurement devices. *Ergonomics*, *44*(13), 1233–1261. https://doi.org/10.1080/00140130110085583

Chang, W., Grönqvist, R., Leclercq, S., Myung, R., Makkonen, L., Strandberg, L., Brungraber, R. J., Mattke, U., &

Thorpe, S. C. (2001). The role of friction in the measurement of slipperiness, Part 1: Friction mechanisms and definition of test conditions The role of friction in the measurement of slipperiness, Part 1: Friction mechanisms and definition of test conditions. *Ergonomics*, *44*(13). https://doi.org/10.1080/00140130110085574

Colbeck, S. C. (1992). A review of the processes that control snow friction. *Cold Regions Research and Engineering Laboratory, CRREL Monograph*, *April*.

Courtney, T. K., Sorock, G. S., Manning, D. P., Collins, J. W., & Holbein-Jenny, M. A. (2001). Occupational slip, trip, and fall-related injuries can the contribution of slipperiness be isolated? *Ergonomics*, *44*(13), 1118–1137. https://doi.org/10.1080/00140130110085538

Fulop, T., & Isitman, N. A. (2020). Frictional characteristics of rubber on ice. *Rubber World*, *262*(6).

Gao, C., & Abeysekera, J. (2002). The assessment of the integration of slip resistance, thermal insulation and wearability of footwear on icy surfaces. *Safety Science*, *40*(7–8). https://doi.org/10.1016/S0925-7535(01)00062-5

Gao, C., Abeysekera, J., Hirvonen, M., & Grönqvist, R. (2004). Slip resistant properties of footwear on ice. *Ergonomics*, *47*(6). https://doi.org/10.1080/00140130410001658673

Gauvin, C., Pearsall, D., Damavandi, M., Michaud-Paquette, Y., Farbos, B., & Imbeau, D. (2015). *Risk Factors for Slip Accidents among Police Officers and School Crossing Guards* . www.csst.qc.ca/AbonnementPAT

Giudici, H., Dahl Fenre, M., Klein-Paste, A., & Rekilä, K.-P. (2017). A technical description of LARS and Lumi: Two apparatus for studying tire-pavement interactions. *Routes/Roads Magazine*, 49–54.

Grönqvist, R., Chang, W., Courtney, T. K., Leamon, T. B., Redfern, M. S., K, T., B, T., & S, M. (2001). Measurement of slipperiness : fundamental concepts and definitions. *Ergonomics*, *44*(13), 1117. https://doi.org/10.1080/0014013011008552

Grönqvist, R., & Hirvonen, M. (1995). Slipperiness of footwear and mechanisms of walking friction on icy surfaces. *International Journal of Industrial Ergonomics*, *16*(3). https://doi.org/10.1016/0169-8141(94)00095-K

Hanson, J. P., Redfern, M. S., & Mazumdar, M. (1999). Predicting slips and falls considering required and available friction. *Ergonomics*, *42*(12), 1619–1633. https://doi.org/10.1080/001401399184712

Hsu, J., Shaw, R., Novak, A., Li, Y., Ormerod, M., Newton, R., Dutta, T., & Fernie, G. (2016). Slip resistance of winter footwear on snow and ice measured using maximum achievable incline. *Ergonomics*, *59*(5), 717–728. https://doi.org/10.1080/00140139.2015.1084051

Iraqi, A., Cham, R., Redfern, M. S., & Beschorner, K. E. (2018). Coefficient of friction testing parameters influence the prediction of human slips. *Applied Ergonomics*, *70*(July 2017), 118–126. https://doi.org/10.1016/j.apergo.2018.02.017

Iraqi, A., Cham, R., Redfern, M. S., Vidic, N. S., & Beschorner, K. E. (2018). Kinematics and kinetics of the shoe during human slips. *Journal of Biomechanics Journal*, *74*(6 June 2018), 57–63. https://doi.org/10.1016/j.jbiomech.2018.04.018

Jakobsen, L., Lysdal, Gertz, F., Bagehorn, T., Kersting, U., & Sivebaek, Marius, I. (2022). The Effect of Footwear Outsole Material on Slip Resistance on Dry and Contaminated Surfaces with Geometrically Controlled Outsoles. *Ergonomics*. https://doi.org/https://doi.org/10.1080/00140139.2022.2081364

Jakobsen, L., Lysdal, F. G., & Sivebaek, I. M. (2021). Dynamic mechanical analysis as a predictor for slip resistance and traction in footwear. *Footwear Science*, *13*(S1), S57–S58. https://doi.org/10.1080/19424280.2021.1917680

Jones, T., Iraqi, A., & Beschorner, K. (2018). Performance testing of work shoes labeled as slip resistant. *Applied Ergonomics*, *68*, 304–312. https://doi.org/10.1016/j.apergo.2017.12.008

Kietzig, A. M., Hatzikiriakos, S. G., & Englezos, P. (2009). Ice friction: The effects of surface roughness, structure, and hydrophobicity. *Journal of Applied Physics*, *106*(2). https://doi.org/10.1063/1.3173346

Klapproth, C., Kessel, T. M., Wiese, K., & Wies, B. (2016). An advanced viscous model for rubber-ice-friction. *Tribology International*, *99*. https://doi.org/10.1016/j.triboint.2015.09.012

Klein-Paste, A., & Wåhlin, J. (2013). Wet pavement anti-icing - A physical mechanism. *Cold Regions Science and Technology*, *96*. https://doi.org/10.1016/j.coldregions.2013.09.002

Lahayne, O., Pichler, B., Reihsner, R., Eberhardsteiner, J., Suh, J., Kim, D., Nam, S., Paek, H., Lorenz, B., & Persson, B. N. J. (2016). Rubber Friction on Ice: Experiments and Modeling. *Tribology Letters*, *62*(2). https://doi.org/10.1007/s11249-016-0665-z

Lloyd, D., & Stevenson, M. G. (1989). Measurement of slip resistance of shoes on floor surfaces. Part 2: Effect of a

bevelled heel. *Journal of Occupational Health and Safety - Australia and New Zealand*, *5*(3).

Manning., D. P., & Jones, C. (1994). The superior slip-resistance of footwear soling compound T66/103. *Safety Science*, *18*(1). https://doi.org/10.1016/0925-7535(94)90040-X

Manning, D., Jones, C., & Bruce, M. (1985). Boots for oily surfaces. *Ergonomics*, *28*(7), 1011–1019. https://doi.org/10.1080/00140138508963223

Menard, K., & Menard, N. (2020). *Dynamic Mechanical Analysis* (3rd ed.). CRC Press. https://doi.org/10.1007/978-3-540-29805-2_1224

Moriyasu, K., Nishiwaki, T., Shibata, K., Yamaguchi, T., & Hokkirigawa, K. (2019). Friction control of a resin foam/rubber laminated block material. *Tribology International*, *136*. https://doi.org/10.1016/j.triboint.2019.04.024

Oksanen, P., & Keinonen, J. (1982). The mechanism of friction of ice. *Wear*, *78*(3). https://doi.org/10.1016/0043-1648(82)90242-3

Persson, B. N. J. (2001). Theory of rubber friction and contact mechanics. *Journal of Chemical Physics*. https://doi.org/10.1063/1.1388626

Rizvi, R., Naguib, H., Fernie, G., & Dutta, T. (2015). High friction on ice provided by elastomeric fiber composites with textured surfaces. *Applied Physics Letters*, *106*(11). https://doi.org/10.1063/1.4913676

Sato, S., Yamaguchi, T., Shibata, K., Nishi, T., Moriyasu, K., Harano, K., & Hokkirigawa, K. (2020). Dry sliding friction and Wear behavior of thermoplastic polyurethane against abrasive paper. *Biotribology*, *23*. https://doi.org/10.1016/j.biotri.2020.100130

Shaghayegh Bagheri, Z., Anwer, A., Fernie, G., Naguib, H. E., & Dutta, T. (2019). Effects of multi-functional surface-texturing on the ice friction and abrasion characteristics of hybrid composite materials for footwear. *Wear*, *418–419*. https://doi.org/10.1016/j.wear.2018.11.030

Skouvaklis, G., Blackford, J. R., & Koutsos, V. (2012). Friction of rubber on ice: A new machine, influence of rubber properties and sliding parameters. *Tribology International*, *49*. https://doi.org/10.1016/j.triboint.2011.12.015

Southern, E., & Walker, R. W. (1972). Friction of Rubber on Ice. *Nature Physical Science*, *237*(78).

https://doi.org/10.1038/physci237142a0

Standard, I. (2019). *Personal protective equipment – Footwear – Test method for slip resistance (ISO 13287:2019)*.

Standard, I. (2021). *Geometrical product specifications (GPS) – Surface texture: Areal – Part 2: Terms, definitions and surface texture parameters : DS/ISO 25178-2:2021*.

Statistics Norway. Fall vanligste arbeidsulykke. (2021). https://www.ssb.no/helse/helseforhold-og-levevaner/statistikk/arbeidsulykker/artikler/fall-vanligste-arbeidsulykke

Sundhedsstyrelsen. (2016). *Sygdomsbyrden i Danmark, Ulykker, Selvskade og Selvmord 2016*. www.sst.dk

Tisserand, M. (1985). Progress in the prevention of falls caused by slipping. *ERGONOMICS*, *28*(7), 1027–1042. https://doi.org/10.1080/00140138508963225

Tuononen, A. J., Kriston, A., & Persson, B. (2016). Multiscale physics of rubber-ice friction. *Journal of Chemical Physics*, *145*(11). https://doi.org/10.1063/1.4962576

Wåhlin, J., Leisinger, S., & Klein-Paste, A. (2014). The effect of sodium chloride solution on the hardness of compacted snow. *Cold Regions Science and Technology*, *102*, 1–7. https://doi.org/10.1016/j.coldregions.2014.02.002

Yamaguchi, T., Hatanaka, S., & Hokkirigawa, K. (2008). Effect of Step Length and Walking Speed on Traction Coefficient and Slip between Shoe Sole and Walkway. *Tribology Online*, *3*(2). https://doi.org/10.2474/trol.3.59

Yamaguchi, T., Hsu, J., Li, Y., & Maki, B. E. (2015). Efficacy of a rubber outsole with a hybrid surface pattern for preventing slips on icy surfaces. *Applied Ergonomics*, *51*. https://doi.org/10.1016/j.apergo.2015.04.001

Yamaguchi, T., Katsurashima, Y., & Hokkirigawa, K. (2017). Effect of rubber block height and orientation on the coefficients of friction against smooth steel surface lubricated with glycerol solution. *Tribology International*, *110*. https://doi.org/10.1016/j.triboint.2017.02.015

Yamaguchi, T., Umetsu, T., Ishizuka, Y., Kasuga, K., Ito, T., Ishizawa, S., & Hokkirigawa, K. (2012). Development of new footwear sole surface pattern for prevention of slip-related falls. *Safety Science*, *50*(4). https://doi.org/10.1016/j.ssci.2011.12.017

7. Appendix

-10 °C							
Average COF	Material	0.3 m/s	1 m/s	2 m/s	3 m/s	4 m/s	5 m/s
Dynamic	PU	0.292 ±0.0008	0.257 ±0.00014	0.212 ±0.0016	0.188 ±0.0031	0.165 ±0.0005	0.154 ±0.0014
	RU	0.399 ±0.0027	0.286 ±0.0034	0.224 ±0.0023	0.189 ±0.0004	0.178 ±0.0007	0.160 ±0.0008
	TPU	0.296 ±0.011	0.223 ±0.0018	0.168 ±0.0018	0.142 ±0.0005	0.126 ±0.00017	0.115 ±0.0011
Static	PU	0.216 ±0.0055	0.198 ±0.0045	0.223 ±0.005	0.254 ±0.0055	0.284 ±0.0055	0.308 ±0.0084
	RU	0.694 ±0.0312	0.427 ±0.0159	0.443 ±0.0237	0.582 ±0.0256	0.625 ±0.0755	0.596 ±0.0400
	TPU	0.451 ±0.0211	0.313 ±0.0256	0.439 ±0.0182	0.338 ±0.0043	0.410 ±0.0429	0.432 ±0.0395

Table 3 Average dynamic coefficient of friction (DCOF) and static coefficient of friction (SCOF) ± standard deviation at -10 °C.

-5 °C							
Average COF	Material	0.3 m/s	1 m/s	2 m/s	3 m/s	4 m/s	5 m/s
Dynamic	PU	0.213 ±0.005	0.165 ±0.001	0.139 ±0.000	0.128 ±0.0183	0.124 ±0.002	0.113 ±0.000
	RU	0.260 ±0.002	0.173 ±0.000	0.137 ±0.000	0.118 ±0.0006	0.109 ±0.000	0.104 ±0.000
	TPU	0.212 ±0.000	0.142 ±0.000	0.111 ±0.000	0.099 ±0.000	0.087 ±0.000	0.082 ±0.001
Static	PU	0.286 ±0.015	0.243 ±0.018	0.255 ±0.0124	0.310 ±0.018	0.401 ±0.017	0.363 ±0.012
	RU	0.521 ±0.009	0.4201 ±0.009	0.498 ±0.049	0.574 ±0.004	0.622 ±0.015	0.604 ±0.012
	TPU	0.271 ±0.009	0.226 ±0.013	0.245 ±0.008	0.313 ±0.020	0.294 ±0.015	0.315 ±0.013

Table 4 Average dynamic coefficient of friction (DCOF) and static coefficient of friction (SCOF) ± standard deviation at -5 °C.

-2 °C							
Average COF	Material	0.3 m/s	1 m/s	2 m/s	3 m/s	4 m/s	5 m/s
Dynamic	PU	0.143 ±0.001	0.106 ±0.001	0.165 ±0.008	0.091 ±0.001	0.125 ±0.033	0.127 ±0.023
	RU	0.134 ±0.001	0.095 ±0.000	0.081 ±0.000	0.077 ±0.000	0.074 ±0.000	0.073 ±0.000
	TPU	0.116 ±0.003	0.081 ±0.000	0.075 ±0.000	0.067 ±0.000	0.065 ±0.000	0.065 ±0.000
Static	PU	0.348 ±0.009	0.318 ±0.011	0.250 ±0.011	0.444 ±0.005	0.457 ±0.057	0.482 ±0.048
	RU	0.475 ±0.005	0.389±0.004	0.428±0.005	0.517 ±0.018	0.519 ±0.006	0.587 ±0.008
	TPU	0.412 ±0.010	0.364±0.01	0.422 ±0.018	0.424 ±0.011	0.472 ±0.008	0.557 ±0.014

Table 5 Average dynamic coefficient of friction (DCOF) and static coefficient of friction (SCOF) ± standard deviation at -2 °C.

0 °C							
Average COF	Material	0.3 m/s	1 m/s	2 m/s	3 m/s	4 m/s	5 m/s
Dynamic	PU	0.048 ±0.000	0.055±0.000	0.059 ±0.000	0.065 ±0.000	0.064 ±0.000	0.070 ±0.000
	RU	0.042 ±0.000	0.038±0.000	0.041 ±0.000	0.042 ±0.000	0.044 ±0.000	0.046 ±0.000
	TPU	0.038 ±0.000	0.039±0.005	0.040 ±0.000	0.043 ±0.000	0.043 ±0.000	0.045 ±0.000
Static	PU	0.730 ±0.021	0.744±0.008	0.871 ±0.005	0.899 ±0.028	1.083 ±0.005	1.116 ±0.011
	RU	0.157 ±0.004	0.116±0.004	0.155 ±0.005	0.173 ±0.004	0.218 ±0.004	0.226 ±0.005
	TPU	0.322 ±0.007	0.291±0.005	0.336 ±0.011	0.380 ±0.006	0.412 ±0.006	0.462 ±0.015

Table 6 Average dynamic coefficient of friction (DCOF) and static coefficient of friction (SCOF) ± standard deviation at 0 °C.

Comparison of mechanical friction evaluations from occupational footwear certified as slip resistant

Lasse Jakobsen[a*], Timo Bagehorn[b], Ion Marius Sivebaek[a] and Filip Gertz Lysdal[a]

[a]Department of Civil and Mechanical Engineering, Technical University of Denmark, Kgs. Lyngby, Denmark

[b]Department of Health Science and Technology, Aalborg University, Aalborg, Denmark

*Corresponding author: lasjak@mek.dtu.dk

Abstract

Slipping is a major cause of occupational accidents that incites from insufficient friction between footwear and surface, often due to contamination of the walking surface. Proper footwear that preserves sufficient friction is therefore crucial to avoid the occurrence of slipping accidents. Many factors and features, including footwear composition and geometry, as well as the testing conditions, all affect an individual shoe's ability to resist slipping. It is therefore of high importance to test occupational footwear under various conditions to assert its resistance towards slipping, while it also remains unknown, whether certified slip resistant footwear will also show high slip resistance in a biofidelic test, and thus likely protect better against slipping. Therefore, the aim of this study was to compare slip resistance certification data from five certified shoes with measurements performed on a hydraulic actuated robotic test setup in accordance with the ISO 20347:2012 standard, as well as determining their performance in a biofidelic setup that resembles the biomechanics of slipping. Pre-obtained certification data attributed Shoe #3 with the highest slip resistance. However, our mechanical assessment of the same footwear models showed that Shoe #2 had the higher slip resistance and was superior to all shoes under more biofidelic testing parameters. Based on our mechanical evaluations, it seems that a manufacturer can advantageously increase both the heel beveling as well as the midsole thickness for an increased slip resistance. However, it remains to be investigated in a clinical setting how this might affect slip probability and ultimately occupational safety.

Keywords

friction, footwear, traction, slips trips and falls, occupational safety

1. Introduction

Falls are among the major causes of work-related accidents and a significant socioeconomically burden (Arbejdstilsynet, 2017; U.S. Department of Labor- Bureau of Labor Statistics, 2019). In Denmark alone, fall accidents are accountable of an annual expense of DKK 3.4 billion (€460.000.000) as consequence of lost production, absence from work, and direct expenses of the public healthcare system (Sundhedsstyrelsen, 2016). Slipping is a typical cause of these falling accidents (Chang et al., 2016) and incites from insufficient friction between footwear and surface, often due to contamination of the walking surface (Chang et al., 2001; Grönqvist et al., 2001; Hanson et al., 1999).

One obvious way to increase slip resistance in contaminated environments is to increase the roughness of the floor surface (Khaday et al., 2021). Increasing the surface roughness, however, complicates the cleanliness and is often not a viable approach in occupational settings where hygiene is of high priority, such as in the food industry. Consequently, this leaves the footwear counterpart as the modifiable option to accommodate the challenge of increasing the slip resistance on these typically smooth, and often contaminated, floors.

Occupational footwear for the food industry can be certified according to the ISO 20347 standard (ISO, 2012). In order to obtain this certification, the specific footwear must, among other criteria, achieve a certain level of slip resistance. During these tests, the available coefficient of friction (ACOF) is determined from mechanical testing under various conditions, and derived from the dynamic coefficient of friction between footwear and surface during sliding (Chang et al., 2001). These testing standards might be good for a uniform description of slip resistance behavior. However, they do not seem to resemble actual slipping events (Beschorner et al., 2019; Blanchette & Powers, 2015), and even the slightest alteration to the testing parameters can influence the outcome of the ACOF measurements (Beschorner et al., 2007). As a consequence, new testing parameters that are arguably more representative of real slipping events in terms of normal load, sliding velocity, static contact time and shoe-surface contact angle have been proposed as an alternative (Redfern et al., 2001), and are often referred to as “biofidelic” mechanical tests (Iraqi et al., 2018).

Many factors and features, including material choice (Beschorner et al., 2009; Jakobsen et al., 2022a; Strobel et al., 2012) outsole geometry/tread pattern (Beschorner et al., 2009; Derler et al., 2007; Li and Chen, 2004; Moore et al., 2012) and hardness (Grönqvist, 1995; Tsai and Powers, 2009), all affect the individual shoe’s ability to resist slipping. These design features might affect the ACOF in various ways, and it is therefore of high importance to test how a

specific shoe performs under the various conditions of the test standard, and whether a new shoe design can achieve the EN ISO 20347 certification. Here, it also remains unknown, whether a shoe that shows high slip resistance in the standard test will also show high slip restistance in a biofidelic test, and thus likely protect better against slipping.

Therefore, the objectives of this study were to (a) determine the ACOF of slip resistant footwear models when undergoing standard testing in a new modifiable robotic test setup, and (b) compare these ACOF measurements to EN ISO 20347 certifications from independent testing, and finally (c) to adapt the mechanical test parameters to conduct biofidelic measurements for a complete mechanical evaluation of the slip resistance of footwear models.

2. Methods

Five different footwear models pre-certified as “slip resistant” were mechanically tested in this study. All five shoes underwent ACOF measurements according to the ISO 20347 standard (ISO, 2012), as well as a more biofidelic ACOF mechanical test. Pre-obtained slip resistance certifications were provided beforehand by SIKA Footwear A/S for comparison.

2.1. Footwear

The evaluated five shoes were all left-sided, size EU 42 models, made with varying designs, geometries and material compositions (Table 1). Shoe #1 (Figure 1) comprised of a rubber outsole and ethylene-vinyl acetate (EVA) midsole. As did Shoe #2 (Figure 2), Shoe #3 (Figure 3), and Shoe #4 (Figure 4). Both the outsole and midsole of Shoe #5 (Figure 5) comprised of polyurethane (PU). The upper and brand names are removed from the respective figures for anonymization.

Figure 1. Shoe #1 outsole pattern (top) and profile (bottom).

Figure 2. Shoe #2 outsole pattern (top) and profile (bottom).

Figure 3. Shoe #3 outsole pattern (top) and profile (bottom).

Figure 4. **Shoe #4 outsole pattern (top) and profile (bottom).**

Figure 5. **Shoe #5 outsole pattern (top) and profile (bottom).**

Table 1. Geometry and material composition of the shoes

Shoe	Outsole material	Midsole material	Outsole hardness [Shore A]	Midsole thickness [mm]		Outsole thickness [mm]		Midsole/outsole thickness aspect ratio		Sagittal heel angle [°]	Outsole tread depth [mm]	Outsole tread width [mm]
				Heel	Forefoot	Heel	Forefoot	Heel	Forefoot			
#1	Rubber	EVA	58.8	17.0	6.0	6.0	6.0	2.8	1.0	7.0	3.0	1.5
#2	Rubber	EVA	62.4	22.0	12.5	6.0	6.0	3.7	2.1	10.7	3.5	2.0
#3	Rubber	EVA	68.0	20.0	6.0	6.0	6.0	3.3	1.0	0.0	2.5	2.0
#4	Rubber	EVA	69.2	12.5	6.0	7.2	7.2	1.7	0.8	7.0	1.0	1.0
#5	PU	PU	70.4	18.6	6.0	3.0	3.0	6.2	2.0	7.0	4.0	6.0

2.2. Surfaces and contaminants

We evaluated slip resistance against two different surfaces with two different contaminants, as specified in the test standard (ISO, 2012). The first surface was a ceramic tile (Eurotile 2) contaminated with a detergent solution containing a mass fraction of 0.5% sodium lauryl sulfate (SLS) in demineralized water. The second surface was a calibrated steel plate (number 1.4301 (AISI304)) contaminated with an 85-percent glycerin solution (85% glycerol and 15% water by volume solution with a viscosity of 110 cP at 20° C). Fifty ml of contamination was distributed over an area of 10 by 40 cm in all tests, with full contamination of the entire area between shoe and surface ensured by visual inspection.

The roughness of both surfaces was measured beforehand using a 2D contact profilometer (Surtronic S-100, Taylor-Hobson, AMETEK, Leicester, England) over a scan length of 8.0 mm. The ceramic tile had an arithmetic mean roughness (Ra) of 3.2 μm (0.8 mm cutoff length), and the steel surface had a mean Ra of 0.2 μm (0.25 mm cutoff length).

2.3. Test procedure

The five shoes were tested for slip resistance in an actuated force plate-based robotic test setup (Figure 6) previously described in Jakobsen et al. (2022b). This setup is developed to accommodate the test method for slip resistance described in ISO 13287:2019 (ISO, 2019). Furthermore, the setup is highly modifiable and can be adapted to

investigate various shoe-surface contact scenarios (Bagehorn et al., n.d.; Ismail et al., 2020, n.d.; Jakobsen et al., 2022b; Lysdal et al., 2022), and in this study modified to also accompany biofidelic footwear slip-resistance testing.

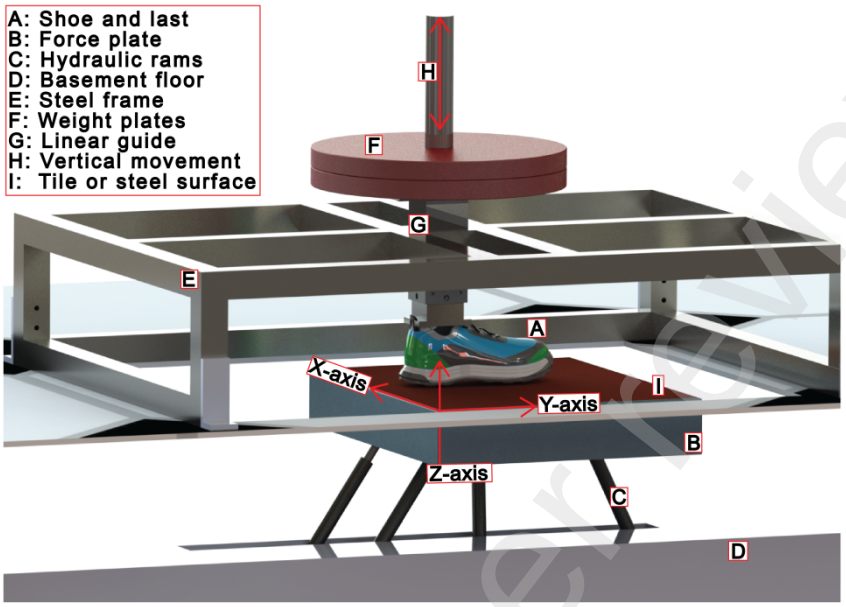

Figure 6. Illustration of the actuated force plate-based robotic test setup.

Reused with permission from Jakobsen et al. (2022b)

The shoes were cleaned and prepared following the specifications of the ISO 13287:2019 (ISO, 2019). This included pre-abrasion of the shoe soles with 400 grit sandpaper, cleaning the outsoles with ethanol, scrubbing with a clean medium stiff brush, washing with demineralized water, and drying with clean dry compressed air. Following this procedure, the shoes rested at the room temperature for a minimum of one hour before testing. The surfaces were cleaned with ethanol, rinsed with demineralized water, and dried using clean dry compressed air. This procedure was repeated every time surfaces and contaminants were changed.

According to EN ISO 20347:2012 (ISO, 2012), occupational shoes are to be tested in accordance with the ISO 13287 (ISO, 2019). This includes a sliding velocity of 0.3 m/s, a normal force of 500 N, a one-second static contact time, and sliding at 0° (flat contact) and 7° heel contact angle (Figure 7). In order to achieve certification as 'slip resistant' under the respective conditions, the tested footwear shall fulfill the following requirements:

A) Footwear resistant to slip on a Eurotile 2 contaminated with SLS must obtain a coefficient of friction of $\mu \geq 0.32$ for forward flat slip, and $\mu \geq 0.28$ for forward heel slip at 7° angled contact (ISO, 2012). B) Footwear resistant to slip

on a steel surface contaminated with glycerin must obtain a coefficient of friction of $\mu \geq 0.18$ for forward flat slip, and $\mu \geq 0.13$ for forward heel slip at 7° angled contact (ISO, 2012).

For the biofidelic measurements, we lowered the static contact time to 0.5 s (Chang et al., 2001b), increased the sliding velocity to 0.5 m/s (Blanchette and Powers, 2015), reduced the normal load to 400 N, and increased the heel/surface contact angle to 17° (Beschorner et al., 2019) (Figure 7).

In total, the five shoes underwent five different testing conditions: 1) Eurotile contaminated with SLS at flat contact, 2) Eurotile contaminated with SLS at 7° contact, 3) Steel contaminated with glycerin at flat contact, 4) Steel contaminated with glycerin at 7° contact, and 5) Biofidelic testing on steel with glycerin contamination.

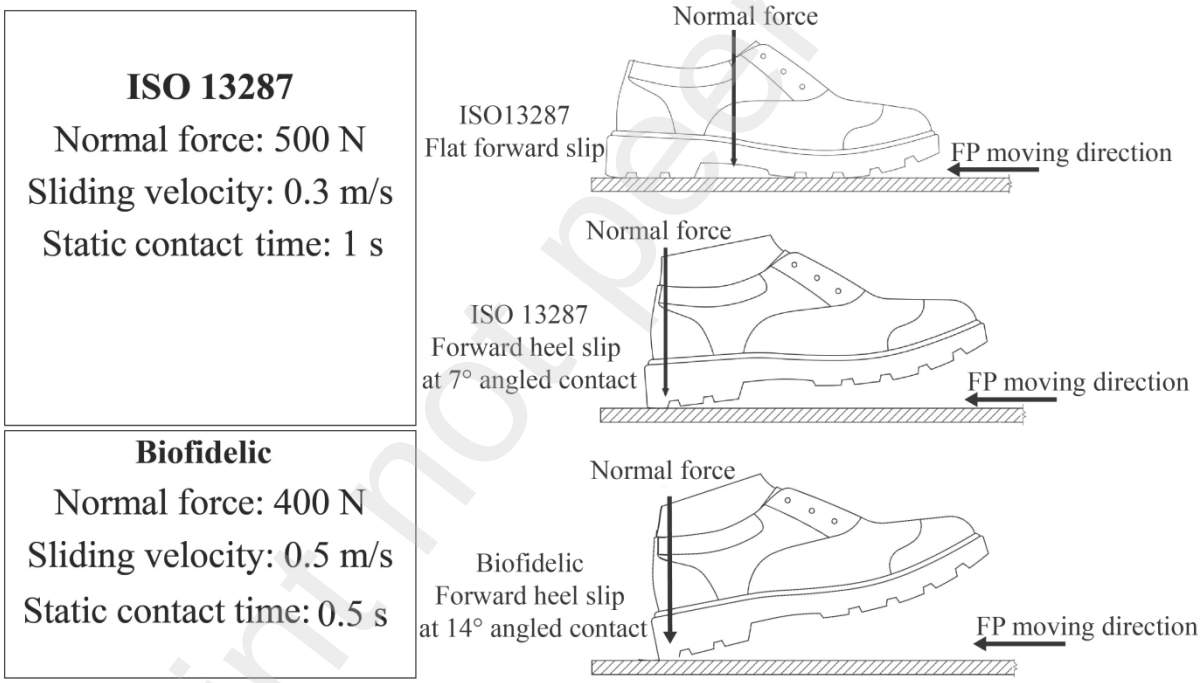

Figure 7. Testing parameters in accordance the ISO 13287 test standard and testing optimized for biofidelic parameters. Adapted from (ISO, 2019) with permission from Danish Standards (ISO 13287:2019).

2.4. Data processing

The dynamic coefficient of friction was used as a measure of slip resistance and was calculated using a customized script in MATLAB version R2020b (MathWorks, Massachusetts, USA) by dividing the sum of the horizontal reaction forces, F_x and F_y (friction forces) with the vertical reaction force F_z (normal force) (Jakobsen et al., 2022c).

3. Results

3.1. Eurotile surface contaminated with SLS

On the Eurotile contaminated with SLS, shoe #2 ranked highest in the robotic test during the flat forward slip with an ACOF of 0.698 (± 0.003). Under this condition, the certification data ranked shoe #3 highest with an ACOF of 0.7. All shoes achieved the minimum required ACOF ($\mu \geq 0.32$) (Figure 8), with shoe #4 achieving the lowest ACOF in the robotic test (0.410 ± 0.006), and shoe #5 the lowest according to the certification data (ACOF = 0.38) (Supplementary Appendix).

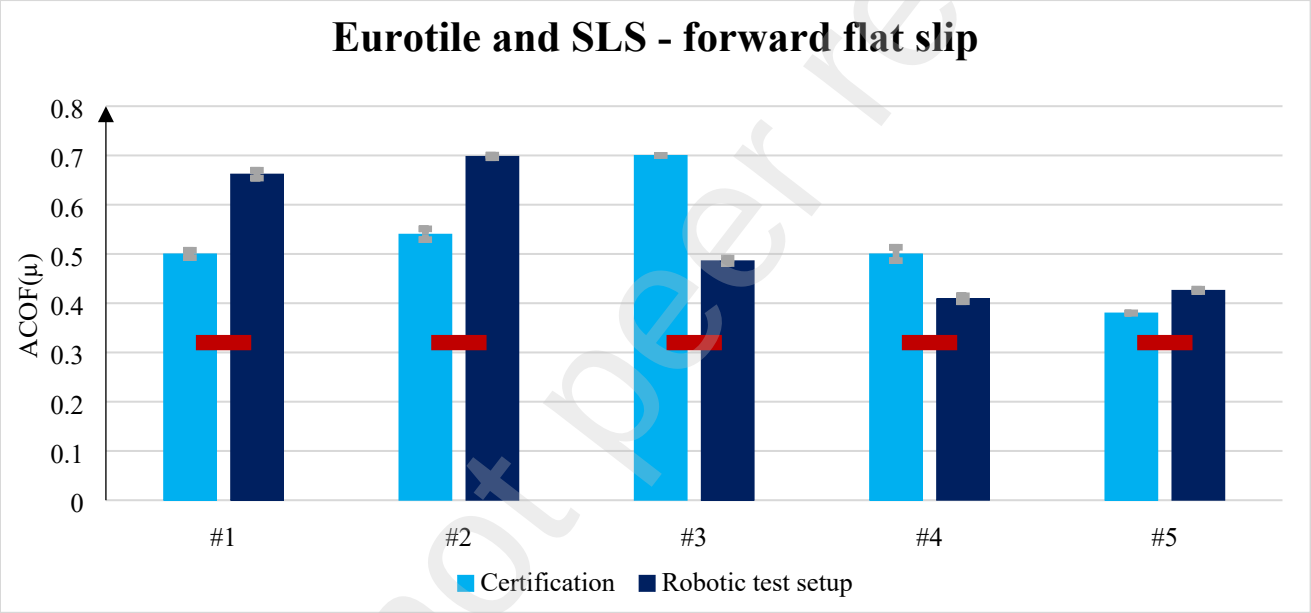

Figure 8. Certification and robotic test setup measurements on Eurotile surface contaminated with SLS during the forward flat slip. The red line represents the minimum ACOF required to meet ISO 20347 certification ($\mu \geq 0.32$). The error bars represent ± standard deviation for five measurements and are presented when available.

During the 7° forward heel slip under the same conditions, shoe #2 again ranked highest in the robotic test with an ACOF of 0.643 (± 0.003). Certification data ranked shoe #3 higher with an ACOF of 0.6. All shoes achieved the minimum required ACOF ($\mu \geq 0.28$) (Figure 9), with shoe #4 achieving the lowest ACOF in the robotic test (0.315 ± 0.003), and shoe #5 the lowest according to the certification data (ACOF = 0.38) (Supplementary Appendix).

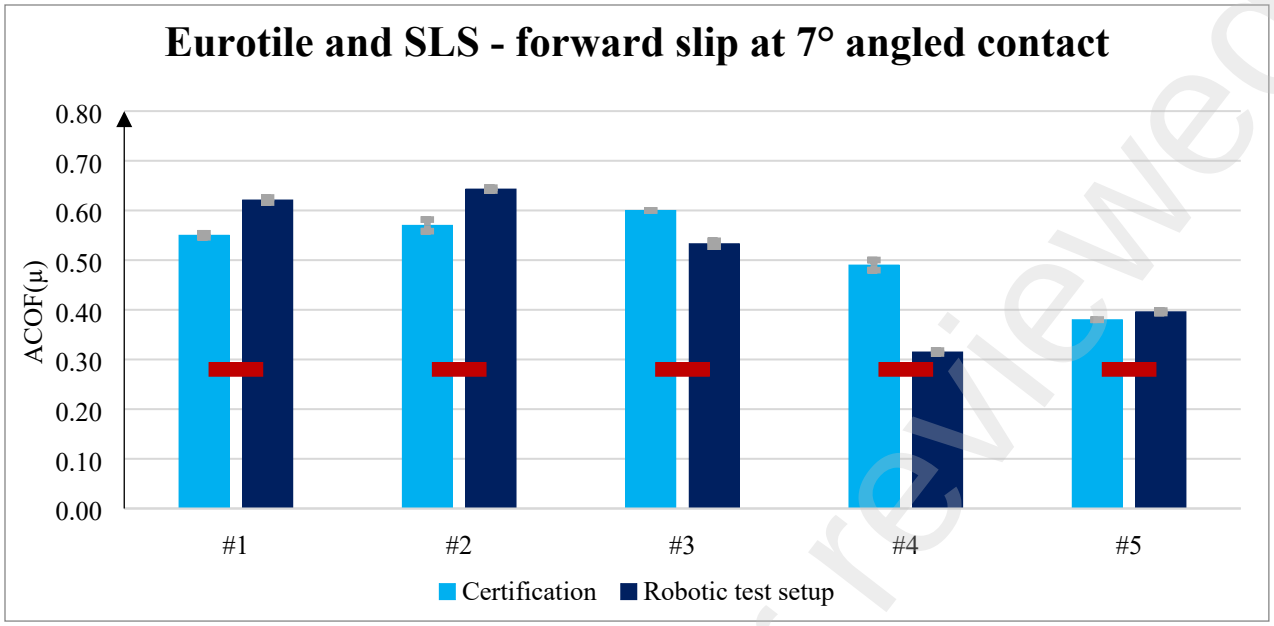

Figure 9. Certification and robotic test setup measurements on Eurotile surface contaminated with SLS during the 7° forward heel slip. The red line represents the minimum ACOF required to meet ISO 20347 certification (μ ≥ 0.28). The error bars represent ± standard deviation for five measurements and are presented when available.

3.2. Steel surface contaminated with glycerin

On the steel surface contaminated with glycerin, shoe #2 ranked highest in the robotic test during the flat forward slip with an ACOF of 0.543 (± 0.002). Here, the certification data ranked shoe #3 highest with an ACOF of 0.67.

Shoe #1 achieved the lowest friction in the robotic test with an ACOF of 0.159 (± 0.005), while shoe #4 achieved the lowest according to the certification data (ACOF = 0.18). All shoes had received the 'slip resistant' certificate for this condition beforehand by achieving the minimum required ACOF (μ ≥ 0.18). Shoe #1, shoe #4 and shoe #5, however, did not pass the minimum required level of friction in the robotic test setup (Figure 10) (Supplementary Appendix).

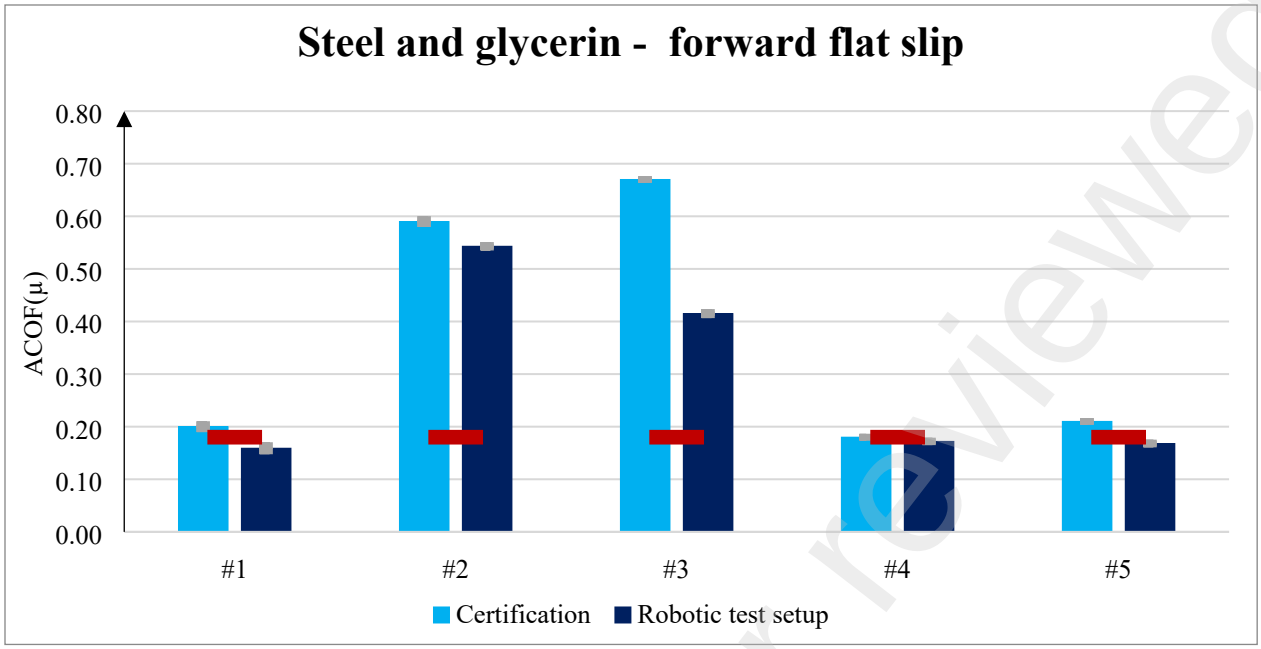

Figure 10. Certification and robotic test setup measurements on steel surface contaminated with glycerin during the forward flat slip. The red line represents the minimum ACOF required to meet ISO 20347 certification (μ ≥ 0.18). The error bars represent ± standard deviation for five measurements and are presented when available.

During the 7° forward heel slip on the steel surface, shoe #3 ranked highest in the robotic test with an ACOF of 0.495 (± 0.002). Certification data also ranked shoe #3 highest with an ACOF of 0.5. All shoes achieved the minimum required ACOF (μ ≥ 0.13) (Figure 11), with shoe #5 achieving the lowest ACOF in the robotic test (0.144 ± 0.000), and shoe #4 the lowest according to the certification data (ACOF = 0.13) (Supplementary Appendix).

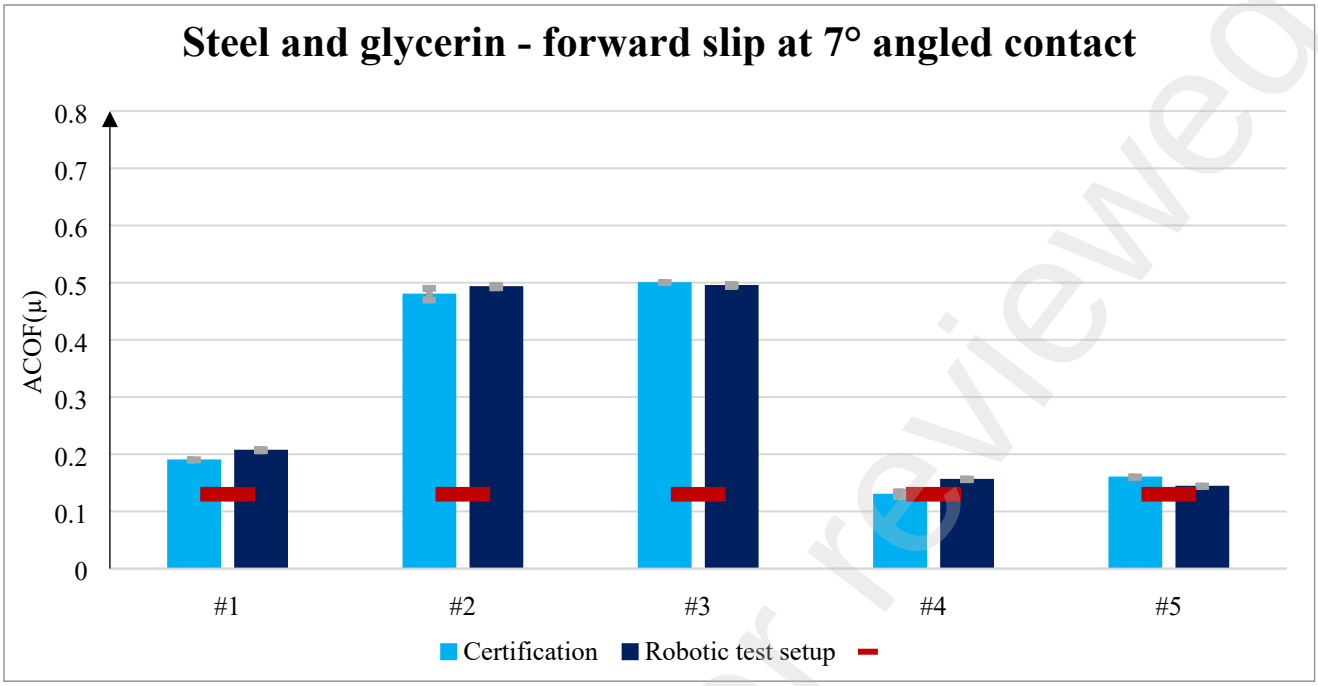

Figure 11. Certification and robotic test setup measurements on steel surface contaminated with glycerin during the 7° forward heel slip. The red line represents the minimum ACOF required to meet ISO 20347 certification (μ ≥ 0.28). The error bars represent ± standard deviation for five measurements and are presented when available.

3.3. Biofidelic measurements on steel surface contaminated with glycerin

Shoe #2 showed the highest slip resistance during the biofidelic testing with an ACOF of 0.478 (± 0.003), and shoe #5 achieved the lowest (ACOF = 0.112 ± 0.001). All shoes achieved lower ACOF during biofidelic testing measurements compared to the standard 7° forward heel slip from both the certification data and robotic test setup measurements (Figure 12), with shoe #3 revealing the largest absolute (0.12-0.13) and relative (25%) reduction in ACOF (Supplementary Appendix).

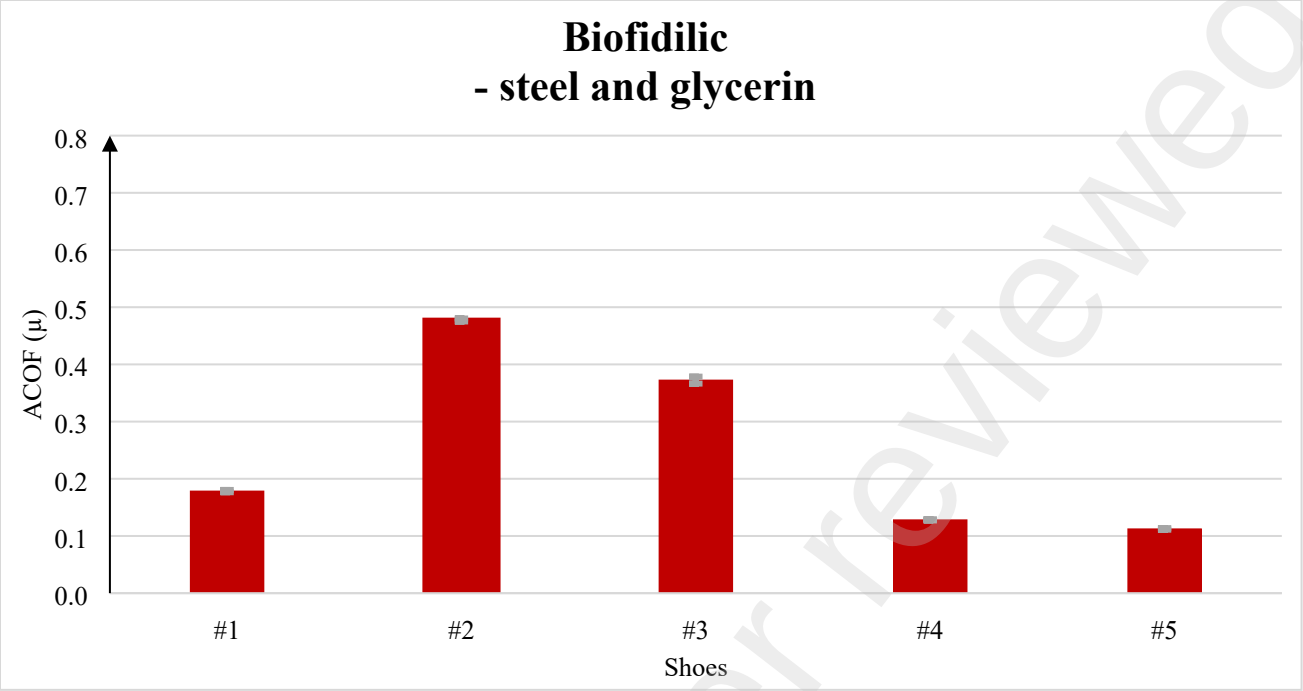

Figure 12. Biofidelic measurements from robotic test setup. The error bars represent ± standard deviation for five measurements.

4. Discussion

In this study, we evaluated the mechanical slip resistance of five different occupational footwear models in compliance with the EN ISO 20347 test standard, and in a more biofidelic test, by using a modifiable actuated force plate based robotic test setup. The five shoes had all previously been certified as slip resistant under each of the four test conditions in the EN ISO 20347 standard. From these certifications, Shoe #3 was consistently ranked the more slip-resistant shoe of the five models. In our mechanical evaluation, however, Shoe #2 appeared as the most slip resistant model. This shoe ranked highest under all conditions, except for the 7° forward heel slip on steel with glycerin contamination (where it performed similar to Shoe #3). This pattern was also supported in the biofidelic test where Shoe #2 achieved a 22% higher ACOF than Shoe #3.

4.1. Effect of test conditions

On the Eurotile contaminated with SLS, the average ACOF in the robotic test for the forward flat slip was 0.54, ranging from 0.41 to 0.70, with Shoe #2 having the highest slip resistance and Shoe #4 the lowest. The minimum

required ACOF for EN ISO 20437 slip resistance certification is 0.32 under this condition. All shoes in both the certifications and in the robotic tests achieved this requirement. In the 7° forward heel slip, the average ACOF was 0.50, ranging from 0.32 (Shoe #4) to 0.64 (Shoe #2), with the same ranking of the shoes as in the forward flat slip, and all shoes achieved the minimum required ACOF of 0.28 in both certification and robotic test.

On the steel surface contaminated with glycerin, the average ACOF for the forward flat slip was 0.29, ranging from 0.16 to 0.54, with Shoe #2 achieving the highest slip resistance. The minimum required ACOF is 0.18 under this condition, and although that requirement had been met by all shoe models in the pre-obtained external certification data, this level of ACOF could not be achieved by three of the shoes (Shoe #1, Shoe #,4 and Shoe #5) in the robotic tests. In the 7° forward heel slip, the average ACOF was 0.30, ranging from 0.14 (Shoe #5) to 0.50 (Shoe #3). Thus, all shoes achieved the minimum required ACOF of 0.13 under this condition in both certifications and robotic tests.

On average, the forward flat slip ACOF was 46% (0.54 to 0.29) lower on the steel surface with glycerin than on the Eurotile with SLS. In the 7° forward heel slip, the ACOF difference between the surfaces (and contaminations) was 41%, and again lower ACOF on the steel surface with glycerin. The lower ACOF on the steel surface is likely a direct result of the lower surface roughness compared to the Eurotile, where higher roughness increases friction when contaminants are present (Cowap et al., 2015). This also justifies the lower minimum required ACOF on the steel surface for certification as slip resistant (ISO, 2012). The observed differences between conditions are likely also factored by the type of contamination, with this being a known contributor to the level of ACOF during mechanical slipping (Chanda et al., 2018).

Differences between certification data and measurements from the robotic test setup differed unsystematically among the surface/contaminant/heel angle conditions. Small ACOF differences between certification measurements and robotic test setup measurements were found when the steel surface was contaminated with glycerin and a 7° heel contact was used. However, larger differences between certification data and robotic test setup measurements were found when the Eurotile was contaminated with SLS with a flat shoe/surface contact. The Eurotile 2 has been found to decrease in slip resistance due to wear (Engels, 2018), which might contribute to the observed differences, since it is unknown how many measurement cycles the Eurotile 2 from the certification measurements and robotic test setup had been through.

Considerable ACOF differences were found between the shoe models, even though all are certified as slip resistant. All shoes tested in this study revealed lower ACOF values during the biofidelic measurements, compared to 7° angled forward slip measurements conducted on the robotic test setup and compared to certification data for the five shoes available. Hence, this study supports the idea that the testing parameters from the ISO 13287 may overestimate the ACOF compared to realistic testing conditions given by biofidelic testing parameters (Hunwin et al., 2010). This is in line with experiments revealing that increased sliding velocity decreases slip resistance and that a complex interaction exists between normal force and footwear/surface contact angle (Beschorner et al., 2007).

The ACOF results for the commercially available slip resistant footwear in this study are comparable to a previous study with similar methodology (Jones et al., 2018). Jones and colleagues found ACOF of ~ 0.5 to 0.65, which is somewhat comparable to our findings performed on the Eurotile contaminated with SLS for Shoe #3 (ACOF = 0.533), which had a similar outsole pattern to the shoes in their study (Jones et al., 2018). The small difference may be explained by a difference in contact angle, suggesting that 7° contact angle will lead to a higher contact area compared to 17°, and thus higher friction coefficient (Iraqi et al., 2020). On the other hand, Jones and colleagues used a lower normal force (225–275 N) compared to the 400 N in the present study. A low normal force typically results in a higher friction coefficient compared to high normal force for polymer materials (Briscoe and Tabor, 1975). It therefore remains unknown which of the two parameters (normal force or contact area) that contributed the most to the observed difference between our findings and Jones et al (2018).

4.2. Effect of footwear characteristics

The relatively large variations between shoe models found in this study can possibly be explained by differences in materials, material hardness, outsole tread patterns, outsole shape/geometry and sole foam thickness. Polyurethane outsoles have previously been shown to outperform rubber outsoles on contaminated surfaces (Jakobsen et al., 2022b), which however was not the case in this study, where shoe #5 was the only shoe constructed with a polyurethane outsole, with the remaining shoes constructed of rubber outsoles. Especially on the steel surface contaminated with glycerin at angled contact, shoe #5 had low ACOF. In addition, shoe #5 also had the second highest hardness among the tested shoes. Harder outsoles have previously been associated with reduced friction (Grönqvist, 1995) and may contribute to lower ACOF for shoe #5. This might also explain why shoe #1, with the softest outsole (shore A = 58.8)

perform well on the rougher Eurotile contaminated with SLS. Hardness is, however, a static measure that does not reveal the dynamic properties of viscoelastic materials (Lorenz et al., 2011). A recent pilot study using dynamic mechanical analysis (DMA) indicated that the static hardness measure could extend the characterization of viscoelastic outsole materials, and that outsole stiffness is highly dependent on load frequency, and thus the sliding velocity (Jakobsen et al., 2021).

It should be noted though, that the difference in outsole hardness among shoe #3 - #5 is very low. In addition, shoe #5 had considerably different outsole tread pattern design, thus the material choice and characteristics cannot be isolated as an explanatory factor for lower ACOF alone.

Thread pattern is related to shoes fluid drainage capabilities and have long been considered important for slip resistant footwear (Strandberg, 1985), why slip resistant footwear often have numerus tread channels. The five shoes in this study are no exception and the thread channels vary greatly in design. Oblique and perpendicular (to sliding direction) tread patterns have in controlled studies been found superior to parallel patterns (Li and Chen, 2004; Li and Chin, 2005). Increased tread depth has previously shown increased slip resistance (Li et al., 2006). This is supported by our findings where Shoe #2 and Shoe #3, with deeper treads, achieved higher ACOF compared to Shoe #4 and Shoe #5 with low treads. It is however important that these treads do not become too high and narrow. This may cause a reduced contact area during sliding, caused by a bending of the tread block due to insufficient stiffness (Yamaguchi et al., 2017).

A beveled heel design is another geometric factor that affects footwear slip resistance. This can provide a larger contact area between shoe and floor during heel contact (Lloyd and Stevenson, 1989). A beveled heel is especially pronounced for Shoe #2, which has the largest heel angle (10.7°) of all the shoes tested in this study. This is probably why Shoe #2 outperforms the other shoes during the biofidelic measurements (0.48), where the shoe/surface contact angle was 14°. Shoe #3, on the other hand, had the highest ACOF certification (0.50) but its 0° sagittal heel angle, is the likely explanation behind the reduced ACOF during the biofidelic measurements, likely caused by a smaller contact area at 14° angled contact.

The heel part outsole designs for shoe #1, #4 and #5 varies from shoe #2, and they all have perpendicular (to sliding direction) outsole patterns. On a glycerin contaminated smooth steel surface, these perpendicular outsole patterns may cause a boundary or mixed lubrication regime, partly separating the outsole and surface and ultimately reducing the

friction coefficient (Yamaguchi et al., 2017). In addition, the thicker midsole of Shoe#2 compared to the other shoe models might also explain the higher ACOF. Thicker foam layers (i.e., midsole height) above a uniform layer of rubber (i.e., outsole) have previously been shown to increase friction, arguably due to a higher midsole shear (Moriyasu et al., 2019).

4.3. Limitations

This study is not without limitations. First, we did not have access to the exact shoe samples that were tested in the pre-obtained certifications. While we did test the exact same shoe models and sizes, we simply cannot rule out that small differences in e.g., material properties and sole roughness might exist between production batches and individual samples. Second, we were limited in our access to data from the individual external measurements preceding the obtained certifications from some of the shoe models. In these instances, we only received the average measure of the five tests, and thus could not report the accuracy of the certification. It is however a requirement to the EN ISO 13287 standard that the slip resistance testing device can measure forces with an accuracy of 2% or better, why we must assume a high precision in all pre-obtained external slip resistance certifications. Finally, it may be argued that our study is limited by using mechanical research methods to inform on what is unquestionably a biomechanical challenge. The robotic test setup used in this study is, however, able to detect changes in friction coefficient with high precision, and its relevance to the field of occupational safety was sought improved by including biofidelic testing that resembles "real world" slipping scenarios, in addition to the standard testing regulations. However, it remains unknown how the tested shoes would perform in a real-life setting, where movements such as twisting and rotating occur.

5. Conclusion

Based on our mechanical evaluation of five different certified slip resistant occupational footwear models, it seems that a manufacturer can advantageously increase both the heel beveling as well as the midsole thickness for an increased slip resistance. However, it remains to be investigated in a clinical setting how this might affect slip probability and ultimately occupational safety.

6. Acknowledgments

This study was funded by the Danish Working Environment Research Fund (grant number: 20195100816). SIKA Footwear A/S provided the shoes used in this study. SIKA Footwear A/S had no scientific role in the interpretation and presentation of the results. The authors wish to thank Kasper Vejergang Jepsen Lundh and Jane Bjerregaard Nielsen from SIKA Footwear for their extensive help and very fast execution. The authors have no conflicts of interest to declare.

7. Appendix

Ceramic tile contaminated with SLS (Flat contact)				
Shoes	Certification	Standard deviation	Robotic test setup	Standard deviation
#1	0.5	0.00748	0.662	0.007949679
#2	0.54	0.01095	0.698	0.002638366
#3	0.7	Na	0.486	0.005457214
#4	0.5	0.01356	0.409	0.006006341
#5	0.38	Na	0.426	0.002437492

Ceramic tile contaminated with SLS (7° heel contact)				
Shoes	Certification	Standard deviation	Robotic test setup	Standard deviation
#1	0.55	0.004	0.621	0.00509
#2	0.57	0.01166	0.643	0.00288
#3	0.6	Na	0.533	0.00588
#4	0.49	0.0102	0.315	0.00291
#5	0.38	Na	0.396	0.00246

Steel/Glycerin (Flat contact)				
Shoes	Certification	Standard deviation	Robotic test setup	Standard deviation
#1	0.20	0.004	0.159	0.0051
#2	0.59	0.004	0.543	0.00168
#3	0.67	Na	0.415	0.00224
#4	0.18	0	0.172	0.00075
#5	0.21	Na	0.168	0.00101

Steel/Glycerin (7° heel contact)				
Shoes	Certification	Standard deviation	Robotic test setup	Standard deviation
#1	0.19	0	0.207	0.0011
#2	0.48	0.0102	0.493	0.00202
#3	0.5	Na	0.495	0.0016
#4	0.13	0.004	0.156	0.00065
#5	0.16	Na	0.144	0.00033

Biofidelic		
Shoes	Robotic test setup	Standard deviation
#1	0.178	0.002009947
#2	0.478	0.002590953
#3	0.373	0.006074498
#4	0.128	0.001042584
#5	0.112	0.00136624

REFERENCES

Arbejdstilsynet, 2017. Baggrundsnotat om snubleulykker (2017).

Bagehorn, T., Lysdal, G.F., Jakobsen, L., de Zee, M., Kersting, U.G., n.d. Medio-lateral and lateral edge friction in indoor sports shoes. Unpubl. results.

Beschorner, K., Lovell, M., Higgs, C.F., Redfern, M.S., Beschorner, K., Lovell, M., Fred Higgs Iii, C., Redfern, M.S., Fred Higgs Iii, C., 2009. Modeling mixed-lubrication of a shoe-floor interface applied to a pin-on-disk apparatus. Tribol. Trans. 52, 560–568. https://doi.org/10.1080/10402000902825705

Beschorner, K.E., Iraqi, A., Redfern, M.S., Cham, R., Li, Y., 2019. Predicting slips based on the STM 603 whole-footwear tribometer under different coefficient of friction testing conditions. https://doi.org/10.1080/00140139.2019.1567828

Beschorner, K.E., Redfern, M.S., Porter, W.L., Debski, R.E., 2007. Effects of slip testing parameters on measured coefficient of friction. Appl. Ergon. 38, 773–780. https://doi.org/10.1016/j.apergo.2006.10.005

Blanchette, M.G., Powers, C.M., 2015. Slip Prediction Accuracy and Bias of the SATRA STM 603 Whole Shoe Tester. J. Test. Eval. 43, 20130308. https://doi.org/10.1520/JTE20130308

Briscoe, B.J., Tabor, D., 1975. The effect of pressure on the frictional properties of polymers. Wear 34, 29–38. https://doi.org/https://dx.doi.org/10.1016/0043-1648(75)90306-3

Chanda, A., Fellow, P., Jones, T.G., Beschorner, K.E., 2018. Generalizability of Footwear Traction Performance

across Flooring and Contaminant Conditions HHS Public Access. IISE Trans Occup Erg. Hum Factors 6, 98–108. https://doi.org/10.1080/24725838.2018.1517702

Chang, W., Grönqvist, R., Leclercq, S., Brungraber, R.J., Mattke, U., Strandberg, L., Thorpe, S.C., Myung, R., Makkonen, L., Courtney, T.K., 2001a. The role of friction in the measurement of slipperiness, Part 2: Survey of friction measurement devices. Ergonomics 44, 1233–1261. https://doi.org/10.1080/00140130110085583

Chang, W., Grönqvist, R., Leclercq, S., Myung, R., Makkonen, L., Strandberg, L., Brungraber, R.J., Mattke, U., Thorpe, S.C., 2001b. The role of friction in the measurement of slipperiness, Part 1: Friction mechanisms and definition of test conditions The role of friction in the measurement of slipperiness, Part 1: Friction mechanisms and definition of test conditions. Ergonomics 44. https://doi.org/10.1080/00140130110085574

Chang, W.R., Leclercq, S., Lockhart, T.E., Haslam, R., 2016. State of science: occupational slips, trips and falls on the same level State of science: occupational slips, trips and falls on the same level. Ergonomics 59, 861–883. https://doi.org/10.1080/00140139.2016.1157214

Cowap, M.J.H., Moghaddam, S.R.M., Menezes, P.L., Beschorner, K.E., 2015. Contributions of adhesion and hysteresis to coefficient of friction between shoe and floor surfaces: Effects of floor roughness and sliding speed. Tribol. - Mater. Surfaces Interfaces 9. https://doi.org/10.1179/1751584X15Y.0000000005

Derler, S., Kausch, F., Huber, R., 2007. Analysis of factors influencing the friction coefficients of shoe sole materials. Saf. Sci. 822–832. https://doi.org/10.1016/j.ssci.2007.01.010

Engels, M., 2018. Recerence Materials - UK Slip Resistance Group.

Grönqvist, R., 1995. Mechanisms of friction and assessment of slip resistance of new and used footwear soles on contaminated floors. Ergonomics 38, 224–241. https://doi.org/10.1080/00140139508925100

Grönqvist, R., Chang, W., Courtney, T.K., Leamon, T.B., Redfern, M.S., K, T., B, T., S, M., 2001. Measurement of slipperiness : fundamental concepts and definitions. Ergonomics 44, 1117. https://doi.org/10.1080/0014013011008552

Hanson, J.P., Redfern, M.S., Mazumdar, M., 1999. Predicting slips and falls considering required and available friction. Ergonomics 42, 1619–1633. https://doi.org/10.1080/001401399184712

Hunwin, G., Thorpe, S., Hallas, K., 2010. Improvements to the EN slip resistance test for footwear. Contemp. Ergon.

Hum. Factors 2010 Proceeding, 471–479.

Iraqi, A., Cham, R., Redfern, M.S., Beschorner, K.E., 2018. Coefficient of friction testing parameters influence the prediction of human slips. Appl. Ergon. 70, 118–126. https://doi.org/10.1016/j.apergo.2018.02.017

Iraqi, A., Vidic, N.S., Redfern, M.S., Beschorner, K.E., 2020. Prediction of coefficient of friction based on footwear outsole features. Appl. Ergon. 82, 102963. https://doi.org/10.1016/j.apergo.2019.102963

Ismail, S.I., Nunome, H., Lysdal, G.F., Kersting, U.G., Tamura, Y., n.d. Futsal Playing Surface Characteristics Significantly Affects Perceived Traction and Change of Direction Performance Among Experienced Futsal Players. Unpubl. results.

Ismail, S.I., Nunome, H., Tamura, Y., 2020. Does visual representation of futsal shoes outsole tread groove design resemblance its mechanical traction, dynamic human traction performance, and perceived traction during change of direction and straight sprint tasks? Footwear Sci. 0, 1–11. https://doi.org/10.1080/19424280.2020.1825534

ISO, 2019. Personal protective equipment - Footwear - Test method for slip resistance (ISO 13287:2019). CEN, Eur. Comm. Stand. 13287.

ISO, 2012. Personal protective equipment – Occupational footwear (ISO 20347:2012). CEN, Eur. Comm. Stand. 20347.

Jakobsen, L., Lysdal, Gertz, F., Bagehorn, T., Kersting, U., Sivebaek, Marius, I., 2022a. The Effect of Footwear Outsole Material on Slip Resistance on Dry and Contaminated Surfaces with Geometrically Controlled Outsoles. Ergonomics. https://doi.org/https://doi.org/10.1080/00140139.2022.2081364

Jakobsen, L., Lysdal, F.G., Bagehorn, T., Kersting, U., Sivebaek, I.M., 2022b. The effect of footwear outsole material on slip resistance on dry and contaminated surfaces with geometrically controlled outsoles. Ergonomics. https://doi.org/10.1080/00140139.2022.2081364

Jakobsen, L., Lysdal, F.G., Bagehorn, T., Kersting, U.G., Sivebaek, I.M., 2022c. Evaluation of an actuated force plate-based robotic test setup to assess the slip resistance of footwear. Int. J. Ind. Ergon. 88, 103253. https://doi.org/10.1016/J.ERGON.2021.103253

Jakobsen, L., Lysdal, F.G., Sivebaek, I.M., 2021. Dynamic mechanical analysis as a predictor for slip resistance and traction in footwear. Footwear Sci. 13, S57–S58. https://doi.org/10.1080/19424280.2021.1917680

Jones, T., Iraqi, A., Beschorner, K., 2018. Performance testing of work shoes labeled as slip resistant. Appl. Ergon. 68, 304–312. https://doi.org/10.1016/j.apergo.2017.12.008

Khaday, S., Li, K.W., Peng, L., Chen, C.C., 2021. Relationship between friction coefficient and surface roughness of stone and ceramic floors. Coatings 11. https://doi.org/10.3390/coatings11101254

Li, K.W., Chen, C.J., 2004. The effect of shoe soling tread groove width on the coefficient of friction with different sole materials, floors, and contaminants. Appl. Ergon. 35, 499–507. https://doi.org/10.1016/j.apergo.2004.06.010

Li, K.W., Chin, J.C., 2005. Effects of tread groove orientation and width of the footwear pads on measured friction coefficients, in: Safety Science. https://doi.org/10.1016/j.ssci.2005.08.006

Li, K.W., Wu, H.H., Lin, Y.-C., 2006. The effect of shoe sole tread groove depth on the friction coefficient with different tread groove widths, floors and contaminants. Appl. Ergon. 37, 743–748. https://doi.org/10.1016/j.apergo.2005.11.007

Lloyd, D., Stevenson, M.G., 1989. Measurement of slip resistance of shoes on floor surfaces. Part 2: Effect of a bevelled heel. J. Occup. Heal. Saf. - Aust. New Zeal. 5.

Lorenz, B., Persson, B.N.J., Dieluweit, S., Tada, T., 2011. Rubber friction: Comparison of theory with experiment. Eur. Phys. J. E 34. https://doi.org/10.1140/epje/i2011-11129-1

Lysdal, F.G., Grønlykke, T.B., Kersting, U.G., 2022. Spraino: A novel low-friction device for prevention of lateral ankle sprain injuries in indoor sports. Med. Nov. Technol. Devices 16, 100141. https://doi.org/https://doi.org/10.1016/j.medntd.2022.100141

Moore, C.T., Menezes, P.L., Lovell, M.R., Beschorner, K.E., 2012. Analysis of Shoe Friction During Sliding Against Floor Material: Role of Fluid Contaminant. J. Tribol. 134, 041104. https://doi.org/10.1115/1.4007346

Moriyasu, K., Nishiwaki, T., Shibata, K., Yamaguchi, T., Hokkirigawa, K., 2019. Friction control of a resin foam/rubber laminated block material. Tribol. Int. 136. https://doi.org/10.1016/j.triboint.2019.04.024

Redfern, M.S., Cham, R., Gielo-Perczak, K., Grönqvist, R., Hirvonen, M., Lanshammar, H., Marpet, M., Yi-Chung Pai, C.I., Powers, C., Redfern, S., Yi-Chung Pai, C., Â Cham, R., Gielo-perczak, K., Gro È Nqvist, R., Ê Kan Lanshammar, H., Yi-chung Pai, C., 2001. Biomechanics of slips. Ergonomics 44, 1138–1166.

https://doi.org/10.1080/00140130110085547

Strandberg, L., 1985. The effect of conditions underfoot on falling and overexertion accidents. Ergonomics 28, 131–147. https://doi.org/10.1080/00140138508963123

Strobel, C.M., Menezes, P.L., Lovell, M.R., Beschorner, K.E., 2012. Analysis of the contribution of adhesion and hysteresis to shoe-floor lubricated friction in the boundary lubrication regime. Tribol. Lett. 47, 341–347. https://doi.org/10.1007/s11249-012-9989-5

Sundhedsstyrelsen, 2016. Sygdomsbyrden i Danmark, Ulykker, Selvskade og Selvmord 2016. Copenhagen S.

Tsai, Y.J., Powers, C.M., 2009. Increased shoe sole hardness results in compensatory changes in the utilized coefficient of friction during walking. Gait Posture 30, 303–306. https://doi.org/10.1016/j.gaitpost.2009.05.019

U.S. Department of Labor- Bureau of Labor Statistics, 2019. TABLE R4. Number of Nonfatal Occupational Injuries and Illnesses Involving Days Away from Work by Industry and Selected Events or Exposures Leading to Injury or Illness, vol. 2019.

Yamaguchi, T., Katsurashima, Y., Hokkirigawa, K., 2017. Effect of rubber block height and orientation on the coefficients of friction against smooth steel surface lubricated with glycerol solution. Tribol. Int. 110. https://doi.org/10.1016/j.triboint.2017.02.015

Footwear Outsole Friction on Steel and Tile Surfaces: Experiments and Modelling

L. Jakobsen,[1,2] A. Tiwari,[1,3,4] I.M. Sivebaek,[1,2] and B.N.J. Persson[1,3]

[1] *Peter Grünberg Institute (PGI-1), Forschungszentrum Jülich, 52425 Jülich, Germany*
[2] *Technical University of Denmark, Civil and Mechanical Engineering, 2800 Lyngby, Denmark*
[3] *www.MultiscaleConsulting.com*
[4] *Laerdal Medical AS, Tanke Svildsgate 30, Stavanger 4002, Norway*

Understanding and modeling friction between the footwear outsoles and different substrates is important to avoid slips, trips, and falls (STF). In this study footwear outsole materials friction is measured against steel and tile surfaces. We used three chemically different shoe outsole materials namely vulcanized rubber (RU), thermoplastic polyurethane (TPU), and polyurethane (PU), and their viscoelastic and friction properties were characterized. We measured friction as a function of sliding velocity using two different tribometers and the surface roughness power spectrum of the sliding substrates (steel and tile) was measured using stylus instrument. Persson's multiscale contact mechanics approach was used to model the friction which takes as input two quantities namely the surface roughness power spectrum of substrates and viscoelastic properties of the outsole materials.

Introduction

Slips, trips and falls (STF) is a frequent cause of both non-fatal [1] and fatal [2] occupational accidents. In fact, STF is the most frequent cause of absence of work [2]. STF is however subdivided into falls to a lower level (e.g. fall from a scaffolding), or falls on the same level (e.g. slipping on a greasy surface or stumbling over an object). The latter is the most frequent with approximately a factor of three. Furthermore, slipping has been acknowledged as the most frequent cause of STF on the same level [3]. Notably, in a five year time period most work related injuries has decreased except from STF injuries, which have increased [4, 5]. Hence, STF preventive actions are demanded and have great potential for increasing occupational safety and reducing expenses in terms of absence from work [6] and hospitalization [7].

The challenge of slipping prevention has received attention in the scientific community [8, 9], with effort put into optimizing surfaces [10–13] and footwear outsoles [14] to increase slip resistance. Especially increased surface roughness has shown a positive effect on slip resistance on contaminated surfaces [15, 16]. However, medical- and food industries often lacks the ability to increase surface roughness due to hygiene requirements [17, 18]. Thus, attempts to optimize footwear slip resistance in terms of outsole patterns [19–23], outsole hardness [24–26] and outsole materials [21, 27, 28] have also been done.

Footwear outsoles are constructed of viscoelastic elastomers [9], which have complicated material properties affecting the slip resistance [29]. The slip resistance between footwear and surface is often quantified using the coefficient of friction (COF) [8, 28], thus a higher COF between footwear and surface will ultimately increase the slip resistance. The adhesive and hysteresis components' contribution to the friction of rubber compounds has previously been described [30–32]. In relation to footwear slip resistance these components have been addressed [9, 14, 33], however sparsely investigated [15, 34]. Dynamic Mechanical Analysis (DMA) is valuable tool to determine elastomers viscoelastic properties as function of temperature and frequency. Viscoelasticity of the rubber compounds has direct relation to the hystersis/viscoelastic contribution to friction and has been linked to footwear slip resistance on ice surface [35] and has been used in similar contact situations such as tire/road contact by many earlier studies [36, 37]. The sliding velocities in real slip events simulated in biomechanical tests are as high as 2.5 m/s [8] and in standardized tests the footwear slip resistance is often determined at a much lower sliding velocity of 0.3 m/s [38]. Hence, there exists a gap in sliding velocities between real slip events and standardized test measurements. Therefore, in this study, we experimentally determine the friction properties of three common elastomer footwear outsole materials in sliding velocities covering six decades in velocity from 1 μm/s to 2.4 m/s and the friction results are modelled and explained using Persson's multiscale contact mechanics approach.

Surface roughness power spectra

The most important information about the surface topography of a rough surface is the surface roughness power spectrum. For a one-dimensional (1D) line scan $z = h(x)$ the power spectrum is given by

$$C_{1\mathrm{D}}(q) = \frac{1}{2\pi}\int_{-\infty}^{\infty} dx\ \langle h(x)h(0)\rangle e^{iqx}$$

where $\langle..\rangle$ stands for ensemble averaging. For surfaces with isotropic roughness the 2D power spectrum $C(q)$ can be obtained directly from $C_{1\mathrm{D}}(q)$ as described elsewhere [39–41]. For randomly rough surfaces, all the (ensemble averaged) information about the surface is contained in the power spectrum $C(q)$. For this reason the only information about the surface roughness which enter in contact mechanics theories (with or without adhesion) is the function $C(q)$. Thus, the (ensemble averaged) area of real contact, the interfacial stress distribution and the

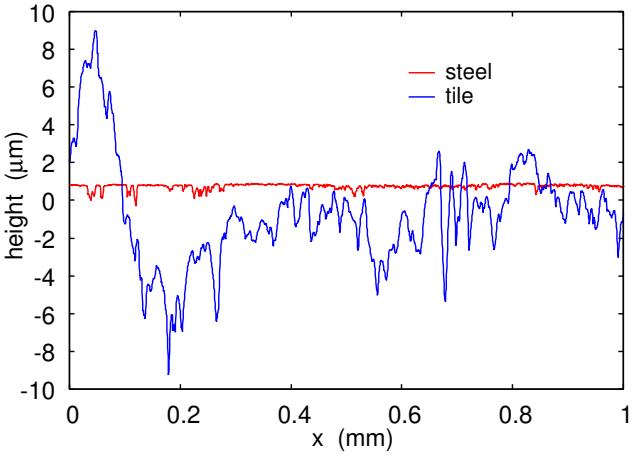

FIG. 1: The surface height $h(x)$ of the steel surface and the tile surface as a function of the distance x.

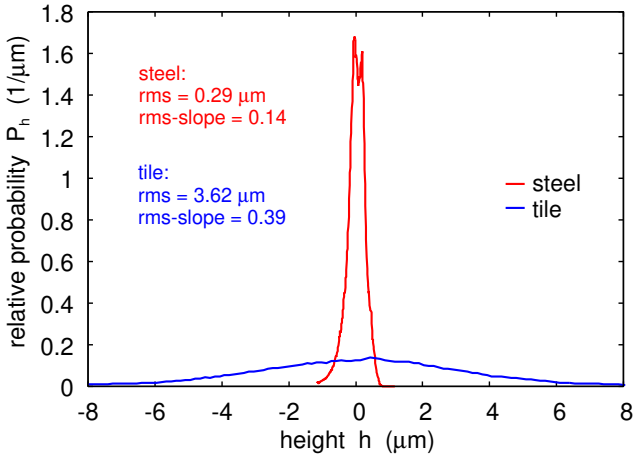

FIG. 2: The surface height probability distribution P_h of the steel surface and the tile surface as a function of the surface height h.

distribution of interfacial separations, are all determined by $C(q)$[42, 43].

Note that moments of the power spectrum determine standard quantities which are output of most stylus instruments and often quoted. Thus, for example, the mean-square (ms) roughness amplitude $\langle h^2 \rangle$ is given by

$$\langle h^2 \rangle = 2 \int_0^\infty dq \; C_{1D}(q).$$

Using an engineering stylus instrument we have studied the surface topography of a tile (eurotile 2) and steel surface (steel number 1.4301) used in this work. The topography measurements was performed using Mitutoyo Portable Surface Roughness Measurement Surftest SJ-410 with a diamond tip with the radius of curvature R = 1 μm, and with the tip-substrate repulsive force F_N = 0.75 mN. The scan length L = 25 mm and the tip speed v = 50 μm/s.

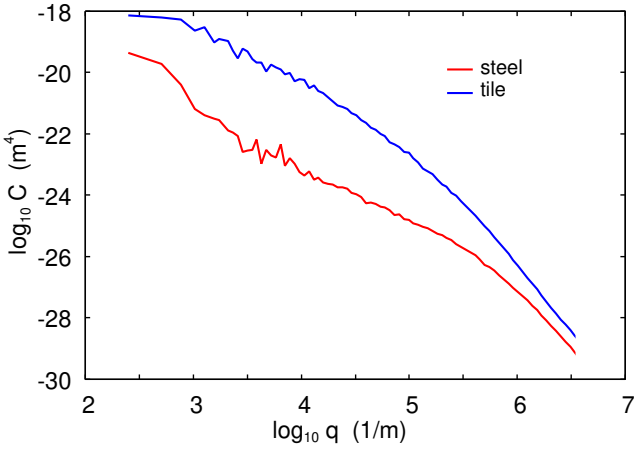

FIG. 3: The surface roughness power spectra of the steel surface and the tile surface as a function of the wavenumber (log-log scale).

TABLE I: Summary of the glass transition temperatures of the PU and TPU compounds. The glass transition temperature is defined as the maximum of tanδ as a function of temperature for the frequency ω_0 = 0.01 s^{-1}. The RU compound is a mixture of two different rubber compounds and exhibit two separate peaks in the tanδ as a function of temperature curve.

compound	T_g	maximum of tanδ
PU	−22.7°C	0.61
TPU	−37.7°C	0.69

Fig. 1 shows the surface height $h(x)$ of the steel surface and the tile surface as a function of the distance x. Fig. 2 shows the surface height probability distribution P_h, and Fig. 3 the surface roughness power spectra of the same surfaces.

Viscoelastic modulus

For determining the viscoleastic contribution to rubber/elastomer friction it is necessary to have information about the complex elastic modulus over a rather large frequency range, as well as at different strain values including very large strain of order 100%. A standard way of measuring the viscoelastic modulus is to use DMA instrument where one oscillatory deforms the rubber sample with a constant strain or stress amplitude. This is done at different frequencies and then repeated at different temperatures. The results measured at different temperatures can be time-temperature shifted to form a mastercurve at a chosen reference temperature covering a broad range of frequencies.

In this section we present results for the viscoelastic properties for three different elastomer compounds namely TPU, PU and RU. These materials have also

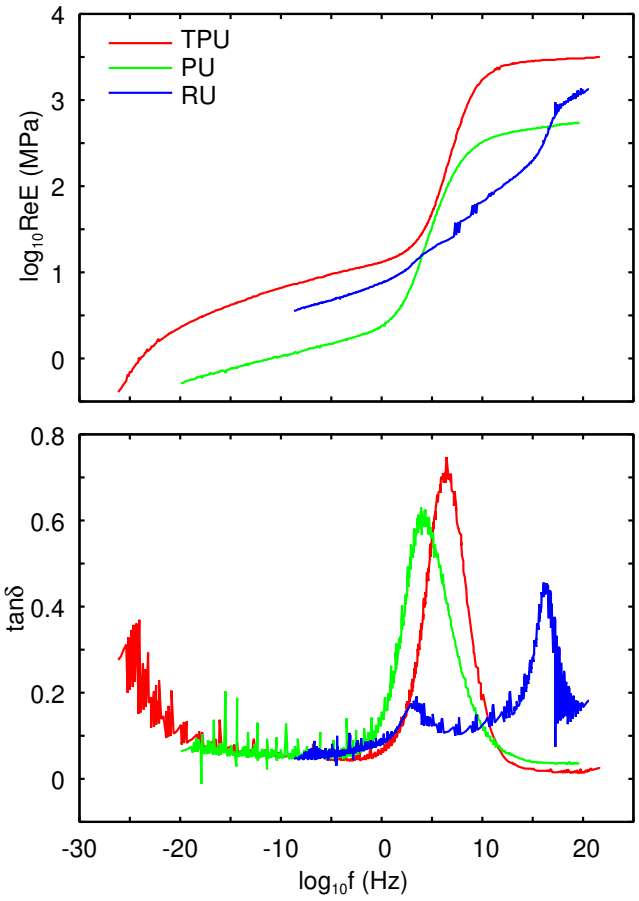

FIG. 4: (a): The real part ReE of the viscoelastic modulus E as a function of frequency (log-log scale). (b): The ratio ImE/ReE as a function of the logarithm of the frequency.

been molded as whole footwear outsoles in a real shoe samples and slip resistance was determined on contaminated surfaces [44] and as blocks on ice surface [35].

We use a Q800 Dynamic Mechanical Analysis (DMA) instrument produced by TA Instruments.The machine is run in tension mode, meaning that a strip or a fiber of elastomer clamped on both sides, is elongated in an oscillatory manner. The complex viscoelastic modulus is first measured in constant strain mode with a strain amplitude of 0.04% strain and at different frequencies starting from 28 Hz and changed in steps until 0.25 Hz is reached (10 frequency points: 28.0, 25.0, 14.0, 7.9, 4.4, 2.5, 1.4, 0.79, 0.44, and 0.25 Hz). The rather small strain amplitude is chosen in order to avoid strain softening effects. We have found that a strain amplitude of 0.04% is reasonable good for typical filled rubber compounds. Measuring the elastomer sample in tension mode also requires to prestrain the sample with a static strain that has to be larger then the dynamic strain during oscillation. The prestrain in the experiments has been set to 0.06% to avoid compressing the sample during the DMA measurement.

The experiment usually starts at −75°C and after measuring the modulus at all frequencies mentioned above, the temperature is increased in steps by 5°C, and the procedure is repeated until 120°C is reached. Note that it may be necessary to choose smaller temperature steps when reaching the glass transition temperature T_g where the viscoelastic response of the rubber material changes strongly with frequency (and temperature). This makes sure that the curves measured at different temperatures overlap with each other, which is necessary for the shift procedure. The results are then shifted in order to form a smooth ReE master curve.

We have measured the viscoelastic modulus of the PU, TPU and RU elastomer compounds used in this study. Fig. 4(a) shows the frequency dependency of the real part of the low strain ($\epsilon = 0.0004$) modulus E for the PU, TPU and RU compounds for the $T = 20$°C. In Fig. 4(b) we show for the same compounds the ratio ImE/ReE. The RU compound is a mixture of two rubber compounds with different glass transition temperatures giving two separate peaks in the Im$E(T)$/Re$E(T)$ curve. In Table I we give the glass transition temperatures and the maximum of the Im$E(T)$/Re$E(T)$ curve for the TPU and PU compounds.

Fig. 4(a) shows that TPU has the largest modulus in the rubbery region, followed by RU and then PU. This is also clear from the shore A hardness values which are 80 for the TPU compound, 68 for the RU compound and 56 for the PU compound. Note that the chain molecules in TPU are not chemically crosslinked like typical crosslinked rubber compounds and at high temperatures or very low frequencies it behaves as a viscous fluid. This can be seen in Fig. 4(a) where ReE decreases for very low frequencies as expected for a fluid for which Re$E = 0$ at zero frequency.

Rubber friction

Friction measurements in Jülich We performed friction measurements using our low-temperature linear friction slider. In this setup the temperature can be changed from room temperature down to −40°C. Square samples (2.5 cm * 2.5 cm) of the elastomer blocks are glued on a sample holder (aluminum plate) which gets attached to the force cell. The elastomer sample can move with the carriage in the vertical direction to adapt to the substrate profile. The normal load can be changed by adding steel plates on top of the force cell. The substrate sample gets attached to the machine table which is moved by a servo drive via a gearbox in a translational manner. We control the relative velocity between the elastomer sample and the surface while the force cell acquires information about normal force as well as friction force.

To change the temperature the whole set-up is placed inside a deep freezer capable of cooling down the exper-

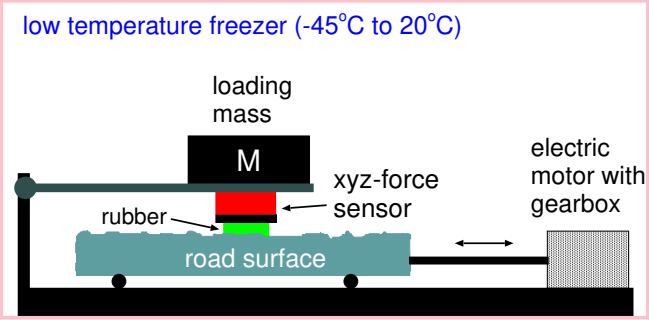

FIG. 5: Schematic picture of low-temperature friction instrument allowing for linear reciprocal motion. A rubber segment is glued on the aluminum sample holder which gets attached to the force cell (red box in the figure). The rubber specimen can move with the carriage in the vertical direction to adapt to the substrate profile. The normal load can simply be changed by adding additional steel plates on top of the force cell. The substrate sample gets attached to the machine table which is moved by a servo drive via a gearbox in a translational manner. Here we control the relative velocity between the rubber specimen and the substrate sample while the force cell acquires information about normal force as well as friction force.

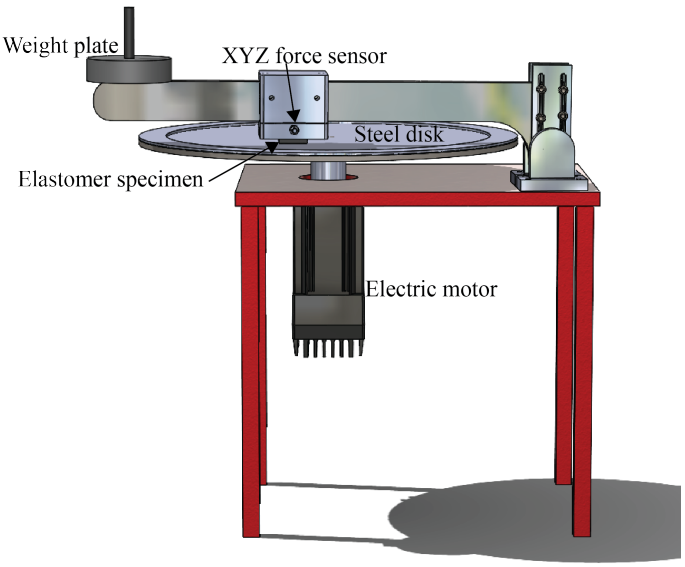

FIG. 6: Illustration of the large-scale pin-on-disk tribosystem for measuring the elastomers frictional properties.

iment to −40°C. We then slide the elastomer samples over the tile and steel surface with different velocities to gain information on the velocity, load (normal force) and temperature dependency of the friction coefficient and the wear rate. Fig. 5 shows the set-up placed inside the deep freezer while an experiment is performed. With the current configuration it is possible to move the elastomer specimen with velocities from 1 μm/s to 10 mm/s [37]. The temperature inside the deep freezer can be varied from 30°C to −40°C. For increasing the temperature again after an experiment is finished there is also a heating system built into the set-up. The smallest normal force on the elastomer sample possible is about $F_z \approx 280$ N and one can add additional steel plates up to 63 kg giving the normal force $F_z \approx 900$ N.

Friction measurements at DTU

We designed a large-scale pin-on-disk tribometer, and instrumented a 3-axis force sensor (K3D120 Force sensor, ME-Meßsysteme GmbH, Germany) on a beam, and an 8000 mm steel plate (steel number 1.4301) "disk". The disk was powered by a servo motor (MAC1200, JVL A/S, Denmark) that was mounted on a steel frame below the attached disk. Fig. 6 shows the large-scale pin-on-disk setup.

The tangential velocity in the contact point between the elastomer specimen and the steel disk was adjustable between 0-2.5 m/s. Square samples (2.5 mm * 2.5 mm) of the RU, PU, and TPU samples were cut and glued to an aluminum plate, which was attached to the force sensor. Normal force was applied with weight plates on top of the beam, hence a normal pressure of 0.5 MPa was achieved. Each material specimen was subjected to sliding velocities of 30 cm/s, 1 m/s and 2.4 m/s for maximal 1 s in dry conditions. The tile surface cannot be mounted on the tribometer, hence only the steel surface is used.

Experimental results

Fig. 7 shows the measured friction coefficient on the (a) the tile surface and (b) the steel surface as a function of the sliding velocity. The temperature T = 20°C and the nominal contact pressure p_0 = 0.5 MPa.

Although the TPU compound gives very high friction, the friction force decreases with sliding velocities above 0.1 mm/s on both the steel and tile surface. Thus if a slip occur at velocities above 0.1 mm/s accelerated (runaway) slip would occur (the banana-effect) which, in the context of footwear, could result in a slip event. For the PU and RU compounds the friction force is much smaller but increases monotonically with the sliding velocity up to the highest sliding velocity studied (v = 0.5 m/s).

Analysis of the experimental results

We have calculated (estimated) the viscoelastic contribution to the friction using the rubber friction theory developed elsewhere [42]. In the calculations we have used the power spectra shown in Fig. 3. Thus the viscoelastic contribution to the friction only include the roughness with wavenumber $q < 3 \times 10^6$ m^{-1}.

Fig. 8 shows the calculated viscoelastic contribution to the friction coefficient and Fig. 9 the calculated projected relative contact area A/A_0 for (a) the tile surface and (b) the steel surface as a function of the sliding velocity at the temperature T = 20°C and the nominal contact pressure p_0 = 0.5 MPa. The viscoelastic contribution to

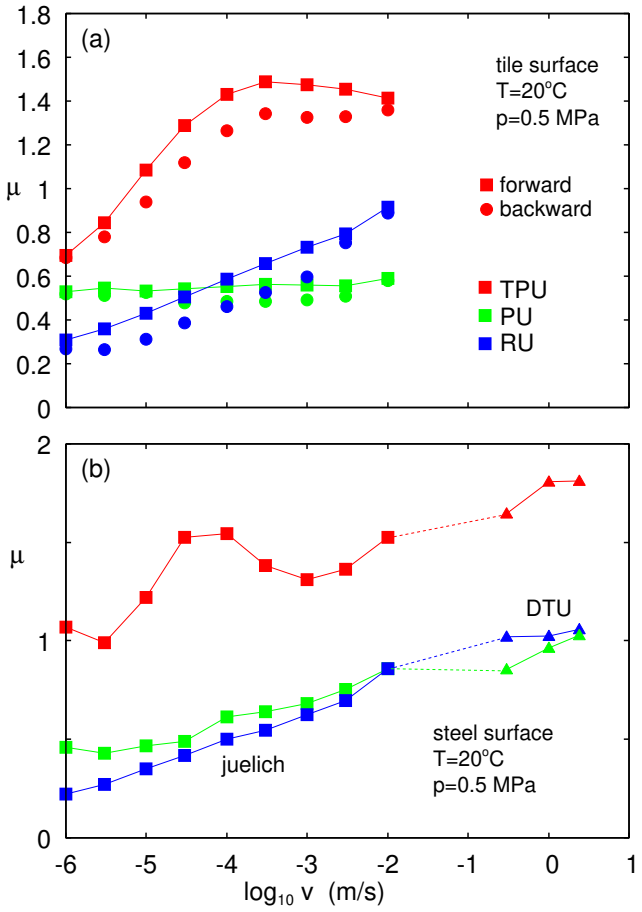

FIG. 7: The measured friction coefficient on the (a) the tile surface and (b) the steel surface as a function of the sliding velocity. The temperature $T = 20^{\circ}$C and the nominal contact pressure $p_0 = 0.5$ MPa.

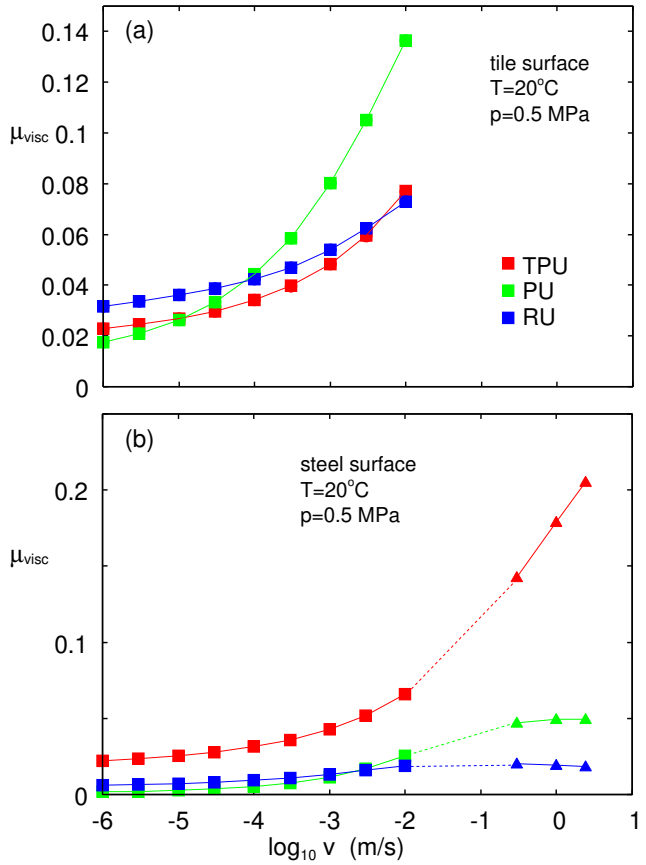

FIG. 8: The calculated viscoelastic contribution to the friction coefficient on (a) the tile surface and (b) the steel surface as a function of the sliding velocity. The temperature $T = 20^{\circ}$C and the nominal contact pressure $p_0 = 0.5$ MPa.

the friction coefficient is very small for all three materials, relative to the total friction coefficient. This means that the adhesive contribution to the friction coefficient is large. Hard elastomer materials have previously been found to have higher adhesive friction contribution compared to softer elastomer materials [34], which is in line with the findings from this study with the TPU showing high adhesive friction contribution. The fact that the contact area decreases as function of sliding velocity is in line with previous findings for polyurethane outsole specimen sliding on a tile surface [27].

Fig. 10 shows the effective frictional shear stress acting in the area of real contact on (a) the tile surface and (b) the steel surface as a function of the sliding velocity. The shear stress was obtained by subtracting from the measured friction force and the calculated viscoelastic contribution to the friction force, and dividing with the calculated area of real contact.

$$\tau_{\rm f} = p_0 \frac{A_0}{A} \left(\mu - \mu_{\rm visc}\right)$$

We note that this is the frictional shear stress in the contact regions observed at the magnification $\zeta = q_1/q_0$. At higher magnification, the area of real contact may be smaller and the effective frictional shear stress higher. Due to the high friction coefficient for TPU and the relatively low projected contact area, the frictional shear stress is much higher.

Summary and footwear implications

This study provides a fundamental insight into the friction mechanisms of three common outsole materials, by estimating the viscoelastic contribution to friction, the projected relative contact area and frictional shear stress in dry state. In this dry state the TPU showed superior friction coefficient compared to the PU and RU material, which could be explained by the viscous behavior at high temperatures, caused by its thermoplastic nature. While the RU and PU compounds exhibit very similar (effective) frictional shear stress, the TPU compound exhibit much higher frictional shear stress. The microscopic origin of this is not obvious but may also be related to the fact that the RU and PU compounds are have more chemical covalent crosslinks, while the TPU

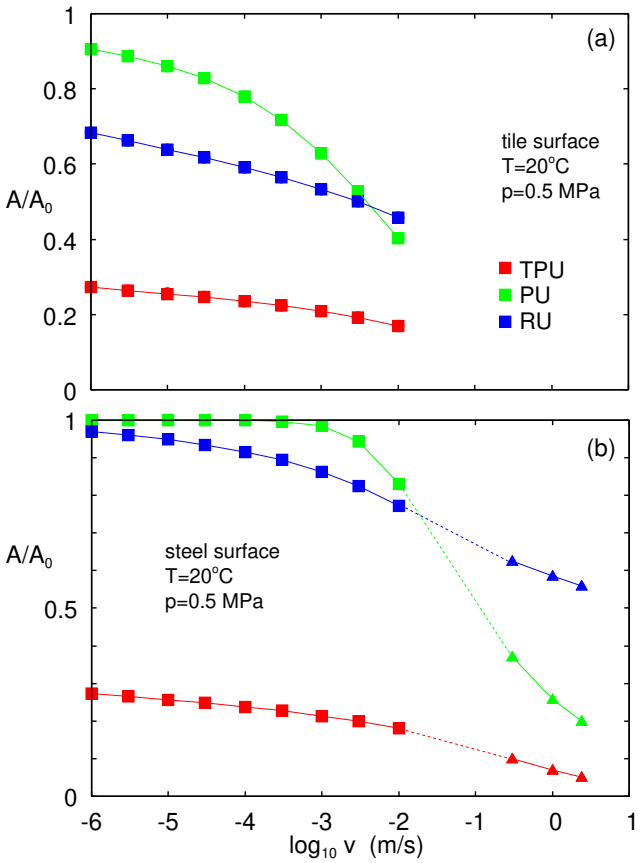

FIG. 9: The calculated projected relative contact area A/A_0 for the (a) the tile surface and (b) the steel surface as a function of the sliding velocity. The temperature T = 20°C and the nominal contact pressure p_0 = 0.5 MPa.

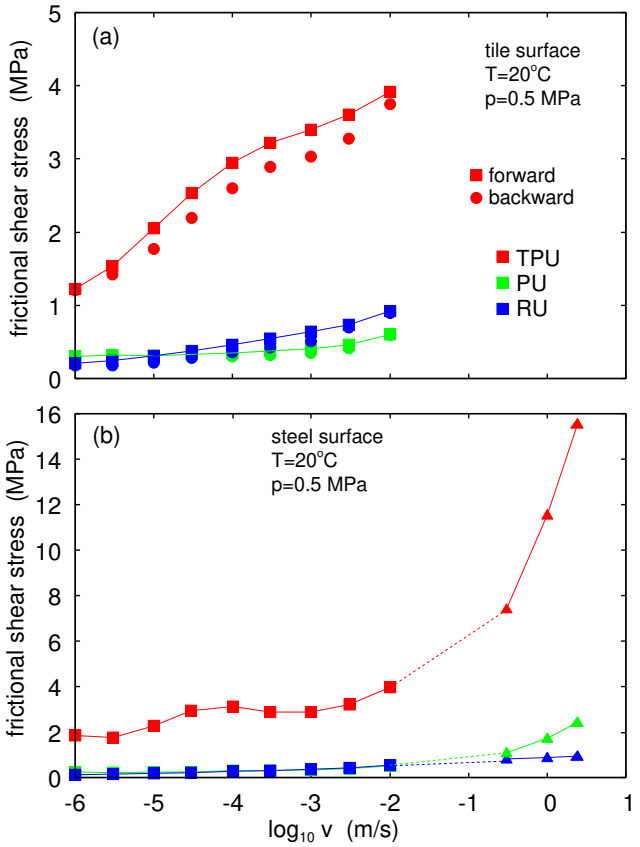

FIG. 10: The frictional shear stress acting in the area of real contact on (a) the tile surface and (b) the steel surface as a function of the sliding velocity. The shear stress was obtained by subtracting from the measured friction force in FIG 7 and the calculated viscoelastic contribution to the friction force in FIG 8, and dividing with the calculated area of real contact. The temperature T = 20°C and the nominal contact pressure p_0 = 0.5 MPa.

compounds have more of physical crosslinks. Thus at high-temperature TPU melts while RU decomposes by pyrolysis (thermal decomposition). The fact that only weak bonds keep the chain molecules together in TPU may result in more dissipative processes occurring in the TPU-substrate contact regions, such as chain pull-out and slippage. It should be noted that slipping accidents often occur on contaminated surfaces, which makes the viscoelastic contribution and the contact area important. The PU material showed highest viscoelastic friction contribution (Fig 9) and highest contact area (Fig 10), when sliding on the tile surface. This is a possible explanation for the higher friction coefficient found in previous research with the PU material, when sliding on glycerine and canola oil contaminated tile surface [44] as well as ice surfaces close to the melting point [35].

[1] Hoon-Yong Yoon and Thurmon E Lockhart. Nonfatal occupational injuries associated with slips and falls in the united states. *International journal of industrial ergonomics*, 36(1):83–92, 2006.

[2] U.S. Department of Labor-Bureau of Labor Statistics. National census of fatal occupational injuries in 2019. bureau of labor statistics., 2020.

[3] Theodore K Courtney, Gary S Sorock, Derek P Manning, James W Collins, and Mary Ann Holbein-Jenny. Occupational slip, trip, and fall-related injuries can the contribution of slipperiness be isolated? *Ergonomics*, 44(13):1118–1137, 2001.

[4] Wen-Ruey Chang, Sylvie Leclercq, Thurmon E Lockhart, and Roger Haslam. State of science: occupational slips, trips and falls on the same level. *Ergonomics*, 59(7):861–883, 2016.

[5] Caijun Zhao, Kai Way Li, Jiayi Lu, and Zhu Li. Risk of tripping, minimum foot clearance, and step length when crossing a barrier. *International Journal of Industrial Ergonomics*, 83:103138, 2021.

[6] C Gauvin, D Pearsall, M Damavandi, Y Michaud-Paquette, B Farbos, and D Imbeau. Risk factors for slip accidents among police officers and school crossing guards—exploratory study. *IRSST Research Report R-*

893.

[7] Larry A Layne and Keshia M Pollack. Nonfatal occupational injuries from slips, trips, and falls among older workers treated in hospital emergency departments, united states 1998. *American journal of industrial medicine*, 46(1):32–41, 2004.

[8] Wen-Ruey Chang, Raoul Grönqvist, Sylvie Leclercq, Robert J Brungraber, Ulrich Mattke, Lennart Strandberg, Steve C Thorpe, Rohae Myung, Lasse Makkonen, and Theodore K Courtney. The role of friction in the measurement of slipperiness, part 2: Survey of friction measurement devices. *Ergonomics*, 44(13):1233–1261, 2001.

[9] M Tisserand. Progress in the prevention of falls caused by slipping. *Ergonomics*, 28(7):1027–1042, 1985.

[10] Arnab Chanda, Taylor G Jones, and Kurt E Beschorner. Generalizability of footwear traction performance across flooring and contaminant conditions. *IISE transactions on occupational ergonomics and human factors*, 6(2):98–108, 2018.

[11] Ruikang Ding, Abhijeet Gujrati, Matthew M Pendolino, Kurt E Beschorner, and Tevis DB Jacobs. Going beyond traditional roughness metrics for floor tiles: Measuring topography down to the nanoscale. *Tribology Letters*, 69(3):1–12, 2021.

[12] In-Ju Kim. Identifying shoe wear mechanisms and associated tribological characteristics: Importance for slip resistance evaluation. *Wear*, 360:77–86, 2016.

[13] D Manning, Craig Jones, and M Bruce. Boots for oily surfaces. *Ergonomics*, 28(7):1011–1019, 1985.

[14] Raoul Grönqvist. Mechanisms of friction and assessment of slip resistance of new and used footwear soles on contaminated floors. *Ergonomics*, 38(2):224–241, 1995.

[15] Matthew JH Cowap, Seyed RM Moghaddam, Pradeep L Menezes, and Kurt E Beschorner. Contributions of adhesion and hysteresis to coefficient of friction between shoe and floor surfaces: effects of floor roughness and sliding speed. *Tribology-Materials, Surfaces & Interfaces*, 9(2):77–84, 2015.

[16] In-Ju Kim, Hongwei Hsiao, and Peter Simeonov. Functional levels of floor surface roughness for the prevention of slips and falls: Clean-and-dry and soapsuds-covered wet surfaces. *Applied Ergonomics*, 44(1):58–64, 2013.

[17] Wen-Ruey Chang, Kai Way Li, Alfred Filiaggi, Yueng-Hsiang Huang, and Theodore K Courtney. Friction variation in common working areas of fast-food restaurants in the usa. *Ergonomics*, 51(12):1998–2012, 2008.

[18] Collette Staal, Barbra White, Bruce Brasser, Larry LeForge, et al. Reducing employee slips, trips, and falls during employee-assisted patient activities. *Rehabilitation Nursing*, 29(6):211, 2004.

[19] Kurt E Beschorner, Arian Iraqi, Mark S Redfern, Rakié Cham, and Yue Li. Predicting slips based on the stm 603 whole-footwear tribometer under different coefficient of friction testing conditions. *Ergonomics*, 62(5):668–681, 2019.

[20] Kai Way Li, Horng Huei Wu, and Yu-Chang Lin. The effect of shoe sole tread groove depth on the friction coefficient with different tread groove widths, floors and contaminants. *Applied ergonomics*, 37(6):743–748, 2006.

[21] Kai Way Li and Chin Jung Chen. The effect of shoe soling tread groove width on the coefficient of friction with different sole materials, floors, and contaminants. *Applied ergonomics*, 35(6):499–507, 2004.

[22] Takeshi Yamaguchi and Kazuo Hokkirigawa. Development of a high slip-resistant footwear outsole using a hybrid rubber surface pattern. *Industrial health*, 2014.

[23] Mansour Ziaei, Hamidreza Mokhtarinia, Farhad Tabatabai Ghomshe, and Maryam Maghsoudipour. Coefficient of friction, walking speed and cadence on slippery and dry surfaces: shoes with different groove depths. *International journal of occupational safety and ergonomics*, 2018.

[24] Yi-Ju Tsai and Christopher M Powers. The influence of footwear sole hardness on slip initiation in young adults. *Journal of forensic sciences*, 53(4):884–888, 2008.

[25] Yi-Ju Tsai and Christopher M Powers. Increased shoe sole hardness results in compensatory changes in the utilized coefficient of friction during walking. *Gait & posture*, 30(3):303–306, 2009.

[26] Paul J Walter, Claire M Tushak, Sarah L Hemler, and Kurt E Beschorner. Effect of tread design and hardness on interfacial fluid force and friction in artificially worn shoes. *Footwear Science*, 13(3):245–254, 2021.

[27] Kurt Beschorner, Michael Lovell, C Fred Higgs III, and Mark S Redfern. Modeling mixed-lubrication of a shoe-floor interface applied to a pin-on-disk apparatus. *Tribology Transactions*, 52(4):560–568, 2009.

[28] S Derler, F Kausch, and R Huber. Analysis of factors influencing the friction coefficients of shoe sole materials. *Safety Science*, 46(5):822–832, 2008.

[29] MR Shariatmadari, R English, and G Rothwell. Finite element study into the effect of footwear temperature on the forces transmitted to the foot during quasi-static compression loading. In *IOP Conference Series: Materials Science and Engineering*, volume 10, page 012126. IOP Publishing, 2010.

[30] KA Grosch. The relation between the friction and viscoelastic properties of rubber. *Proceedings of the Royal Society of London. Series A. Mathematical and Physical Sciences*, 274(1356):21–39, 1963.

[31] Qiang Li, Andrey Dimaki, Mikhail Popov, Sergey G Psakhie, and Valentin L Popov. Kinetics of the coefficient of friction of elastomers. *Scientific reports*, 4(1):1–5, 2014.

[32] BNJ Persson and Erio Tosatti. The effect of surface roughness on the adhesion of elastic solids. *The Journal of Chemical Physics*, 115(12):5597–5610, 2001.

[33] Raoul Grönqvist, Wen-Ruey Chang, Theodore K Courtney, Tom B Leamon, Mark S Redfern, and Lennart Strandberg. Measurement of slipperiness: fundamental concepts and definitions. *Ergonomics*, 44(13):1102–1117, 2001.

[34] Caitlin Moore Strobel, Pradeep L Menezes, Michael R Lovell, and Kurt E Beschorner. Analysis of the contribution of adhesion and hysteresis to shoe–floor lubricated friction in the boundary lubrication regime. *Tribology Letters*, 47(3):341–347, 2012.

[35] Lasse Jakobsen, Bergtun Auganæs, Buene Sondre, Audun Formo, Marius Ion Sivebaek, and Alex Klein-Paste. Dynamic and static friction measurements of elastomer footwear blocks on ice surface. *Tribology International*, 0(0):0, 2022.

[36] Mona Mahboob Kanafi, Ari Juhani Tuononen, Leonid Dorogin, and Bo NJ Persson. Rubber friction on 3d-printed randomly rough surfaces at low and high sliding speeds. *Wear*, 376:1200–1206, 2017.

[37] Avinash Tiwari, N Miyashita, Nuria Espallargas, and

Bo NJ Persson. Rubber friction: The contribution from the area of real contact. *The Journal of chemical physics*, 148(22):224701, 2018.

[38] International Organization for Standardization. Personal protective equipment – footwear – test method for slip resistance (iso 13287. 2019.

[39] Bo NJ Persson, O Albohr, Ugo Tartaglino, AI Volokitin, and Erio Tosatti. On the nature of surface roughness with application to contact mechanics, sealing, rubber friction and adhesion. *Journal of physics: Condensed matter*, 17(1):R1, 2004.

[40] Giuseppe Carbone, Boris Lorenz, Bo NJ Persson, and Alexander Wohlers. Contact mechanics and rubber friction for randomly rough surfaces with anisotropic statistical properties. *The European Physical Journal E*, 29(3):275–284, 2009.

[41] P Ranganath Nayak. Random process model of rough surfaces. *WEAR*, 21(21):406, 1971.

[42] Bo NJ Persson. Theory of rubber friction and contact mechanics. *The Journal of Chemical Physics*, 115(8):3840–3861, 2001.

[43] Andreas Almqvist, C Campana, N Prodanov, and BNJ Persson. Interfacial separation between elastic solids with randomly rough surfaces: comparison between theory and numerical techniques. *Journal of the Mechanics and Physics of Solids*, 59(11):2355–2369, 2011.

[44] Lasse Jakobsen, Filip Gertz Lysdal, Timo Bagehorn, Uwe G Kersting, and Ion Marius Sivebaek. The effect of footwear outsole material on slip resistance on dry and contaminated surfaces with geometrically controlled outsoles. *Ergonomics*, pages 1–8, 2022.

DTU Construct
Section of Manufacturing Engineering
Technical University of Denmark

Produktionstorvet, Bld. 425
DK-2800 Kgs. Lyngby
Denmark

Tlf.: +45 4525 4763
Fax: +45 4525 1961

www.construct.dtu.dk

March 2023

ISBN: 978-87-7475-707-8